이학박사학위논문

애기장대 히스톤 아세틸화 효소 HAG1의 발달전이 및 식물세포 전형성능 관련 기능에 대한 연구

A Study on the Role of Arabidopsis Histone Acetyltransferase HAG1 in Developmental Transition and Plant Cell Totipotency

2016년 8월

서울대학교 대학원

생명과학부

김 지 연

Abstract

A Study on the Role of Arabidopsis Histone Acetyltransferase HAG1 in Developmental Transition and Plant Cell Totipotency

Ji-Yun Kim

Department of Biological Sciences

The Graduate School

Seoul National University

Every cell in an organism carries an identical genome. However, multicellular eukaryotes are composed of different cell types that show different morphology and carry out diverse functions. Each cell types are characterized by distinct gene expression patterns that are generated during development and stably maintained. The main mechanism by which the information stored in the genome can be selectively controlled is based on epigenetics. Epigenetic regulation is referred to the stable control of gene expression caused by mechanisms that are not dependent

on underlying DNA sequence. Epigenetic mechanisms include DNA methylation, chromatin remodeling by ATP-dependent remodelers or histone modifications, nuclear positioning, histone variant incorporation, and regulation by noncoding RNAs.

Histone acetylation is an epigenetic modification associated with euchromatin and is catalyzed by histone acetyltransferases (HATs). HATs transfer the acetyl group from acetyl-CoA to lysine residues within the N-terminal histone tails. The negative charge of the acetyl group (CH_3COO^-) neutralizes the positive charges of histones, reducing their affinity to negatively charged DNA. This renders DNA more accessible to the transcriptional machinery or generates binding sites for acetyl lysine-binding proteins to spread the modification, leading to transcriptional activation.

In this study, I address two distinct roles HAG1/AtGCN5, a member of the Arabidopsis Gcn5-related N-acetyltransferase (GNAT) family of HATs. In the first part, I show that the HAG1 and PRZ1/ADA2b-containing SAGA-like histone acetyltransferase (HAT) complex controls the juvenile-to-adult phase transition. In Arabidopsis, vegetative phase transitions are regulated by SQUAMOSA PROMOTER BINDING PROTEIN-LIKE (SPL) factors that are post-transcriptionally regulated by miR156 in an age-dependent manner. I demonstrate that HAG1 and PRZ1 directly controls the transcription of *SPLs* by catalyzing H3Ac of their chromatin, and thus determines the time for juvenile-to-adult phase transition. Furthermore, this epigenetic mechanism is also crucial for miR156-independent induction of *SPLs* and acceleration of phase transition by light and

photoperiod or during post-embryonic growth.

In the second part, I address the role of HAG1 in the acquisition of pluripotency in callus during *de novo* organogenesis. For decades, callus was considered as an unorganized mass of undifferentiated cells. However, recent studies have provided evidences that callus is formed by the proliferation of a subset of existing stem cell-like pericycle cells adjacent to the xylem poles. These studies have also shown that callus cells have gene-expression profiles similar to those of root primordia. I demonstrate that HAG1 protein is induced in developing calli and plays a pivotal role in the activation of root meristem genes. Upon callus induction, histone acetylation at the root meristem genes, namely *WOX5/WOX14*, *SCARECROW* (*SCR*), *PLETHORA 1* (*PLT1*), and *PLT2*, is increased in a HAG1-dependent manner. This allows a high transcriptional output of the root meristem genes, and then the transcription factors encoded by the root meristem genes act as potency factors conferring competence for regeneration that is necessary for *de novo* shoot formation.

Key words: HAG1, callus, *de novo* shoot regeneration, histone acetylation, juvenile-to-adult transition

Student Number: 2007-22838

Contents

List of tables

Chapter I

Chapter II

Chapter III

List of figures

Chapter II

Chapter III

Abbreviations

2,4-D	2,4-dichlorophenoxyacetic acid
2IP	isopentenyladenine
AGL42	AGAMOUS-LIKE 42
AP1	APETALA 1
ChIP	chromatin immunoprecipitation
ChIP-seq	chromatin immunoprecipitation followed by sequencing
CIM	callus induction media
CUC2	CUP-SHAPED COTYLEDON 2
DEG	differentially expressed gene
DEX	dexamethasone
FDR	false discovery rate
FT	FLOWERING LOCUS T
FUL	FRUITFULL
GCN5	General Control Nonrepressed 5
GFP	green fluorescence protein
GNAT	GCN5-related N-acetyltransferase
GR	glucocorticoid receptor
GUS	β-glucuronidase
HA	hemagglutinin

HAT	histone acetyltransferase
IAA	indole-3-acetic acid
KRP7	KIP –RELATED PROTEIN 7
LD	long day
LFY	LEAFY
MIR156	MicroRNA 156
mRNA	messenger ribonucleic acid
MS	Murashige and Skoog
NC	no-change in expression
PCR	polymerase chain reaction
PI	propidium iodide
PLTI	PLETHORA1
PLT2	PLETHORA 2
PRZ1	PROPORZ 1
qPCR	quantitative polymerase chain reaction
RIM	root induction media
RNA POLII	RNA polymerase II
RNA-seq	RNA sequencing
RT	reverse-transcription
SAGA	SPT-ADA-GCN5-acetyltransferase complex
SCR	SCARECROW
SD	short day

SE	standard error
SHR	SHORT ROOT
SIM	shoot induction media
SOC1	SUPPRESSOR OF OVEREXPRESSION OF CONSTANS 1
SPL	SQUAMOSA PROMOTER BINDING PROTEIN-LIKE
T-DNA	transfer DNA
TES	transcription end site
TSS	transcription start site
UBQ	Ubiquitin
UTR	untranslated region
WUS	WUSCHEL
YFP	yellow fluorescence protein

Chapter I

General introduction

1.1 Epigenetic regulation of gene expression

The genome encodes all the RNA and proteins needed to construct the organism. However, knowing the complete genome sequence does not enable us to reconstruct the organism. The organism is composed of different cell types which show different morphology and carry out diverse functions. Each cell type is characterized by distinct gene expression patterns that are generated during development and stably maintained. Therefore, although the information stored in the DNA is important, how the information is selectively expressed in the correct cell type is what determines the cellular fate.

The main mechanism by which the information stored in the genome can be selectively controlled is based on epigenetics. Epigenetic regulation is referred to the stable control of gene expression caused by mechanisms that are not dependent on the underlying DNA sequence. Epigenetic modifications are usually stable and inherited in some instances, although they change dynamically in response to environmental stimuli in other instances. Epigenetic mechanisms include DNA methylation, chromatin remodeling by ATP-dependent remodelers or histone modifications, nuclear positioning, histone variant incorporation, and regulation by noncoding RNAs. These epigenetic mechanisms alter the chromatin structure and modulate the transcriptional potential of eukaryotic cells.

1.1.1 DNA methylation

DNA methylation is a well-studied epigenetic modification known to be involved in many biological processes. When first discovered, the primary biological role of DNA methylation was proposed to be a defense mechanism in higher eukaryotes to protect their genome integrity against viral invasion and the propagation of endogenous selfish DNA elements such as transposons (Yoder *et al*., 1997; Zilberman, 2008). Further reports have provided evidence that DNA methylation is also involved in gene-expression control during development and in response to environmental cues (Bird, 2002; Zhang *et al*., 2006; Zilberman *et al*., 2007).

Arabidopsis DNA is methylated on cytosine residues in all DNA contexts (CG, CHG, and CHH, where H represents A, T, or C). CG methylation is the most common modification and is mainly catalyzed by DNA METHYLTRANSFERASE 1 (MET1). MET1 is recruited to the DNA replication site and replicates the CG methylation pattern in a semi-conservative manner (Finnegan & Kovac, 2000; Lindroth *et al*., 2001). In addition to MET1, VARIANT IN METHYLATION 1 (VIM1; Woo *et al*., 2008), DECREASE IN DNA METHYLATION 1 (DDM1), and the histone deacetylase HDA6 are also known to control CG methylation (Chan *et al*., 2005). CG methylation of promoters and heterochromatin usually leads to transcriptional silencing and gene repression. On the other hand, CG methylation in gene bodies, which occurs in the transcribed regions of the gene away from the 3' and 5'end, is involved in gene activation (Coleman-Derr & Zilberman, 2012). Gene body methylation is also considered to prevent aberrant transcription from cryptic promoters within genes (Seisenberger *et al*., 2013) or influence the responsiveness of genes to internal or external cues (Cantone & Fisher, 2013).

CHG methylation is mediated by the plant-specific CHROMOMETHYLASE 2 (CMT2) and CMT3 and maintained by a feedback loop involving histone H3 lysine 9 dimethylation (H3K9me2; Johnson *et al*., 2007). *De novo* methylation is mainly catalyzed by DOMAINS REARRANGED METHYLTRANSFERASE 1 (DRM1) and DRM2 with some contribution from CMT3 through RNA-directed DNA methylation (RdDM) pathway. DRM1 and DRM2 are targeted to *de novo* DNAmethylation sites by small interfering RNAs (siRNAs) generated by RdDM pathway.

An important feature of DNA methylation is the crosstalk to other epigenetic modifications such as covalent histone modifications. For instance, methylated cytosines can be recognized by methyl CpG binding-domain (MBD) proteins which further recruit histone deacetylases or methyltransferases to regulate target gene expression (Fraga *et al*., 2003; Rauch *et al*., 2005).

DNA methylation is reversible. The methylated state of DNA might be changed in response to developmental or environmental stimuli. Reduction in cytosine methylation can occur either passively by being replaced with unmethylated cytosines following rounds of DNA replication or actively through the action of enzymes with DNA glycosylase activity. In Arabidopsis, active DNA demethylation is achieved by four DNA glycosylases, DEMETER (DME), DEMETER-LIKE 2 (DML2), DML3, and REPRESSOR OF SILENCING 1 (ROS1). These DNA glycosylases actively remove 5-methylcytosine from the DNA in the absence of DNA replication (Choi *et al*., 2002).

1.1.2 Chromatin remodeling

In contrast to the prokaryotic genome, the eukaryotic genome is compacted into a complex of macromolecules called chromatin. Chromatin is composed of DNA, proteins, and RNAs. The basic unit of chromatin is nucleosome. Nucleosomes are consisted of approximately 146 base pairs (bp) of DNA wrapped around a nucleosome core with a 15-55 bp linker DNA connecting the nucleosome core particles (Luger *et al*., 1997). The nucleosome core is consisted of two molecules of each histone proteins H2A, H2B, H3, and H4 forming a histone octamer. The core histones are tightly packed into a globular structure, whereas their amino-terminal tails are extended from the globular core region. These amino terminal tails are accessible to various histone modifying enzymes. Besides core histone proteins, nucleosomes contain an additional histone referred histone H1. H1 interacts with DNA and nucleosomes to compact chromatin into higher-order structures. Nucleosome positioning along the DNA is determined by DNA sequence itself and the presence or nature of proteins bound to the DNA.

The chromatin can be divided into two distinct functional states in non-dividing cells: euchromatin or heterochromatin. Euchromatin is the region in which active genes are abundant. The conformation of euchromatin is ‘open’ due to relaxed nucleosomal arrangement. It is less condensed and more accessible to RNA polymerase and transcription factors.

On the other hand, heterochromatin is the region where DNA is tightly packaged and condensed. This ‘closed’ conformation makes it difficult for transcription factors or chromatin-associated proteins to reach the DNA template. Therefore, genomic regions within heterochromatin consist transcriptionally

inactive repressed genes and repetitive sequences.

The assembly and compaction of chromatin are regulated by several mechanisms. These involve mechanisms by ATP-dependent chromatin remodelers that can reposition nucleosomes, the replication-independent incorporation of histone variants, and covalent histone-modifying complexes catalyzing the addition or removal of various chemical groups on histones. These chromatin remodelers, together with other dynamic epigenetic modifications, balance, crosstalk, and influence each other's action to control the ON/OFF switch of target gene expression.

1.1.2.1 ATP-dependent remodeling and incorporation of histone variants

Control of gene expression by nucleosome positioning is achieved through ATP-dependent chromatin remodeling complexes. ATP-dependent chromatin remodeling complexes contain the ATPase subunit. They gain energy from ATP hydrolysis to induce conformational changes in the histone-DNA interaction or displace the histone octamer from the DNA. This causes sliding, reconstruction, or ejection of the nucleosome, and leaves nucleosome-free regions of DNA which facilitate the exchange of histone variants or enhance the chromatin accessibility for the RNA polymerase II and transcription factors.

In addition, chromatin structure can also be modified by replacing canonical histones with histone variants. Histone variants share structural and amino-acid sequence similarities to canonical core histones. Chromatin immunoprecipitation (ChIP) analyses using specific antibodies revealed that H2A.Z, a histone variant highly conserved among eukaryotes, is enriched in the

gene body of transcriptionally variable genes (Raisner *et al*., 2005). Although the incorporation of H2A.Z does not directly correlate with transcriptional activation, the instability of H2A.Z containing nucleosome facilitates the nucleosome removal in gene bodies and maintains region of chromatin poised to a transcriptionally competent state in order to respond rapidly to intracellular or extracellular cues (Taiko *et al*., 2013).

1.1.2.2 Histone modification

The amino terminal (N-terminal) tails of histones are loosely extended from the core histones and subjected to different combination of covalent modifications. These modifications include acetylation, methylation, phosphorylation, ADP ribosylation, ubiquitination, and sumoylation. Most post-translational modifications of histones are reversible, and enzymes referred to as 'writers' and 'erasers' are involved in the addition and removal of these modifications, respectively. These enzymes usually exist as members of multi-subunit complexes and modify specific residues of target histones.

Histone modification can directly affect the chromatin compaction by modulating histone-DNA interactions. In addition, the modification itself can also serve as a binding platform for other proteins to be recruited to the local chromatin. Proteins often referred to as 'readers' recognize the modifications and are recruited through their specific domains. For instance, acetylation is recognized by the bromodomain-containing proteins and methylation is recognized by the PHD, chromo, WD40, Tudor, or MBT domain-containing proteins. Importantly, these reader proteins can recruit other 'effector' proteins. The effector proteins can be

chromatin architectural proteins, additional chromatin remodelers, or machineries that are directly involved in DNA metabolism. Therefore, regulation of gene expression through histone modification is basically achieved through several steps which can occur consecutively or simultaneously; setting the modification by the writers and erasers, recognizing the message by the readers, and finally triggering action by the effectors to determine the final outcome of the modification.

Until today, hundreds of different histone modifications have been described. The complexity of these modifications rises with the fact that it is difficult to predict the outcome of a single histone mark without understanding the combinatorial co-occurrence with other marks. This concept is generally referred to as the 'histone-code hypothesis' (Strahl & Allis, 2000). According to this notion, various histone modifications at one gene can interact and make crosstalk with other modifications to constitute the code. There are several mechanisms of crosstalk among histone modifications. In some cases, the initial modification of one residue can trigger the activity of the adjacent residue. In other cases, the modification can create a binding site and anchor another histone modification complex to the nearby nucleosome. Modifications of nearby residues can also enhance or prevent the recognition of the substrate.

Recent studies using genome-wide profiling approaches helped us to better investigate the crosstalk among various histone modifications. As hypothesized, those results have demonstrated that histone modifications change dynamically, and multiple modifications make crosstalk simultaneously. Moreover, multiple studies have revealed that some regions of the genome are enriched with modifications that are associated with both repression (i.e. H3K27me3 mediated by

the Polycomb Group (PcG) proteins) and activation marks (i.e. H3K4me3 mediated by the Trithorax Group (TrxG) proteins), making the process even more complicated. This signature is referred to as 'bivalent'. The bivalent chromatin marks are usually present in genes involved in making lineage-fate decisions. The active and repressive histone marks suppress the expression of target genes while at the same time 'poise' such genes for efficient induction on subsequent activation signals.

Together, regulation of gene expression by histone modification is a complex yet elaborate mechanism that is evolutionarily conserved and shared by most eukaryotes. The pattern of distribution, the timing when the modification is set, and the balance between different modifications account for the readout of the histone code.

1.1.2.3 Histone acetylation and deacetylation

In general, histone acetylation is enriched within euchromatin. Acetylation of lysine within the N-terminal histone tails is known to alter the histone-DNA interaction. The negative charge of the acetyl group (CH_3COO^-) neutralizes the positive charges of histones, reducing their affinity to negatively charged DNA. This causes loosening of the interaction between histone and DNA and renders DNA more accessible to the transcriptional machinery including general transcription factors, sequence-specific DNA-binding activators, and non-DNA-binding transcription coactivators. The acetylated histones also generate binding sites for acetyl lysine-binding bromodomain containing proteins to spread the modification or recruit other effector proteins (Hassan *et al*., 2002).

Histone acetylation is catalyzed by histone acetyltransferases (HATs). HATs transfer the acetyl group from acetyl-CoA to the NH_3^+ groups of lysine residues to form ε-N-acetyl lysine. HATs are traditionally grouped into two classes according to their subcellular localizations. Type-A HATs are located in the nucleus, and many of them contain the bromodomain. They are involved in the regulation of gene expression and act as transcriptional coactivators. Type-B HATs are located in the cytoplasm. Type-B HATs lack the bromodomain and recognize unacetylated free histones prior to their assembly into nucleosomes.

Type-A HATs are further categorized into four families based on their functional analogy and sequence homology of their catalytic domains. These include the GNAT (Gcn5-related N-acetyltransferase), MYST (MOZ, Ybt2, Sas2, Tip60-like), p300/CBP, and $TAF_{II}250$ families. Mammals have an extra group of HATs which includes the nuclear hormone-related STEROID RECEPTOR ACTIVATOR 1 (SRC1) and STEROID RECEPTOR ACTIVATOR 3 (SRC3) (Sterner & Berger, 2000). This group is not present in plants, fungi, or lower animals. GNAT, MYST, and p300/CBP HATs are co-activators that are involved in gene activation during conditional gene induction or enhancer-dependent activation. TAFII250 families are subunits of transcription factor II D (TFIID) and are components of the transcription machinery required for pre-mRNA transcription by RNA polymerase II (Mizzen *et al*., 1996).

Members of the HAT families are well conserved in Arabidopsis (Table 1). Mutation analyses have shown that many HATs play pivotal roles during various aspects of the plant life cycle. For instance, mutations in HAG1, the homolog of GENERAL CONTROL NON-DEREPRESSIBLE5 (GCN5), show pleiotropic

phenotypes such as reduced chlorophyll accumulation, defects in light response, dwarfism, loss of apical dominance, serrated leaves, abnormal root morphology, aberrant meristem function, abnormal trichome distribution, abnormal floral organ identity, and infertility. Further analyses have shown that HAG1 is involved in cold tolerance, floral development, embryonic cell-fate patterning, and light responsiveness (Benhamed *et al*., 2006; Bertrand *et al*., 2003; Long *et al*., 2006; Stockinger *et al*., 2001; Vlachonasios *et al*., 2003).

HAF2, one of the two TAFII250 homologs in Arabidopsis, is involved in the activation of light-induced genes (Benhamed *et al*., 2006; Bertrand *et al*., 2005). HAC1, HAC5, and HAC12 of the CBP family have been shown to be involved in regulating flowering time (Han *et al*., 2007) and ethylene signaling pathway (Li *et al*., 2014).

Histone acetylation is a reversible modification. The acetyl groups transferred to histone lysine residues by HATs are removed by histone deacetylases (HDACs). Because the function of HATs and HDACs are antagonistic, they were long considered to be found on different states of the chromatin; HATs in open chromatin and HDACs in closed or inactive chromatin. However, genome-wide mapping analysis of HATs and HDACs demonstrated that this is actually not the case. Surprisingly, HDACs are not only bound to silent genes but are enriched with HATs at actively transcribed genes (Wang *et al*., 2009). This indicates that the role of HDACs is not restricted to deacetylating histones at inactive genes. The larger role of HDACs is actually in actively transcribed or primed genes. The association of HDACs to HAT-associated active genes allows HDACs to reset chromatin enriched with acetyl groups that are added by HATs during transcription. The

resetting of chromatin state can prevent cryptic initiation of unwanted transcription. HDACs are also transiently associated with primed genes. HDACs bind to poised chromatin marked by H3K4me3 and remove the acetyl groups added by transient HAT activity. This allows the dynamic cycling of acetylation and deacetylation to poise primed genes for future action.

In Arabidopsis, there are three major families of histone deacetylases. These include the REDUCED POTASSIUM DEFICIENCY 3 (RPD3) family, the plant specific HD-TUINS (HDT) family, and the SIRTUINS (SRT) family that are homologous to the yeast NAD-dependent enzyme SILENT INFORMATION REGULATOR 2 (SIR2) (Pandey *et al*., 2002). Members of the RPD3 family are known to play diverse roles at various aspects of the plant life cycle including seed development, hypocotyl growth, flowering, root hair development, light signaling, leaf morphogenesis, stress responses, and circadian regulation (Georgieva *et al*., 1991; Perrella *et al*., 2013, Tanaka *et al*., 2008; Choi *et al*., 2012; To *et al*., 2011; Tessadori *et al*., 2011; Kang *et al*., 2015; Wang *et al*., 2013; Liu *et al*., 2013). Members of the HDT family are also known to affect leaf morphogenesis, salt-stress responses, and seed dormancy and germination (Kidner & Martienssen, 2004; Ueno *et al*., 2007; Yano *et al*., 2013; Luo *et al*., 2012; Colville *et al*., 2011). Although less is revealed about the role of SRT family HDACs, studies using mutants of the SRT family genes have reported their role during basal defense to pathogen and mitochondrial energy metabolism (Wang *et al*., 2010; König *et al*., 2014).

1.1.3 Noncoding RNA-mediated silencing

Genome-wide transcriptome analyses have demonstrated that more than 90% of the eukaryotic genomes are transcribed. However, only a small proportion (1-2%) of the transcribed genes encodes proteins (Wilhelm *et al*. 2008, van Bakel *et al*., 2010; Birney *et al*. 2007). This indicates that the larger proportion of the eukaryotic genome produces RNA molecules that have no protein coding potential. Apart from the housekeeping, non-protein coding RNAs such as rRNAs, tRNAs, small nuclear RNAs (snRNAs), and small nucleolar RNAs (snoRNAs), there are groups of RNAs that are transcribed from DNA but are not translated into proteins. These RNAs are collectively called as noncoding RNAs (ncRNAs).

NcRNAs can be classified into two groups based on their size; short and long. Short ncRNAs are less than 200 nucleotides (nt) long (usually less than 40 nt long) and long ncRNAs (lncRNAs) vary in length from 200 nucleotides to dozens of kilobases (kb). Both short and long ncRNAs are generally transcribed from intergenic regions or as antisense strands of protein-coding genes or pseudogenes and are involved in the epigenetic regulation of gene expression at the transcriptional and post-transcriptional level.

1.1.3.1 Small RNAs

In Arabidopsis, small RNAs are known to play various roles in gene regulation. There are several types of small RNA distinguishable from one another based on how they are generated and act. Among the many types of small RNAs, microRNAs (miRNAs) and short-interfering RNAs (siRNAs) are the most extensively studied. Both miRNAs and siRNAs are derived from the action of

dicer-like endonucleases. MiRNAs are generated from a single stranded mRNA that forms a hairpin structure. Mature miRNAs regulate target mRNAs by binding to their complementary target mRNA sequences and cleaving the mRNAs or inhibiting their translation. On the other hand, siRNAs are formed by the duplex of two RNA strands generated by the activity of the RNA-dependent RNA polymerase. One of their roles is to trigger and maintain DNA methylation and histone methylation, leading to the formation of heterochromatin.

1.1.3.2 LncRNAs

Long noncoding RNAs (lncRNaS) are transcribed from intergenic regions, introns, or protein-coding regions in either sense or antisense direction relative to their neighboring protein-coding transcripts. In Arabidopsis, few yet novel lncRNAs have been identified through tilling DNA microarray, genome-wide transcriptome studies, or full-length targeted cDNA sequencing methods. Functional characterizations have revealed that lncRNAs act as *cis*- or *trans*-regulators and interact with chromatin-modifying complexes to modulate the transcriptional activity of its target genes.

Well characterized function of lncRNA comes from a recent study of the regulation of *FLOWERING LOCUS C* (*FLC*) during vernalization (Heo & Sung, 2011). In Arabidopsis, the floral repressor FLC is one of the key factors determining the time to flower. After a sufficient period of winder cold known as the vernalization period, the transcription of *FLC* is epigenetically repressed allowing plants to acquire the competence to flower in the coming spring. The epigenetic repression of *FLC* is catalyzed by the CURLY LEAF (CLF) methyl

transferase-containing Polycomb Repressive Complex 2 (PRC2) mediating H3K27me3 during vernalization. PRC2 recruitment to *FLC* chromatin involves the action of the lncRNA named COLD ASSISTED INTRONIC NONCODING RNA (COLDAIR). COLDAIR is transcribed from an FLC intron, interacts directly with CLF, and recruits the CLF-containing PRC2 to *FLC* chromatin for silencing (Heo & Sung, 2011). Besides COLDAIR, *FLC* encodes another lncRNA named COOLAIR. COOLAIR is an antisense transcript transcribed from the downstream of the poly-A addition site. COOLAIR levels increase during vernalization prior to the decrease of *FLC* mRNA abundance (Swiezewski *et al*., 2009).

Studies from other eukaryotes provide evidence that the action of lncRNAs is deeply involved yet not restricted to the PRC2. Besides COLDAIR, several reports have revealed that a number of lncRNAs have been co-purified with various types of chromatin-modifying complexes (Tsai *et al*., 2010). This indicates that lncRNAs are likely to interact with various enzymes with different function and play diverse roles in the regulation of eukaryotic gene expression.

1.2 Plant life cycle

1.2.1 The life cycle of Arabidopsis

Arabidopsis thaliana is a model organism widely used for basic research in plant molecular and cellular biology. As a member of the *Brassicaceae* family, Arabidopsis has a relatively small genome and was the first plant to be sequenced. Arabidopsis has a short life span lasting about 6 weeks from germination to seed maturation. It is small in size but produces bulk seeds, which make it easy to cultivate in restricted space. Mutants of genes of interest and various transgenic lines can be generated easily using *Agrobacterium tumefaciens*-mediated transformation. These advantages make Arabidopsis a suitable model organism for studying plant molecular biology.

As in most flowering plants, the life cycle of Arabidopsis progresses through several phase transitions during development. After germination, young juvenile leaves are formed from the first primordia. Following the formation of juvenile leaves, adult leaves are formed. The juvenile-to-adult transition is referred to as vegetative phase change. After vegetative phase change, plants undergo through floral transition. During floral transition, the primary inflorescence grows and gives rise to secondary inflorescences. Finally, the plant progresses through the final phase of its life cycle; the meristem identity transition in which flowers are formed at last.

In the past, plant biologists have noticed several phase-specific traits that can serve as markers for each developmental transition. These include pattern, size

and morphology of leaves, branching patterns, and other bimodal traits. Recent studies on mutants and genetic analyses have provided molecular evidence for factors determining the transition from one phase to another. These evidences have proven that transitions between phases are controlled by distinct yet overlapping genetic circuits that integrate endogenous and environmental cues. By coordinating exogenous and intrinsic cues, plants are able to control the rate and the duration of each transition to ensure maximum reproductive success.

1.2.2 Vegetative transition

Among the distinct phases, vegetative transition is important during the life cycle of plants because it is the period when young plants grow to an adult. Throughout this transition, plants become fit and prepared to acquire the competence to flower when environmental conditions are favorable. In Arabidopsis, vegetative phase change can be distinguished by several phenotypical traits. The production of trichomes on the abaxial leaf surface, decrease in cell size, and increase in length/width (L/W) ratio of the leaf blades are all phenotypic markers of the vegetative-phase change.

Recent studies using various mutants and overexpressors revealed that the vegetative transition is under complex genetic control. These genetic pathways control the onset and duration of the vegetative transition and finally converge into a complex network leading to the activation of the next phase, the floral transition.

1.2.3 MiR156-*SPL* module

In Arabidopsis, the master regulator that controls the juvenile-to-adult transition is miR156, one of the most highly conserved miRNAs in the plant kingdom (Axtell & Bowman, 2008). The overexpression of miR156 prolongs the expression of juvenile traits and leads to moderately delayed floral transition. Contrarily, sequestration of miR156 activity by the overexpression of miR156 target mimicry, MIM156, accelerates the expression of adult traits.

MiR156 is expressed highly during juvenile phase. Its expression decreases gradually as the plants proceed through vegetative-phase change. A recent report has shown that the miR156 repression during the vegetative-phase change is mediated by signals produced in leaf primordia (Yang *et al*., 2011). Another report demonstrated that sugars act upstream of miR156 to repress its expression at the transcriptional and post-transcriptional level (Yu *et al*., 2013). Gradual increase in sugars after seed germination may serve as an endogenous cue for repressing the expression of miR156 and, thus, promotes vegetative transition. However, despite its importance, the precise molecular mechanism underlying the decline of miR156 expression during the vegetative transition remains unknown.

MiR156 targets 10 members of the *SQUAMOSA PROMOTER BINDING PROTEIN-LIKE* (*SPL*) family genes to repress their action in a post-transcriptional manner (Rhoades *et al*., 2002). The *SPL* family genes can be grouped into four clades: *SPL3/SPL4/SPL5*, *SPL2/SPL10/SPL11*, *SPL9/SPL15*, and *SPL6/SPL13* (Guo *et al*., 2008). Phenotypic assays of multiple mutants and overexpression lines of *SPL* family genes show that they display high functional redundancy, and several are involved in various phases in plant development. For instance, single

mutation of *SPL9* and *SPL15* show mild phenotypes. However, *spl9 spl15* double mutants display severe phenotypes including the delay in abaxial trichome production and shortened plastochron (time that elapses between the formation of primordia). Overexpression of either *SPL9* or *SPL15* increases the length of plastochron and accelerates vegetative-phase change and flowering (Wang *et al*., 2008). These demonstrate that genes act redundantly to promote the juvenile-to-adult phase transition and flowering. *SPL3*, *SPL4*, and *SPL5*, members of another clade of *SPL* family genes also act redundantly to control flowering and vegetative-phase change. Single mutations in *SPL3* display slight delay in abaxial trichome production, whereas overexpression of *SPL3*, *SPL4*, or *SPL5* accelerates abaxial trichome production and floral induction, indicating that SPL3, SPL4, and SPL5 act redundantly to promote the vegetative transition and flowering (Wu & Poethig, 2006).

Although the *SPL* family genes are implicated in the regulation of vegetative transition, they are also known to play roles during floral induction. SPL9 and its orthologue SPL10 are known to regulate flowering by directly activating the transcription of miR172. MiR172, in turn, represses the expression of APETALA2 (AP2)-like repressors of the central floral inducer, *FLOWERING LOCUS T* (*FT*) (Yamaguchi *et al*., 2009). SPL9 also controls flowering by promoting the transcription of the floral promoters, *FRUITFULL* (*FUL*), *SUPPRESSOR OF CONSTANS 1* (*SOC1*), and *AGAMOUS-LIKE 42* (*AGL42*) (Yamaguchi *et al*., 2009). SPL3 is reported to directly activate the transcription of the floral promoters, *FUL*, *APETALA 1* (*AP1*), and *LEAFY* (*LFY*) in a miR172- and FT-independent pathway during floral transition (Yamaguchi *et al*., 2009).

Therefore, at young juvenile stage, the high level of miR156 maintains juvenility and prevents precocious onset of adult traits and flower formation. However, as miR156 level declines throughout development, the *SPL* genes are released from the miR156-mediated repression, and their induction triggers the juvenile-to-adult transition. Because floral induction is at least in part dependent on the transition to the adult phase, the high level of *SPLs* in adult phase acts as licensing factors to flowering. Thus, SPLs act as factors connecting and coordinating the changes in the vegetative morphology with changes in reproductive potential (Wu *et al*., 2009).

1.3 Plant-cell pluripotency and *de novo* shoot regeneration

Plants are sessile organisms. While mobile organisms use strategies to fight or flee, plants must optimize their growth to the local environment where they germinated and cope with continuous environmental challenges throughout their life cycle. Plants have evolved to possess the ability to alter their development in response to environmental changes, in other words, to be plastic. The high 'plasticity' of plants allows them to respond to external cues in a permanent or nonpermanent manner and to adapt to their local environment. A second strategy that plants have adopted through evolution is their totipotent feature. The 'totipotency' of plants allows cell division to initiate from most tissues and to regenerate lost parts or even into a whole new plant.

The principle of plant-cell totipotency was first postulated in 1902, when Gottlieb Haberlandt proposed that single plant cells are able to "successfully cultivate artificial embryos from vegetative cells" under proper conditions (Haberlandt, 1902). More than five decades after the Haberlandt's proposal, a classical work of Skoog and Miller demonstrated that plant-cell totipotency and *de novo* organ regeneration could be achieved by modulating the ratio of two phytohormones: auxin and cytokinin (CK) (Skoog & Miller, 1957). This culture technique has been the guiding principle for researches in callus induction and *de novo* shoot regeneration and successfully applied to a wide range of plant species.

The reason for the wide adoption of the Skoog and Miller's method is probably due to its simplicity and easy modulation. Although numerous protocols

have been developed by different groups in the past decades, the fundamental principle underlying the process of *de novo* shoot regeneration has remained constant.

1.3.1 Step 1: Callus formation

The first step for *de novo* shoot regeneration *in vitro* is the induction of the intermediate growing cell mass referred to as 'callus'. Explants of cotyledon, hypocotyl, root, and petal are generally used for regeneration assays. Pieces of tissues are cut and the explants are transferred to an auxin-rich media referred to as the callus-induction media (CIM). Although several factors including age of the explants, light duration, and light intensity are known to influence the callus-formation rate, in general, incubation of root explants in CIM for a minimum of 4 days leads to callus formation (Che *et al*., 2007).

Because callus induction is a prerequisite for proper shoot regeneration, callus was considered a dedifferentiated form of somatic cells possessing totipotency for many decades. However, recent advances in microscopy and the development of specific cell-type markers have proven that callus is not a cluster of dedifferentiated cells but rather a well-organized cell mass (Atta *et al*.,2009). When placed in an auxin-rich media, the pericycle cells (in case of roots) or pericycle-like cells (in case of hypocotyls, cotyledons, and petals) begin to divide. After several round of cell division, by a yet undiscovered mechanism, the lateral root-meristem (LRM) developmental program becomes activated (Sugimoto *et al*., 2010). In concordance with these observations, transcriptome-profiling studies using initiating calli revealed that incubation of tissue explants in CIM causes massive change in gene expression. Notably, root-specific genes such as *WUSCHEL RELATED HOMEOBOX 5* (*WOX5*), *SHORT ROOT* (*SHR*), and *SCARECROW* (*SCR*) are highly expressed in the calli induced from not only root and hypocotyls but also aerial plant parts such as petals or cotyledons (Sugimoto *et al*., 2010). The

expression of J0121, the pericycle-specific marker, was increased in early stages of CIM incubation, indicating that the cell division of the pericycle cells is the initial step of callus formation (Che *et al*., 2007). Mutants of *ABERRANT LATERL ROOT FORMATION 4* (*ALF4*), which display phenotypes defective in lateral-root initiation, show severe defects in callus formation (Sugimoto *et al*., 2010). Therefore, callus formation is not a process in which differentiated cells revert their cellular state to an undifferentiated state, but rather a process in which explants transdifferentiate to a cell mass with ectopic activation of lateral-root developmental program.

The transformation of the pericycle and pericycle-like cells into a callus involves the activation of auxin homeostasis, signaling, and transport genes. For instance, the expression of *PIN-FORMED 1* (*PIN1*), an auxin efflux carrier responsible for polar auxin transport, is highly expressed during CIM incubation and is responsible for the reestablishment and distribution of auxin gradient in the callus (Ke *et al*., 2012). Expression of transcription factors such as LATERAL ORGAN BOUNDARIES DOMAIN (LBD), WRKY, and basic helix-loop helix (bHLH) proteins are also upregulated upon CIM incubation. Among these, the function of LBD16, LBD17, LBD18, and LBD28 are well studied. Ectopic overexpression of *LBD16*, *LBD17*, *LBD18*, or *LBD28* triggers callus formation in media without exogenous hormones, and their mutants show defects in lateral root formation and callus formation. *LBD* genes are also known to act as downstream targets of AUXIN RESPONSIVE FACTOR 7 (ARF7) and ARF19 in the regulation of lateral root initiation and callus formation. Therefore it is likely that the signal derived from the high auxin concentration in CIM is conveyed to ARF7 and

ARF19, which in turn induces the expression of *LBD* genes forming a molecular link connecting auxin signaling and callus formation (Fan *et al*., 2012).

Although auxin is a major player in callus formation, the CIM also contains cytokinin. Despite its low concentration, cytokinin is known to be essential for the maintenance of cell proliferation during callus formation. In planta, cytokinin is implicated during post-embryonic development where it acts as a repressor of lateral root organogenesis. The xylem-pole pericycle cells and the LR founder cells in the initiating primordia are known to be highly sensitive to cytokinin (Laplaze *et al*., 2007). Considering the fact that callus initiation involves the initiation of lateral root program, the role of cytokinin in the repression of lateral root initiation is likely to be conserved and applicable in the callus system.

ARABIDOPSIS RESPONSE REGULATOR (ARR) transcription factors are the final targets of the multistep phosphorelay in the cytokinin signaling pathway. ARR transcription factors can be classified as type-A (ARR3-ARR9, ARR15-ARR17, ARR22, and ARR24) or type-B (ARR1-2, ARR10-14, ARR18-21, and ARR23) based on their domain structure, phylogenetic analyses, and molecular function (D'Agostino & Kieber, 1999; D'Agostino *et al*., 2000). Upon cytokinin signal, type-B ARRs directly promote the transcription of cytokinin-responsive genes and type-A ARRs. In turn, type-A ARRs interfere the activity of type-B ARRs forming a negative feedback loop.

Several members of the type-B ARRs are involved in callus formation. Mutations in *ARR1* and *ARR21* display ectopic callus induction in the absence of exogenous auxin and cytokinin. Moreover, *arr1* mutant calli also produce less shoot, whereas *ARR1* overexpressors show increased shoot regeneration efficiency,

demonstrating its additional function during shoot regeneration (Sakai *et al*., 2001; Tajima *et al*., 2004).

The most significant role of type-B ARRs during callus formation is to connect the pathway linking cytokinin signaling to cell division during callus maintenance. The presumable target of type-B ARRs in regulating cell division during callus formation is *CYCLIN D3* (*CYCD3*) (Riou-Khamlichi *et al*., 1999). CYCD3 is the rate-limiting factor for the transition of the G1/S boundary and is highly induced during callus formation. Overexpression of *CYCD3* causes formation of green callus without exogenous cytokinin. Furthermore, mutation in the three genes encoding CYCD3 (*CYCD3;1*, *CYCD3;2*, and *CYCD3;3*) show that CYCD3 is a potent downstream effector of the cytokinin signaling that regulates the population of proliferating cells and the duration of the mitotic cycle. Whether the type-B ARRs directly activate *CYCD3* is yet to be revealed.

Some other members of the cell cycle-related genes that function in the downstream of the cytokinin-mediated callus formation are *ENHANCED SHOOT REGENERATION 1* (*ESR1*) and its homolog *ESR2*. ESR genes encode APETALLA 2 (AP2)/ETHYLENE RESPONSIVE FACTOR (ERF) transcription factors and are implicated in the by cytokinin signaling pathway (Banno *et al*., 2001; Ikeda *et al*., 2006). Overexpression of *ESR1* and *ESR2* causes callus formation in the absence of auxin and cytokinin (Banno *et al*., 2001; Ikeda *et al*., 2006). ESR2 promotes the expression of *CYCLIN D 1;1* (*CYCD1;1*) and *OBF BINDING PROTEIN 1* (*OBP1*), a DOF transcription factor, in a direct manner. OBP1 in turn, promotes the expression of various cell cycle-related genes including the S phase transcription factor genes *DOF2;3* and *CYCD3;3*. This leads to the

shortening of the G1 phase duration and progression of the cell cycle (Skirycz *et al*., 2008).

In contrast to the roles of type-B ARRs during callus formation, less has been studied on the role of type-A ARRs. One member of the type-A ARRs, ARR5, is known to be differentially expressed during CIM. In roots, *ARR5* is expressed in the root stele, meristem, and lateral root-progenitor cells. When root explants are transferred to CIM, *ARR5* is expressed near the vasculature of the root explants and the proliferating callus cells, and its expression is further expanded to the whole callus, implying its potential role during callus formation (Gordon *et al*., 2007).

In addition to the hormone responsive and cell cycle-related genes, a few shoot-meristem genes are also upregulated in CIM. Recent study using CUP-SHAPED COTYLEDONS 1 (CUC1)-enhancer trap line has shown that the upregulation of *CUC1* is linked to callus formation (Cary *et al*., 2002). Further report using *pCUC2::3xVENUS-N7* has shown that *CUC2*, a gene with partial functional redundancy with *CUC1*, is also induced in CIM (Gordon *et al*., 2007). Conversely, other shoot meristem factors such as *WUSCHEL* (*WUS*), *SHOOT MERISTEMLESS* (*STM*), and *CLAVATA 3* (*CLV3*) are not expressed in the callus. These factors, together with CUC1, CUC2, and the auxin gradient formed by PIN1, play a major role in the acquisition of progenitor identity and new shoot formation during the final step of the *de novo* shoot regeneration process; the stage of actual shoot formation.

1.3.2 Step 2. *De novo* shoot formation

The final step of the *de novo* shoot formation process is achieved by transferring the CIM-incubated explants to the cytokinin-rich shoot induction media (SIM). In contrast to the process of callus formation, the incubation in SIM does not involve massive changes in genome-wide gene expression (Che *et al*., 2002, 2006; Xu *et al*., 2012). However, the differential expression pattern of several genes indicates that this stage is also regulated by genetic and epigenetic mechanisms.

The most notable change of this step is the down regulation of root meristem genes and the upregulation of shoot meristem genes. Upon transfer to SIM, *WUS* and *CUC2* are differentially expressed (Cary *et al*., 2002; Gordon *et al*., 2007). Interestingly, *CUC2* expression is reduced within 1-2 days after transfer to SIM, however, after 1 week in SIM, its expression becomes reactivated in clusters of cells. These cells marked by the expression of *CUC2* together with *WUS* act as shoot progenitor cells (Gordon *et al*., 2007; Duclercq *et al*., 2011). Afterward, genes known to be expressed in the mature shoot meristem such as *STM*, *REVOLUTA* (*REV*), *FILAMENTOUS FLOWER* (*FIL*), *ARABIDOPSIS THALIANA MERISTEM L1 LAYER* (*AtML1*), *PIN1*, and *CLV3* become locally expressed, leading to the formation of the new shoot (Gordon *et al*., 2007).

1.3.3 Molecular link between callus induction and *de novo* shoot regeneration

Recently, three PLETHORA (PLT)-family members, PLT3, PLT5, and PLT7 were reported to act as key regulators in linking callus formation and *de novo* shoot regeneration (Kareem *et al*., 2015). PLT3, PLT5, and PLT7 regulate *de novo* shoot regeneration by controlling the expression of different targets at two distinct steps. In the first step, PLT3, PLT5, and PLT7 activate the root meristem regulators, *PLT1* and *PLT2*. This allows callus cells to acquire the competence necessary for further *de novo* shoot regeneration. In the next step, PLT3, PLT5, and PLT7 regulate a different target, *CUC2*. Introduction of *CUC2* and *PLT1* to the *plt3 plt5 plt7* triple mutant restores its shoot-formation defect. This indicates that PLT3, PLT5, and PLT7 activate different targets at different steps; root meristem-maintenance genes for proper callus induction in the earlier step and shoot regulators to achieve *de novo* shoot regeneration in the later step.

1.3.4 Epigenetic control of callus formation and *de novo* shoot regeneration

According to the hypothesis proposed by Birnbaum and Alvarado, 'almost all regeneration phenomena in one kingdom have a counterpart in the other, despite the diverse array of regeneration mechanisms' (Birnbaum & Alvarado, 2008). One of such convergent mechanisms evolutionarily shared from mammals to plants is the epigenetic mechanism controlling cellular fate. Various epigenetic modifications are reported to play pivotal regulatory roles underlying cellular differentiation, dedifferentiation, and development. In mammals, fully differentiated cells are generally enriched with condensed chromatin state with stable gene expression, whereas the chromatin state of pluripotent cells is open and possesses dynamic gene expression profiles (Gaspar-Maia *et al*., 2011). Several studies in Arabidopsis suggest that, as in mammals, the chromatin state of plants is also differentially regulated depending on cellular state (Zhao *et al*., 2001; Verdeil *et al*., 2007). Analysis using mutants and overexpressors have revealed that many epigenetic factors are deeply involved in the acquisition of pluripotency and cellular differentiation in plants (Berdasco *et al*., 2008; Li *et al*., 2011; Anzola *et al*., 2010; Farrona *et al*., 2008; Bouyer *et al*., 2011; Bratzel *et al*., 2010; Ogas *et al*., 1997, 1999; Furuta *et al*., 2011; Zhang *et al*., 2008, 2012; Qiao *et al*., 2012; Peaucelle *et al*., 2007).

1.3.4.1 DNA methylation

DNA methylation is an important epigenetic mechanism required for the establishment and maintenance of callus pluripotency and shoot regeneration. Several genes including *MAPK12*, *GSTU1*, and *BXL1* transcriptionally silenced in

callus cells are heavily methylated. The promoters of these genes are hypermethylated primarily at CG sites by MET1 and DRM2 and are also associated with histone hypoacetylation (Berdasco *et al*., 2008).

DNA methylation is involved in the process of *de novo* shoot regeneration. Mutations in *MET1* resulted in increased expression of *WUS* and enhanced *de novo* shoot regeneration efficiency (Li *et al*., 2011). Bisulfite sequencing experiments revealed that the level of DNA methylation change dynamically at regions of the *WUS* locus during shoot regeneration. This methylation pattern is lost in the *met1* mutants, indicating that DNA methylation catalyzed by MET1 regulates *de novo* shoot regeneration in part by modulating *WUS* expression (Li *et al*., 2011). Another study reported the importance of CHG methylation and the role of CMT3 during *de novo* shoot regeneration (Shemer *et al*., 2015). Mutations in *CMT3* allow regeneration of new shoots even when root explants were placed directly on SIM without the pre-incubation step in CIM. In wild type, pre-incubation on CIM is required for the induction of *WUS* in SIM. However, in the *cmt3* mutants, this pre-incubation period was not necessary for *WUS* induction. Furthermore, CHG methylation at the *WUS* promoter is significantly reduced in the *cmt3* mutant. These results suggest that the reduction of CHG methylation at the *WUS* locus in *cmt3* increases the potency to regenerate new shoots, implicating the role for CHG methylation in the acquisition of competency for shoot regeneration (Shemer *et al*., 2015). Other report has noted that genomic regions of genes besides *WUS*, such as genes involved in auxin signaling including *INDOLE-3-ACETIC ACID INDUCIBLE 18* (*IAA18*), *ARF3*, and *ARF4* possess differential methylation profile in callus cells and cells undergoing shoot regeneration (Li *et al*., 2011). Expression

of these genes were downregulated in callus in accordance to their methylation profile. Therefore, dynamic DNA methylation modulates callus formation and *de novo* shoot regeneration by regulating the expression of subset of genes including *WUS* and components of the auxin-signaling pathway.

1.3.4.2 Histone modification

Dynamic histone modification is another epigenetic mechanism modulating callus formation and *de novo* shoot regeneration. Various histone-modifying factors are known to be involved in this process.

The transcriptional adaptor PROPORZ 1 (PRZ1) is known to interact with the histone acetyltransferase GCN5/HAG1 to control the expression of specific target genes by promoting H3K9 and H3K14 acetylation (Anzola *et al*, 2010; Servet *et al*, 2010; Cohen *et al*, 2009; Kornet & Scheres, 2009; Benhamed *et al*, 2006; Benhamed *et al*, 2008; Bertrand *et al*, 2003; Sieberer *et al*, 2003; Vlachonasios *et al*, 2003). Mutations in *PRZ1* display hyper-proliferative growth phenotype and ectopic callus formation in the condition where lateral roots should be formed (Anzola *et al*., 2010; Sieberer *et al*., 2003). The role of PRZ1 is implicated in the control of cell cycle-regulatory genes, and it is thought to regulate the switch from cell division to cellular differentiation in response to auxin and cytokinin. One such target of PRZ1 is KIP-RELATED PROTEIN (KRP). *KRP* genes encode cyclin-dependent kinase (CDK) inhibitors and act as negative regulators of cell division. The transcript levels of several *KRP* genes (*KRP2*, *KRP3*, and *KRP7*) are reduced in the *prz1* mutants. Overexpression of *KRP7* partially rescues the over-proliferation phenotype of *prz1*. Moreover, *KRP*-

silencing lines phenocopy the over-proliferative phenotype in *pzr1*. PRZ1 directly binds to the promoter of *KRP* genes and catalyzes H3K9/H3K14 acetylation. Importantly, the expression and the acetylation at the *KRP* locus mediated by PRZ1 are decreased upon auxin treatment (Anzola *et al*., 2010). Therefore, PRZ1-mediated histone modification link auxin signaling and cell-cycle regulation and contributes to the formation of callus.

Other epigenetic factors that play roles during callus formation are the members of the Polycomb Group (PcG) complexes. The PcG protein complexes are evolutionally conserved from plants to animals. They form two important complexes, PRC1 and PRC2, which function sequentially to repress target genes. PRC2 modifies chromatin by tri-methylating H3K27. H3K27me3 acts as a mark to recruit PRC1, which contains a subunit that specifically binds to H3K27me3. PcG-mediated repression can confer a molecular memory to gene regulation (Farrona *et al*., 2008).

In Arabidopsis, loss of function mutants of the PRC1 and PRC2 components show severe phenotypes. For instance, *CLF* and *SWINGER* (*SWN*), or *EMBRYONIC FLOWER 2* (*EMF2*) and *VERNALIZATION 2* (*VRN2*) double mutants form ectopic callus after germination (Schubert *et al*., 2005; Chanvivattana *et al*., 2004). Mutations in *FERTILITZATION INDEPENDENT EMDOSPERM* (*FIE*), another component of PRC2, also lead to similar callus formation phenotypes (Bouyer *et al*., 2011). Mutations in the homologs of the mammalian PRC1, AtBMI1A and AtBMI1B, which are involved in the monoubiquitination of H2A, also display similar phenotypes to the mutants of the members of the PRC2 complex (Bratzel *et al*., 2010). These phenotypes include ectopic callus formation

at early stage and the derepression of embryonic traits in somatic cells. Furthermore, in the *atbmi1a atbmi1b* double mutants, expression of the embryonic regulators *LEAFY COLYLEDON 1* (*LEC1)*, *LEC2*, *AGAMOUS-LIKE 15* (*AGL15*), *FUSCA 3* (*FUS3*), the stem-cell regulators *BABYBOOM* (*BBM*), the shoot-meristem regulators *WUS* and *STM*, and the root-meristem regulator *WOX5* are elevated. This indicates that along with H3K27me3 catalyzed by the PRC2 complex, H2A monoubiquitination catalyzed by AtBMI1A/B is critical for the maintenance of cellular identity in plants. Taken together, members of the PRC1 and PRC2 play roles in the repression of embryonic and stem cell regulators and thus function as negative regulators in callus formation.

Another epigenetic factor that plays a role in callus formation is PICKLE (PKL). PKL, the CHROMODOMAIN-HELICASE-DNA BINDING 3 (CHD3) and CHD4-like chromatin remodeling factor, is also known to repress callus formation. Mutations in *PKL* cause the formation of ectopic callus right after germination (Ogas *et al*., 1997, 1999). PKL is indirectly related to the deposition of H3K27me3 at *LEC1* and *LEC2* loci in seedlings (Zhang *et al*., 2008, 2012). A different allele of *PKL* mutant called *CYTOKININ-HYPERSENSITIVE 2* (*CHK2*) also shows elevated response to exogenous cytokinin and produces green callus in response to low levels of cytokinin (Furuta *et al*., 2011). Gene expression analyses revealed that several genes related with photosynthesis, and cytokinin-regulated genes are affected in the mutant.

Other histone modifiers are also implicated to play roles during *de novo* shoot regeneration. Recent studies reported that dynamic histone modifications such as H3K4me3, H3K9me2, and H3K9Ac affect the expression of *WUS*

transcript during *de novo* shoot regeneration (Li *et al*., 2011). Loss of histone modifiers such as KRYPTONITE (KYP), an H3K9 methytransferase, JUMONJI 14 (JMJ14), an H3K4 demethylase, and HAC1, a histone acetyltransferase, show differential expression of *WUS* transcript and altered shoot regeneration efficiency (Li *et al*., 2011). Thus, various repressive and active marks written and erased by multiple histone modifiers modulate the differential expression of various genes for the maintenance of the pluripotency of callus and *de novo* shoot regeneration.

1.3.4.3 MiRNA-mediated regulation

There are several evidences supporting the role of miRNAs in the process of callus formation and *de novo* shoot regeneration. In Arabidopsis, a group of miRNAs are reported to be differentially expressed during callus formation and *de novo* shoot regeneration (Qiao *et al*., 2012). Among them, miR160 is the most profoundly studied. MiR160 is highly expressed in non-totipotent callus and its expression is reduced in totipotent callus or upon SIM incubation. Overexpression of miR160 causes reduced shoot-regeneration efficiency. MiR160 directs the repression of its target, *ARF10* which in turn affects the transcript levels of *CLV3*, *CUC1*, *CUC2*, and *WUS*. Other miRNAs such as miR165/166 are also known to be involved in the regulation of shoot-meristem maintenance (Jung and Par 2007).

The regenerative potential of plants decreases according to age; younger plants exhibit better shoot-regenerative potential compared to older plants. A previous report has shown that the age-dependency is due to the action of miR156 (Zhang *et al*., 2015). As its role in juvenile-to-adult transition, miR156 represses the action of *SPL9*-group genes during *de novo* shoot regeneration. In old plants,

SPL-transcript levels are high due to the decline of miR156 level. SPL9 protein binds directly to type-B *ARR* genes, inhibits their transcription, and impairs *de novo* shoot regeneration. Therefore, miR156 acts as a timer that governs the regenerative capacity of plants.

Although much is yet to be revealed, post-transcriptional regulation mediated by miRNAs is likely to act as an important mechanism for callus cells to establish and maintain pluripotency and to differentiate during *de novo* shoot regeneration.

Table 1-1 Histone acetyltransferases in *Arabidopsis thaliana*

Family	*Arabidopsis thaliana* protein	Gene ID	Homologous proteins
GNAT-like	HAG1 (AtGCN5)	At3g54610	hsPCAF, scGCN5
	HAG2	At5g56740	hsHAG509, scHAT1
	HAG3	At5g50320	hsHAG510, scELP3
MYST-like	HAM1 (HAG4)	At5g64610	hsTIP60, scESA1
	HAM2 (HAG5)	At5g09740	
CBP-like	HAC1	At1g79000	hsCBP
	HAC2	At1g67220	
	HAC4	At1g55970	
	HAC5	At3g12980	
	HAC12	At1g16710	
TAFII250-like	HAF1	At1g32750	hsTAFII 250, csTAFII 250

Chapter II

Epigenetic control of juvenile-to-adult phase transition by the Arabidopsis SAGA-like complex

---

This chapter was published as "Kim, J.Y., Oh, J.E., Noh, Y.S., Noh, B. (2015). Epigenetic control of juvenile-to-adult phase transition by the Arabidopsis SAGA-like complex. *Plant J* **83(3)**: 537-545"

2.1 Abstract

During growth and development, plants undergo a series of phase transitions from the juvenile-to-adult vegetative phase to the reproductive phase. In Arabidopsis, vegetative phase transitions and flowering are regulated by SQUAMOSA PROMOTER BINDING PROTEIN-LIKE (SPL) factors. *SPL* mRNAs are post-transcriptionally regulated by miR156 in an age-dependent manner; however, the role of other mechanisms in this process is not known. In this study, I demonstrate that the HAG1/GCN5- and PRZ1/ADA2b-containing SAGA-like histone acetyltransferase (HAT) complex directly controls the transcription of *SPLs* and determines the time for juvenile-to-adult phase transition. Thus, epigenetic control by the SAGA-like HAT complex determines the transcriptional output of *SPLs*, which might be a prerequisite for the subsequent post-transcriptional regulation by miR156. Importantly, this epigenetic control mechanism is also crucial for miR156-independent induction of *SPLs* and acceleration of phase transition by light and photoperiod or during post-embryonic growth.

2.2 Introduction

Higher plants pass through a series of morphologically and physiologically distinct developmental phases. Vegetative phase transition from a juvenile to an adult phase in Arabidopsis and maize is controlled by a master regulatory module made of conserved microRNAs of the miR156 family and their target transcription factors, SQUAMOSA PROMOTER BINDING PROTEIN LIKEs (SPLs). In Arabidopsis, miR156 levels, which are highest in seedlings, gradually decrease with age, resulting in a gradual increase in the transcript levels of target *SPLs* (Wang *et al*, 2009; Wu *et al*, 2009; Wu & Poethig, 2006). Besides vegetative phase transition, *SPLs* are also known to be critical factors for the transition from the vegetative to the reproductive phase especially in non-inductive short days (SD; Wang *et al*, 2009). Although miR156 appears to be a major regulator of SPL expression during the developmental time course, recent studies have provided evidence that the expression or activity of SPLs is also regulated in a miR156-indpendent manner in response to environmental cues or the phytohormone gibberellin (Jung *et al*, 2012; Yu *et al*, 2012; Wang *et al*, 2009).

General Control Nonrepressed 5 (GCN5) is a catalytic component of histone acetyltransferase (HAT) complexes that are structurally conserved in yeast, flies, and mammals, e.g., the Spt-Ada-Gcn5-Acetyltransferase (SAGA) complex. Generally, transcriptional activators recruit the SAGA complex to target loci. This leads to loss of chromatin compaction due to acetylating histones, thereby facilitating transcription initiation (Sterner *et al*, 1999; Nagy & Tora, 2007). In addition, the SAGA complex has also been shown to enhance progression of RNA

Polymerase II (PolII) during transcription elongation (Sansó *et al*, 2011; Govind *et al*, 2007).

In Arabidopsis, mutant studies of HAG1 (the Arabidopsis homolog of GCN5) and ADA2b/PROPORZ 1 (hereafter, PRZ1; an Arabidopsis homolog of ADA2) have shown that the Arabidopsis SAGA-like complex plays a critical role in development and responses to environmental cues or endogenous hormones (Anzola *et al*, 2010; Servet *et al*, 2010; Cohen *et al*, 2009; Kornet & Scheres, 2009; Benhamed *et al*, 2006; Benhamed *et al*, 2008; Bertrand *et al*, 2003; Sieberer *et al*, 2003; Vlachonasios *et al*, 2003). A microarray study revealed that ~5% of the genes tested were affected by *hag1* and *prz1* mutations (Vlachonasios *et al*, 2003), suggesting a limited target range of HAG1/PRZ1 in Arabidopsis. Although the effect of HAG1 and PRZ1 in gene expression has been addressed in these studies, their regulatory pathways, direct targets, and molecular mechanisms have yet to be fully elucidated.

Here, I show that HAG1 and PRZ1 play an essential role in the control of *SPL* genes for successful juvenile-to-adult phase transition. HAG1 and PRZ1 establish or maintain high histone acetylation levels at *SPLs* throughout vegetative development, and this allows for high transcriptional output of *SPLs* that is necessary for miR156-mediated fine-tuning. I further demonstrate that HAG1-mediated histone acetylation is crucial for miR156-independent induction of *SPLs* by environmental cues that accelerate phase transitions. Germination-specific targeting of HAG1 to *SPL3* is also required for miR156-independent induction and establishment of early *SPL3* expression in vegetative tissues.

2.3 Materials and methods

2.3.1 Plant materials and growth conditions

Plants were grown under 100 μmol m^{-2} s^{-1} cool white fluorescent lights at 22°C. Unless otherwise noted, plants were grown in long days (LD) with a 16 hr light and 8 hr dark photoperiod (16L/8D). Short day (SD) conditions included an 8L/16D photoperiod. *pSPL9::rSPL9* and *pSPL3::SPL3:GUS/pSPL3::rSPL3:GUS* were provided by Detlef Weigel (Max Planck Institute for Developmental Biology, Tübingen, Germany) and Scott Poethig (University of Pennsylvania, Philadelphia, USA), respectively. Leaf-shape analysis and abaxial trichome scoring were performed as previously described (Wu *et al*, 2009). Flowering time was measured as described (Han *et al*, 2007). *hag1-6* (SALK_150784), *hag1-7* (SALK_106557), *prz1-1* (CS9674), *ada2a-3* (SALK_150349), *hag2-2* (SALK_051832), *ham1-1* (SALK_027726), *ham2-1* (SALK_106046), *haf1-2* (SALK_116607) and *haf2-5* (SALK_105189) were obtained from TAIR (http://www.arabidopsis.org). *elo3-1* was provided by M. Van Lijsebettens.

Table 2-1 Details of the mutant lines used in the study

Gene family	Gene name	Locus	Stock name	Allele	Ecotype	Reference
GNAT	*HAG1*	At3g54610	SALK_150784	*hag1-6*	Col	Long *et al.*, (2006)
		At3g54610	SALK_106557	*hag1-7*	Col	This study
	HAG2	At5g56740	SALK_051832	*hag2-2*	Col	This study
	HAG3	At5g50320	*elo3-1*	*elo3-1*	L*er*	Nelissen *et al.*, (2005)
MYST	*HAM1*	At5g64610	SALK_027726	*ham1-1*	Col	Latrasse *et al.*, (2008)
	HAM2	At5g09740	SALK_106046	*ham2-1*	Col	Latrasse *et al.*, (2008)
				ham1-1 ham2-1	Col	This study
CBP	*HAC1*	At1g79000	SALK_070277	*hac1-2*	Col	Han *et al.*, (2007)
	HAC5	At3g12980	SALK_024278	*hac5-2*	Col	Han *et al.*, (2007)
				hac1-2 hac5-2	Col	Han *et al.*, (2007)
TAFII 250	*HAF1*	At1g32750	SALK_116607	*haf1-2*	Col	This study
	HAF2	At3g19040	SALK_105189	*haf2-5*	Col	This study
				haf1-2 haf5-2	Col	This study
ADA2	*ADA2a*	At3g07740	SALK_150349	*ada2a-3*	Col	Hark *et al.*, (2009)
	PZR1	At4g16420	CS9674	*prz1-1*	Col	Sieberer *et al.*, (2003)

2.3.2 Constructs and plant transformation

To generate *35S::FLAG:HAG1* and *35S::HAG1:YFP:HA* the full-length coding region of *HAG1* was amplified using HAG1 entry-F (5′-CACCATGGACTCTCACTCTTCCCACCT-3′) and HAG1 entry-R (5′-TTGAGATTTAGCACCAGATTGGAG-3′) primers, cloned first into the pENTR™/SD/D-TOPO entry vector (Invitrogen), and subcloned subsequently into the pEarleyGate202 and pEarleyGate101 destination vector (Earley *et al.*, 2006). For *HAC1:HA*, the genomic *HAC1* fragment including the 1.2kb promoter region upstream of start codon was amplified using primers HAC1 promoter-F (5′-CACCCTACAACAGTCTCTGCTTCATTCAACT-3′) and HAC1-R (5′-CCCGGGGCGCGCCCACCCTTACCTGAGCCCCCAGCGACT-3′) and cloned into the pEarleyGate301 destination vector (Earley *et al.*, 2006). *35S::FLAG:HAG1* or *35S::HAG1:YFP:HA* was transformed into heterozygous *hag1-7* or *hag1-6* plants and *HAC1:HA* into WT Col respectively, via *Agrobacterium*-mediated transformation using floral dip method (Clough & Bent, 1998). Homozygous transgenic *35S::FLAG:HAG1 hag1-7* and *35::HAG1:YFP:HA hag1-6* plants were selected in the subsequent generations through genotyping.

2.3.3 RT-PCR or RT-qPCR analysis

Four micrograms of total RNA was reverse transcribed using M-MuLV reverse transcriptase (Fermentas) and oligo(dT) primer. RT-qPCR analysis of *rSPL9*, a gene-specific reverse transcription was performed using qrSPL9_RT-R (5′-TGGTTGATGTGGATTGCTTAACAAGCTTAAG-3′), and UBQ-R (5′-CGACTTGTCATTAGAAAGAAAGAGATAACAGG-3′) was used for the *UBQ10* control. Following RT, either semi-quantitative PCR using i-Taq DNA polymerase (iNtRON Biotechnology) or qPCR was performed on first-strand DNA with gene-specific primers. qPCR was performed with the Applied Biosystems 7300 real-time PCR system by using the SYBR Green I master mix (Kappa). Quantification using standard curves was performed to determine the amount of target genes in each sample. The transcript levels of each gene were normalized to the level of *UBQ10* or *PP2A3*. To detect *SPL9*, *rSPL9*, and *SPL9*+*rSPL9* in *pSPL9::rSPL9* plants using RT-PCR analysis, primer sets were designed within the 15 modified bases in *rSPL9*. While *rSPL9* was detected by using primer pairs that contained the modified miR156 target site, endogenous *SPL9* was detected using primer pairs containing the original miR156 target site. To detect both *SPL9* and *rSPL9* (*SPL9*+*rSPL9*), primers were designed in regions with identical sequences between *SPL9* and *rSPL9*. Primers used for RT-PCR or RT-qPCR analyses are as in Table2-2 and Table 2-3.

Table 2-2 Oligonucleotides used for RT-PCR analyses

Gene	Name	Sequence (5' to 3')
UBQ10	UBQ-F	GATCTTTGCCGGAAAACAATTGGAGGATGGT
	UBQ-R	CGACTTGTCATTAGAAAGAAAGAGATAACAGG
SPL2	SPL2-F	CCGACGTCTCTCAGATCACA
	SPL2-R	TGGTACGTGCTTCGAACTTG
SPL3	SPL3-F	CTTAGCTGGACACAACGAGAGAAGGC
	SPL3-R	GAGAAACAGACAGAGACACAGAGGA
SPL4	SPL4-F	GTAGCATCAATCGTGGTGGC
	SPL4-R	CTTCGCTCATTGTGTCCAGC
SPL5	SPL5-F	CCAGACTCAAGAAAGAAACAGGGTAGACAG
	SPL5-R	TCCGTGTAGGATTTAATACCATGACC
SPL7	SPL7-F	GAGCTGGAGGGCTATATCCG
	SPL7-R	GGAAGAGGCTCGATGACTGT
SPL8	SPL8-F	CGCGAAACACTACCACAGAA
	SPL8-R	GGAGGCTGATTGGTGACATT
SPL9	qSPL9-F	CAAGGTTCAGTTGGTGGAGGA
(*SPL9*+*rSPL9*)	qSPL9-R	TGAAGAAGCTCGCCATGTATTG
SPL10	SPL10-F	GTGTGGGAGAATGCTCAGGAGG
	SPL10-R	GATGATGCAACCCGACTTTT
SPL11	SPL11-F	CCCTTAACGCGAGATCTGAA
	SPL11-R	AAGAGAGAGAGCACGGTGGA
SPL13(*17*)	SPL13-F	GTTCGAGTTATGGGCAGAGC

	SPL13-R	GCACTCGCATTCTCAAACAA
SPL14	SPL14-F	TGGTTTGACTGCTGTGGAAG
	SPL14-R	TTCCTCCTCCGTCGATTATG
SPL15	SPL15-F	TTGGGAGATCCTACTGCGTGGTCAACC
	SPL15-R	AGCCATTGTAACCTTATCGGAGAATGAG
AP1	AP1-F	AGGGAAAAAATTCTTAGGGCTCAACAG
	AP1-R	GCGGCGAAGCAGCCAAGGTTGCAGTTG
CAB2	CAB2-F	GAGTCAAGTTTGGAGAGGC
	CAB2-R	AAGTTGGTGGCAAAGGCCC
SPL9 (endogenous)	SPL9-F	GAGTGATGAGGCGGCCAGTG
	eSPL9-R	GGATTTGACAGAAGAGAGAGAGCAC
rSPL9	SPL9-F	GAGTGATGAGGCGGCCAGTG
	rSPL9-R	GGATTGCTTAACAAGCTTAAGGCGC

Table 2-3 Oligonucleotides used for RT-qPCR analyses

Gene	Name	Sequence (5' to 3')
UBQ10	qUBQ-F	GGCCTTGTATAATCCCTGATGAATAAG
	qUBQ-R	AAAGAGATAACAGGAACGGAAACATAGT
SPL2	SPL2-F	CCGACGTCTCTCAGATCACA
	SPL2-R	TGGTACGTGCTTCGAACTTG
SPL3	SPL3-F	CTTAGCTGGACACAACGAGAGAAGGC
	SPL3-R	GAGAAACAGACAGAGACACAGAGGA
SPL4	SPL4-F	GTAGCATCAATCGTGGTGGC
	SPL4-R	CTTCGCTCATTGTGTCCAGC
SPL5	SPL5-F	CCAGACTCAAGAAAGAAACAGGGTAGACAG
	SPL5-R	TCCGTGTAGGATTTAATACCATGACC
SPL7	SPL7-F	GAGCTGGAGGGCTATATCCG
	SPL7-R	GGAAGAGGCTCGATGACTGT
SPL8	SPL8-F	CGCGAAACACTACCACAGAA
	SPL8-R	GGAGGCTGATTGGTGACATT
SPL9	qSPL9-F	CAAGGTTCAGTTGGTGGAGGA
(*SPL9*+*rSPL9*)	qSPL9-R	TGAAGAAGCTCGCCATGTATTG
SPL10	SPL10-F	GTGTGGGAGAATGCTCAGGAGG
	SPL10-R	GATGATGCAACCCGACTTTT
SPL11	SPL11-F	CCCTTAACGCGAGATCTGAA
	SPL11-R	AAGAGAGAGAGCACGGTGGA
SPL13(*17*)	SPL13-F	GTTCGAGTTATGGGCAGAGC

	SPL13-R	GCACTCGCATTCTCAAACAA
SPL14	SPL14-F	TGGTTTGACTGCTGTGGAAG
	SPL14-R	TTCCTCCTCCGTCGATTATG
SPL15	SPL15-F	TTGGGAGATCCTACTGCGTGGTCAACC
	SPL15-R	AGCCATTGTAACCTTATCGGAGAATGAG
PP2A3	PP2A3-F	TAACGTGGCCAAAATGATGC
	PP2A3-R	GTTCTCCACAACCGCTTGGT
SPL15 (L*er*)	SPL15(L)F	TTGGGAGATCCTACTGCGTGGTCAACC
	SPL15(L)R	AGCCATTGTAACCTTATCGGAGAATGAG
SPL2 (L*er*)	SPL2(L)F	TTGGGACTTCCAGTGACTCTGGCTTC
	SPL2(L)-R	CATCAAACTCAGAGAGACAGTGGAACC
miR156a	miR156a-F	CATCTTGTAGATCTCTGAAGTTGGACT
	miR156a-R	GAGATTGAGACATAGAGAACGAAGACA
miR156b	miR156b-F	GCAGAGATAGGCAACTGACAG
	miR156b-R	GAAGAGGGAGAGATGGTGATTG
miR156c	miR156c-F	GACAACTTTCCTCTTCTCCTTCGG
	miR156c-R	CCCAAAACTCCCTCATCAGTCATC
miR156h	miR156h-F	TGACACGATCACACAACATGG
	miR156h-R	CCACCGTCACTGCTTACTTA
FT	FT-F	CCATTGGTTGGTGACTGATATCC
	FT-R	TTGCCAAAGGTTGTTCCAGTT
SOC1	SOC1-F	TGAGGCATACTAAGGATCGAG
	SOC1-R	GCGTCTCTACTTCAGAACTTGGGC
LFY	LFY-F	ACGCCGTCATTTGCTACTCT

	LFY-R	CTTTCTCCGTCTCTGCTGCT
FUL	FUL-F	TTGCAAGATCACAACAATTCGCTTCTC
	FUL-R	GAGAGTTTGGTTCCGTCAACGACGATG
AP1	AP1-F	AGGGAAAAAATTCTTAGGGCTCAACAG
	AP1-R	GCGGCGAAGCAGCCAAGGTTGCAGTTG
AGL42	AGL42-F	TCATGAAACCAGCAATCACGACTCA
	AGL42-R	AGCCTTTCTTTCTCGGACCTTTCC
TRY	TRY-F	TTGTCGGTGATAGGTGGGATTT
	TRY-R	ACGGTGAGGCTTGGTATGTTTG
TCL1	TCL1-F	AAACCGTCTTCGCCGCCTTCA
	TCL1-R	TCCTTTGCCTCACGTCCCACCA
rSPL9	qrSPL9-F	TTCCTCCACTGAGTCATCCTCT
	qrSPL9-R	GACCACCTGAGGAAGAAGACC
SPL9 (endo)	qeSPL9-F	CACCATCATCAAAGTAGGAGACAG
	qeSPL9-R	AACAAATCAAAATCAAAAGCCATT
GUS	GUS-F	GAACCACTGAACACGTATCTCTACC
	GUS-R	TATTGAAATCCATCACATTGCTCGC

2.3.4 ChIP assay

ChIP assays against PolII, H3Ac, H3K9Ac, H3K14Ac, H3K27Ac, and total H3 were performed essentially as previously described (Han *et al.*, 2007; Johnson *et al.*, 2002). For seed samples, 300 mg seeds were cross-linked in 1% formaldehyde solution. Chromatin complexes were isolated with lysis buffer (50 mM HEPES (pH 7.5), 150 mM NaCl, 1 mM EDTA, 1% Triton X-100, 0.1% deoxycholate, 0.1% SDS, 1 mM PMSF, protease inhibitor cocktail) prior to DNA shearing by sonication. For all samples, insoluble materials were precipitated by several rounds of centrifugation and the chromatin was precleared using salmon sperm DNA/Protein A agarose beads (Upstate 16-157) The antibodies used in ChIP were anti-PolII (Covance 8WG16), anti-H3Ac (Millipore 06-599), anti-H3K9Ac (Millipore 07-352), anti-H3K14Ac (Millipore 07-353), anti-H3K27Ac (Millipore 07-360), and anti-H3 (Abcam ab1791). For the ChIP binding assays, chromatin was prepared as previously described (Kaufmann *et al.*, 2010) with minor modifications. Briefly, seedlings were harvested and fixed to crosslink protein-DNA interaction in MC buffer (10 mM sodium phosphate (pH 7), 50 mM NaCl, 0.1 M sucrose) with 1% formaldehyde. Nuclei were then isolated in M1 buffer (10 mM sodium phosphate (pH 7), 0.1 M NaCl, 1 M 2-methyl 2,4-pentanediol, 10 mM β-mercaptoethanol, protease inhibitor cocktail) and washed several times with M2 (10 mM sodium phosphate (pH 7), 0.1 M NaCl, 1 M 2-methyl 2,4-pentanediol, 10 mM β-mercaptoethanol, 10 mM $MgCl_2$, 0.5% Triton X-100, protease inhibitor cocktail), and M3 (10 mM sodium phosphate (pH 7), 0.1 M NaCl, 10 mM β-mercaptoethanol, protease inhibitor cocktail) buffers. The nuclear pellet was then resuspended in sonic buffer (10 mM sodium phosphate (pH 7), 0.1 M NaCl, 0.5%

Sarkosyl, 10 mM EDTA, protease inhibitor cocktail), and chromatin was sheared such that most DNA fragments were between 200 to 1,200 bp long. After incubation with a specific antibody against HA (Abcam ab9110), antibody-protein/DNA complexes were isolated using salmon sperm DNA/Protein A agarose beads. DNA was then isolated by reverse crosslinking and residual proteins were digested by incubation with proteinase K (Roche). Finally, DNA was purified using the QIAquick PCR purification Kit (Qiagen) and resuspended in 100 µl distilled water. The amount of immunoprecipitated DNA was quantified by qPCR using primer pairs listed in Table 2-4. qPCR was performed with the Applied Biosystems 7300 real time PCR system by using the SYBR Green I master mix (Kappa) or with the Rotor Gene Q real-time PCR cycler (Qiagen) by using the SYBR Premix Dimer Eraser (Takara). Relative amounts of each amplified product were determined by using the comparative $\Delta\Delta C_T$ method (Livak & Schmittgen, 2001). The amount of immunoprecipitated DNA was normalized to the respective input, and the fold enrichment was calculated by comparing the normalized value of each fragment to that of *Actin2/7*, *PP2A3*, or *UBQ11*. For ChIP binding assays, levels of nontransgenic control plants were set to 1 after normalization to the levels of the input DNA.

Table 2-4 Oligonucleotides used for ChIP-qPCR assays

Gene	Name	Sequence (5' to 3')
Actin2/7	Actin2/7-F	GATCCGTTCGCTTGATTTTGC
	Actin2/7-R	ACAAGCACGGATCGAATCACA
PP2A3	PP2A3-F	TAACGTGGCCAAAATGATGC
	PP2A3-R	GTTCTCCACAACCGCTTGGT
CHS	CHS-F	CACAGAAAAGGGGGCTAACA
	CHS-R	AGAGTTTGATGTTGCTGTTGTG
UBQ11	UBQ11-F	TCAGTATATGTCTCGCAGCAAACTATC
	UBQ11-R	GACGACTCGGTCGGTCACG
KRP7	KRP7(K7D3n)F	GTATTTATAGTTCTGTCTCCATGTG
	KRP7(K7u3n)R	GCTGTAGAAATGTGAGTTGTGACAG
SPL3	SPL3A-F	GTGGCCCCGATAGCTAATTT
	SPL3A-R	TTGCACATAAATGTGTCGTAAGG
	SPL3B-F	TTCAGTCTTGCTTTTCCAATCA
	SPL3B-R	GATCATGTTAATGCCGATGCTA
	SPL3C-F	ATAGAGCTGGGTCCTCGTCA
	SPL3C-R	AAGTGGGGAAGGATCTTAGGTG
	SPL3D-F	TTTTTCAAAACTCCTGCAACAA
	SPL3D-R	ATTAACCTTCAAACCGGGATCT
	SPL3E-F	CTTAGCTGGACACAACGAGAGAAGGC
	SPL3E-R	GAGAAACAGACAGAGACACAGAGGA
	SPL3A2-F	TGATACAGAAACTTTAACTACCAAAAA
	SPL3A2-R	GATCATGTTAATGCCGATGCTA

SPL9	SPL9A-F	GGTTTGGTTGGTTCGGATAA
	SPL9A-R	TGTCCATTGCCAATCTACCAT
	SPL9B-F	TCCAATGTTCACTTGCTCCA
	SPL9B-R	ATTTCGGCTTCCCTGATTTT
	SPL9C-F	ACCTAAAGTCACTGTGGCTGGTAT
	SPL9C-R	AGCCTTTAGATTTGATTCACAACAG
	SPL9D-F	TGGTCTTGTGTTTGTTGGACTC
	SPL9D-R	ACACTAGTTTTGTCCCCCTCAA
	SPL9E-F	TTCCGGAATTTGACCTAGAGAA
	SPL9E-R	TCGGTCTTATGTGTCGAGCTTA
	SPL9F-F	TCACCATACCAACTGGTCTCTC
	SPL9F-R	AAAAGCCATTATCTGGCAACAA
	SPL9A2-F	AATCAAAATTTTCAGTATTCGACTAAA
	SPL9A2-R	TTTTTCAAAATGGAAAGAAAACC
	SPL9B2-F	CCCTCGTTTTGCTATGTGGT
	SPL9B2-R	ATTTCGGCTTCCCTGATTTT
	SPL9C2-F	TTCCTCCACTGAGTCATCCTCT
	SPL9C2-R	GACCACCTGAGGAAGAAGACC
SPL5	SPL5A-F	CAGACAAGGCAATTTTAAAACCA
	SPL5A-R	GGATTCCTCTTCCTGCAACC
	SPL5B-F	GTTGCACTGATCAATAAGGTTCAC
	SPL5B-R	AGTTGATACAAGATTGGAGCTGT
	SPL5C-F	GGAAGCAAGCACATCACGTA
	SPL5C-R	TGGGAAGATGATGGTGGATT

SPL5D-F	GAGAATGGCATGGATGGAGA
SPL5D-R	CTGCTTGGCCTCAGTCAAAT
SPL5E-F	GCAGGTATGATTCTTCCCTTCA
SPL5E-R	GCTCATGAAACCTGCTCAAAA

2.3.5 Northern blot analysis

A total of 50 μg of RNA was separated on a 15% polyacrylamide gel containing 8 M urea, transferred to a Hybond™-NX membrane (Amersham), and fixed by UV cross-linking. Blots were then hybridized with a miR156-complementary oligonucleotide (5′-GTGCTCACTC TCTTCTGTCA-3′) labeled with γ-^{32}P-ATP. The same blot was also analyzed with an oligonucleotide probe (5′-AGGGGCCATGCTAATCTTCTC-3′) specific to *U6* snRNA, which was used as a loading control. Images were quantified using Molecular Imaging Software (Kodak) and normalized to *U6* expression.

2.3.6 Histochemical GUS assay

Plants at similar developmental stages were fixed with 90% acetone for 20 min on ice. GUS staining was performed as described (Han *et al*, 2007). The GUS expression pattern was observed with a STEM2000 stereomicroscope (Carl Zeiss)

2.4 Results

2.4.1 Mutations in *HAG1* strongly delay juvenile-to-adult phase transition in Arabidopsis

In the attempts to characterize the phenotypes of *HAG1* loss-of-function mutants, I noticed that the *hag1-6* mutants (Long *et al*, 2006) had severely lower trichome numbers on the abaxial, but not on the adaxial, leaf surface compared to that in wild type (WT) (Figure 2.1a). Quantitative analysis of the abaxial trichome numbers of leaves at various positions indicated that not only were the number of trichomes formed far less, but the developmental onset of trichome production was also severely delayed in *hag1-6* compared to those in WT (Figure 2.1b). Delay in abaxial trichome initiation was also observed in another allele of *HAG1*, *hag1-7* (Figure 2.1c), and the overexpression of either FLAG-tagged (*35S::FLAG:HAG1*) or yellow fluorescence protein (YFP)- and HA-tagged (*35S::HAG1:YFP:HA*) HAG1 fully rescued the phenotypes of *hag1-7* or *hag1-6*, respectively (Figure 2.1c, Figure 2.2a-c). Furthermore, the 7th leaves of both *hag1-6* and *hag1-7* were smaller and rounder as measured by length-to-width ratio, and their petioles were also more elongated than those in WT (Figure 2.1c). The morphological characteristics observed in *hag1* are considered juvenile vegetative traits (Wu *et al*, 2009; Telfer *et al*, 1997), indicating that juvenile-to-adult vegetative phase transition is delayed in *hag1* mutants.

2.4.2 Transcript levels of a group of *SPL*-family genes are reduced in *hag1* mutants

Because the timing of the juvenile-to-adult phase transition is known to be controlled by several members of the SPL-family of transcription factors (e.g., SPL3, SPL4, SPL5, SPL9, SPL15), I investigated whether delayed vegetative phase transition of *hag1* is related to altered expression of *SPL* genes. The transcript levels of *SPL3, SPL4, SPL5, SPL9* and *SPL15* which were higher in older plants than in younger plants irrespective of genotype (Figure 2.1d and Figure 2.3d), were greatly reduced in *hag1-6* compared to WT at all developmental stages examined (Figure 2.1d and Figure 2.3d). Several other *SPLs* were also down-regulated in *hag1* mutants (Figure 2.1e, Figure 2.2d). Among these, *SPL3, SPL4, SPL5, SPL9, SPL11, SPL13(17), SPL15* but not *SPL8* transcripts contain predicted miR156-binding sites (Rhoades *et al*, 2002), suggesting that the regulation of *SPLs* by HAG1 might be independent of miR156. Furthermore, the levels of some predicted miR156-target transcripts including *SPL2* and *SPL10* were not affected by *hag1-6* (Figure 2.1e). In accordance with the rescue of the phase-transition phenotypes, the transcript levels of all *SPLs* down-regulated in *hag1* were restored back to WT levels by the introduction of *35S::FLAG:HAG1* (Figure 2.2d).

2.4.3 Mutations in *HAG1* result in delayed flowering and reduced expression of *SPL*-target genes

SPLs are believed to directly regulate several MADS-box genes associated with reproductive transition and determination of floral meristem identity in a FT/FD-independent manner (Wang *et al*, 2009; Yamaguchi *et al*, 2009). Correspondingly,

HAG1 mutations resulted in decreased levels of *LEAFY* (*LFY*), *FRUITFULL* (*FUL*), *APETALA 1* (*AP1*), *AGAMOUS-LIKE 42* (*AGL42*), and *SUPPRESSOR OF OVEREXPRESSION OF CONSTANS 1* (*SOC1*) transcripts, but not of *FT* transcript, and delayed flowering (Figure 2.5c and Figure2.2e). Consistent with the fact that SPLs are critical factors in an endogenous flowering pathway, flowering delay in *hag1* was more pronounced in non-inductive SD (Figure 2.2f). Expression of *TRY* and *TCL1,* SPL9 targets without flowering-related function (Yu *et al*, 2010), was also severely reduced in *hag1-6* (Figure 2.5c).

2.4.4 miR156-independent transcriptional control of *SPL3* and *SPL9* by HAG1

To test if the reduced expression of *SPLs* in *hag1* was a result of increased miR156 expression, I compared the primary transcript levels of several *MIR156* genes and the level of mature miR156 in the WT and *hag1-6*. The primary transcripts levels of *MIR156A* and *MIR156B* were reduced, whereas those of *MIR156C* and *MIR156H* were slightly increased in *hag1-6* (Figure 2.3a). The level of mature miR156 was ~1.35-fold higher in *hag1-6* than in WT (Figure 2.3b).

Because the extent of the increase in miR156 appeared insufficient to account for the strong down-regulation of *SPLs* and the severe delay in vegetative phase transition in *hag1*, I further analyzed *HAG1* function in plants expressing a miR156-resistant *SPL9* under the *SPL9* promoter (*pSPL9::rSPL9*; Wang *et al*, 2008). The strong acceleration of abaxial trichome production by *pSPL9::rSPL9* was greatly delayed by the *hag1-6* mutation (Figure 2.3c). The floral promotion effect of *pSPL9::rSPL9* was also less effective in the *hag1-6* mutant background

(Figure 2.4a). Consistently, a large reduction in the transcript levels of *rSPL9* as well as endogenous *SPL9* was observed in *hag1-6* at all developmental stages examined (Figure 2.3d and Figure 2.4b), demonstrating that the effects of *HAG1* on *SPL9* is miR156-independent. Expression of SPL-target genes was also reduced in *pSPL9::rSPL9 hag1-6* compared to *pSPL9::rSPL9* (Figure 2.4c).

Like *SPL9*, *HAG1* control of *SPL3* expression was independent of miR156. Both *pSPL3::SPL3:GUS* and *pSPL3::rSPL3:GUS*, expressing miR156-sensitve and -resistant *SPL3* tagged with *β-glucuronidase* (*GUS*) under the *SPL3* promoter, respectively (Yang *et al*, 2011), showed lower GUS expression in *hag1-6* than in WT (Figure 2.3e and Figure 2.4d). I then studied the effect of a *hag1* loss-of-function mutation on PolII activity and found that PolII occupancies in the promoter and transcribed regions of *SPL3* and *SPL9* were severely reduced in *hag1-6* than in WT (Figure 2.3f and 2.3g). Taken together, these results indicate that HAG1 affects the transcriptional activity of *SPLs* independently of the miR156 pathway.

2.4.5 Histone acetylation at the *SPL3* and *SPL9* loci is controlled by the HAG1- and PRZ1-containing HAT complex

Next, I investigated whether *SPL3* and *SPL9* are the direct targets of HAG1. For this, I used *35S::HAG1:YFP:HA hag1-6* plants (Figure 2.2b and 2.2c) and performed ChIP assays using the anti-HA antibody. Enrichment of the HAG1:YFP:HA protein was observed in the promoters and transcribed regions of *SPL3* and *SPL9*, but not at the negative control locus *CHS* (Benhamed *et al*, 2006; Figure 2.5a). Thus, *SPL3* and *SPL9* are likely the direct targets of HAG1.

HAG1:YFP:HA was also enriched at *KRP7*, a PRZ1 target (Anzola *et al*, 2010), supporting the view that HAG1 functions together with ADA2 homologs (ADA2a and PRZ1) in the SAGA-like complex (Mao *et al*, 2006) as in other organisms.

To determine whether the relationship between HAG1 and ADA2 is also observed in the regulation of phase transition, I examined the abaxial trichome phenotypes of *ada2a-3* and *prz1-1* mutant leaves at various positions. The *prz1-1*, but not *ada2a-3* mutation, resulted in a severe delay in the onset of abaxial trichome production (Figure 2.5b). Moreover, the transcript levels of several *SPLs* and *SPL3* and *SPL9* -target genes, which were reduced in *hag1* (Figure 2.1e), were also substantially decreased in *prz1-1* (Figure 2.5c and Figure 2.6a), indicating that the HAG1/PRZ1-containing SAGA-like complex plays a role in the transcriptional control of *SPLs* and subsequent developmental phase transitions.

I then investigated whether the HAG1/PRZ1-containing SAGA-like complex affects histone acetylation at SPL3 and SPL9. ChIP assays using anti-histone H3 (H3) and anti-acetylated histone H3 (H3Ac) antibodies showed that disruption of HAG1 and PRZ1 reduced H3Ac to similar levels without affecting total H3 levels in the promoters and transcribed regions of SPL3 and SPL9 (Figures 2.5d,e and Figure 2.6b). As HAG1 was previously reported to target H3K9, H3K14, and H3K27 for acetylation (Benhamed *et al*., 2006), I then tested H3K9Ac, H3K14Ac, and H3K27Ac levels for limited regions of the SPL3 and SPL9 loci. In line with the previous report, all the three acetylation levels were reduced by the *hag1-6* mutation (Figure 2.7a to 2.7c). These results, together with the finding that SPL3 and SPL9 are direct targets of HAG1, indicate that the SAGA-like complex directly controls SPL transcription through histone acetylation.

2.4.6 HAG1 plays a major role in juvenile-to-adult phase transition and *SPL* activation among Arabidopsis HATs

To determine whether the role of HAG1 in *SPL* regulation and phase transitions is shared by other HATs, I examined the abaxial trichome emergence in the leaves of single or double mutants of several HATs (Figure 2.6c). The timing of abaxial trichome emergence was not significantly altered in the plants lacking the GNAT-family HAT2 (*hag2-2*) or two MYST-family HATs, HAM1 and HAM2 (*ham1-1 ham2-1*). On the other hand, it was moderately delayed in *elo3-1*, *haf1-2 haf2-5*, and *hac1-2 hac5-2* mutants, which lacked the Elongator HAT ELO3/HAG3, two TAF250-family HATs (HAF1 and HAF2), and two CBP-family HATs, HAC1 and HAC5, respectively. Consistent with delayed trichome emergence, the transcript levels of *SPL3, SPL4, SPL5, SPL9 and SPL15* were reduced in *elo3-1*, *haf1-2 haf2-5*, and *hac1-2 hac5-2* compared to those in WT (Figure 2.6d to 2.6f). However, although small decreases were observed in parts of the transcribed regions of *SPL3* and *SPL9* in *hac1-2 hac5-2*, H3Ac levels at *SPL3* and *SPL9* in these mutants were not as substantially altered as in *hag1* or *prz1* (Figure 2.6g, 2.6i, and 2.6j). Furthermore, at *SPL5*, where the transcript levels were most severely reduced, H3Ac levels were not affected at all by the *hac1-2 hac5-2* mutations (Figure 2.6g), indicating a lack of correlation between transcription and histone acetylation. Finally enrichment of HAC1:HA fusion protein was not observed in the *SPL3* and *SPL9* chromatin (Figure 2.6h). Thus, the role of HACs, HAFs, and ELO3 in *SPL* regulation might be either indirect or minor in contrast to that of the HAG1/ PRZ1 complex.

2.4.7 HAG1-mediated H3Ac is important for miR156-independent light and photoperiodic induction of *SPL9*

Photoperiodic induction of *SPL3* and *SPL9* is known to be a miR156-independent process (Jung *et al*, 2012; Wang *et al*, 2009). By studying *rSPL9* expression under light-shifting conditions, I found that *SPL9* is also induced by light in a miR156-independent manner (Figure 2.8a). Light induction of *SPL9* as well as its previously known photoperiodic induction was substantially reduced by the *hag1-6* mutation (Figure 2.8b and Figure 2.9a). This led me to investigate whether the effects of light and photoperiod involve changes in histone acetylation that is mediated by HAG1. These environmental cues clearly increased H3Ac levels at *SPL9* (Figure 2.8c and Figure 2.9b). Notably, H3Ac levels at *SPL9* in *hag1-6* were lower than those in WT under dark conditions and increased in response to light, but only to WT levels in the dark (Figure 2.8c). This indicates that HAG1 plays a role in maintaining basal histone acetylation and establishing additional histone acetylation in response to light signals at *SPL9*, which induce efficient *SPL9* transcription. Reduced yet detectable increase in H3Ac levels at *SPL9* induced by light in *hag1-6* suggests that HATs other than HAG1 might also be involved in this process. Alternatively, a decrease in histone deacetylase activity might be accompanied with increased HAG1 activity.

2.4.8 HAG1-mediated H3Ac is important for miR156-independent induction of *SPL3* during germination

I was curious about how initial expressional status of *SPLs* is established during

post-embryonic growth. I challenged this question using *SPL3* as a test model and noticed that *SPL3* mRNA is substantially increased in germinating seeds (Figure 2.10a). Although the expression level was different, the induction pattern *per se* during the course of germination between the miR156-sensitive *pSPL3::SPL3:GUS* and the miR156-resistant *pSPL3::rSPL3:GUS* was similar (Figure 2.10b), indicating that the inductive process is regulated by other mechanism independent of miR156. Thus, the *SPL3* induction during seed germination was not likely due to the release from miR156 inhibition but rather might be contributed by the onset of transcriptional activation. I investigated whether histone acetylation mediated by HAG1 is required for this transcriptional activation of *SPL3* during germination. Gradual increase of GUS activity encoded by *pSPL3::rSPL3:GUS* during germination and early-seedling growth was substantially dampened by the *hag1-6* mutation (Figure 2.10c). Moreover, the level of H3Ac at the *SPL3* loci was clearly higher in samples 4 days after planting (DAP) compared to 1 DAP samples (Figure 2.10d). Finally, the enrichment of HAG1:YFP:HA fusion protein within *SPL3* chromatin was observed in four DAP but not in one DAP samples (Figure 2.10e). Taken together, these results indicate that the targeting of HAG1-mediated histone acetylation activity is crucial for initial establishment of *SPL3* expression during post-embryonic growth.

2.5 Figures

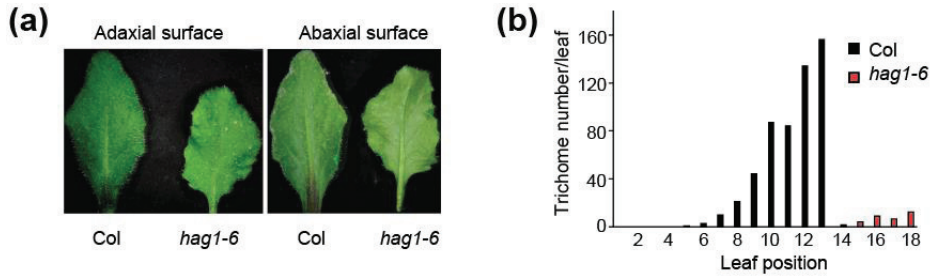

(c)

Genotype	First leaf bearing abaxial trichome (leaf number)	Leaf shape	Length/width of leaf 7
Col	6.5 ± 0.76		2.1 ± 0.34
hag1-6	14.7 ± 0.82		1.6 ± 0.14
hag1-7	11.4 ± 1.21		1.7 ± 0.28
35S::FLAG:HAG1 hag1-7	6.29 ± 0.52		2.0 ± 0.72

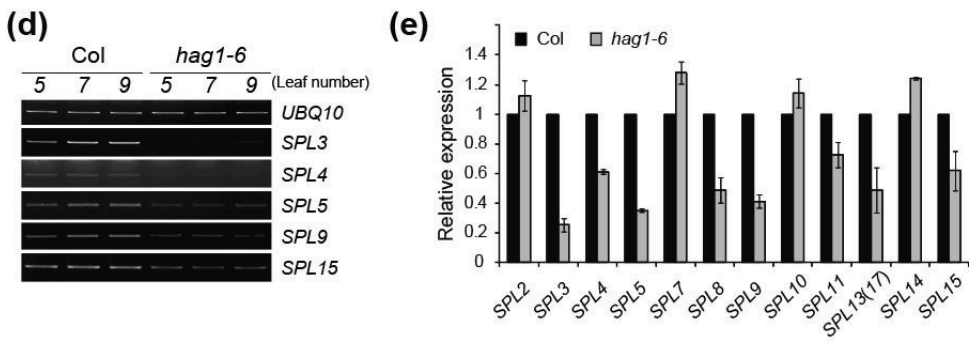

Figure 2.1 *HAG1* is required for the juvenile-to-adult phase transition.

(a) Adaxial and abaxial surfaces of the seventh rosette leaves of wild type (WT) and *hag1-6*. Col: Columbia-0 WT.

(b) Trichome numbers on the abaxial surface of WT (black bars) and *hag1-6* (red bars) leaves at indicated positions.

(c) The leaf shape and the position of the first leaf with abaxial trichome in WT, *hag1-6*, *hag1-7*, and *35S::FLAG:HAG1 hag1-7*. Values are the averages of 20 plants per genotype, and error bars represent standard deviation (SD).

(d) Reverse transcription followed by polymerase change reaction (RT-PCR) analyses of several *SPL* transcripts in WT and *hag1-6* at different developmental stages. RNA was isolated from the above ground tissues in plants with five, seven, or nine visible leaves. *Ubiquitin 10* (*UBQ10*) is an expression control.

(e) Transcript levels of multiple *SPL* genes in WT and *hag1-6* at the seven-leaf stage as determined by RT followed by quantitative real-time PCR (RT-qPCR). *SPL13*(*17*) indicates duplicate *SPL13* and *SPL17* genes (Guo *et al*., 2008). WT levels were set to 1 after normalization to *UBQ10*. Values are the means ± standard error (SE) of three biological replicates.

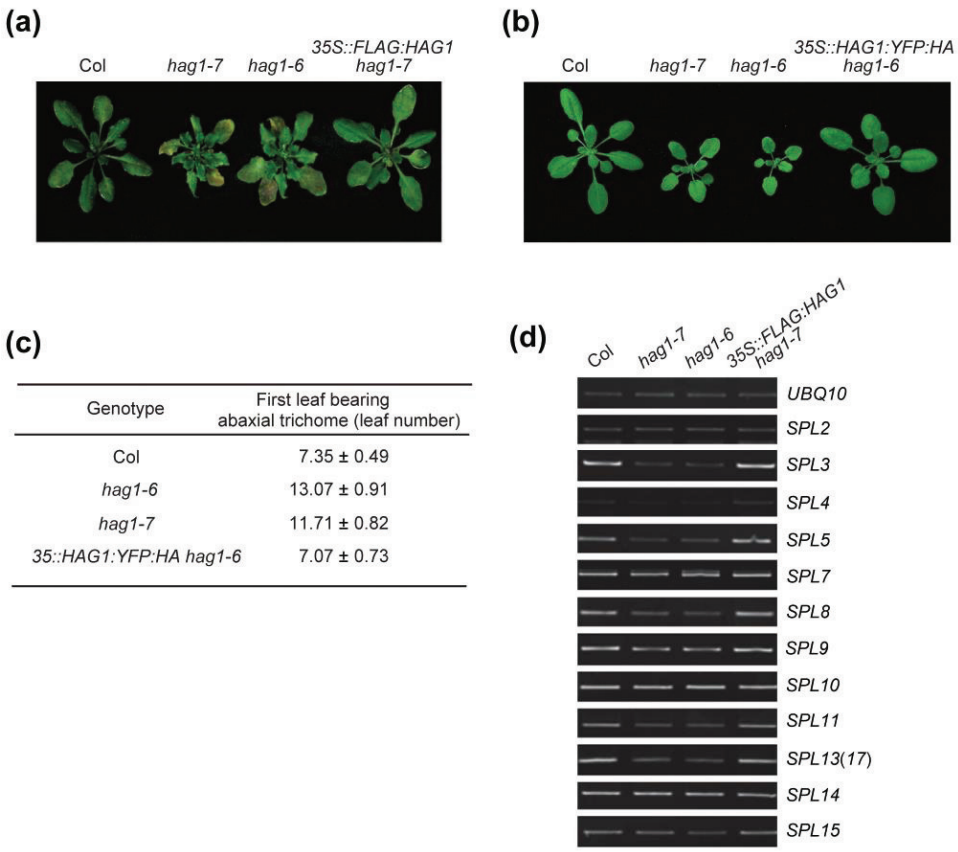

Genotype	First leaf bearing abaxial trichome (leaf number)
Col	7.35 ± 0.49
hag1-6	13.07 ± 0.91
hag1-7	11.71 ± 0.82
35::HAG1:YFP:HA hag1-6	7.07 ± 0.73

Figure 2.2 *hag1* mutant phenotypes and their complementation by *HAG1* overexpression.

(a) Complementation of *hag1-7* by *35S::FLAG:HAG1*.

(b) Complementation of *hag1-6* by *35S::HAG1:YFP:HA*.

(c) Position of the first leaf with abaxial trichome in WT, *hag1-6*, *hag1-7*, and *35S::HAG1:YFP:HA hag1-6*. Values are averages of 20 plants per genotype, and error bars represent sd.

(d) RT-PCR analyses of multiple *SPL* transcripts in WT, *hag1-7, hag1-6*, and *35S::FLAG:HAG1 hag1-7* plants at the seven-leaf stage.

(e) Flowering time of WT, *hag1-7*, and *hag1-6* as scored by primary leaf number formed at flowering. At least 15 individuals were scored for each genotype. Error bars represent sd.

(f) Delayed flowering of *hag1-7* and *hag1-6* in SD.

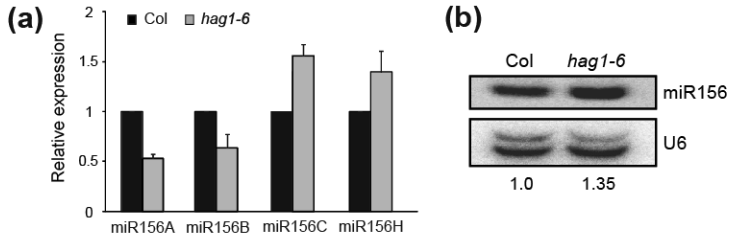

(c)

Genotype	First leaf bearing abaxial trichome (leaf number)
pSPL9::rSPL9	1.08 ± 0.28
pSPL9::rSPL9 hag1-6	12.13 ± 3.54

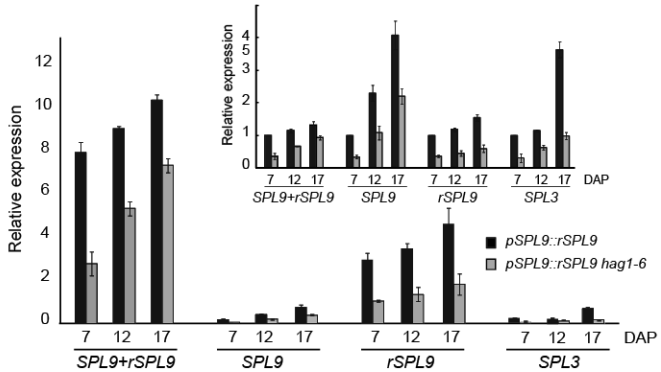

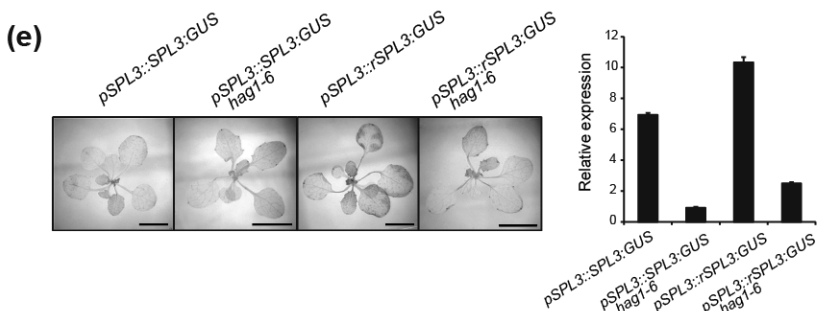

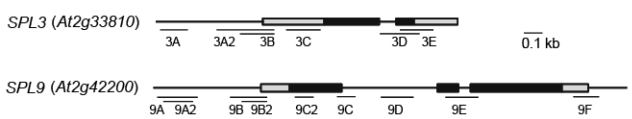

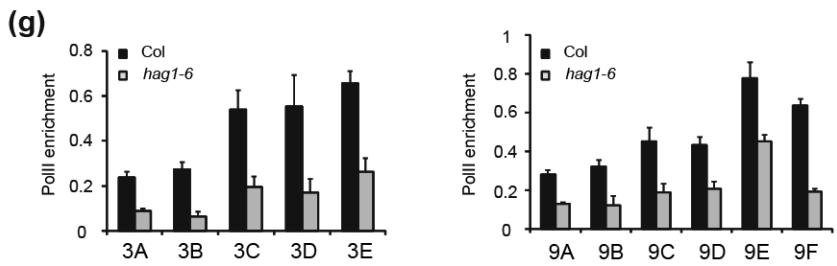

Figure 2.3 miR156-independent transcriptional control of *SPLs* by HAG1.

(a) Primary transcript levels of miR156 genes in WT and *hag1-6*. WT levels were set to 1 after normalization with *UBQ10*. Values are the means ± standard error (SE) of three biological replicates.

(b) Northern blot analysis of miR156. Numbers indicate fold change relative to WT.

(c) Abaxial trichome phenotypes of *pSPL9::rSPL9* and *pSPL9::rSPL9 hag1-6* plants.

(d) Transcript levels of *SPL9*, *rSPL9*, total *SPL9* (*SPL9* + *rSPL9*), and *SPL3* after normalization to *UBQ10* in *pSPL9::rSPL9* and *pSPL9::rSPL9 hag1-6* plants at indicated days after planting (DAP). Values are the means ± SE of three biological replicates. The inset shows relative values to WT at 7 DAP.

(e) Histochemical GUS staining of transgenic plants harboring *pSPL3::SPL3:GUS* or *pSPL3::rSPL3:GUS* in WT or *hag1-6* backgrounds (left). Scale bars: 1 cm. Quantitative analysis of *GUS*-fused transcript levels by RT-qPCR (right). Normalization was to *UBQ10*. Shown are the means ± SE of three biological replicates.

(f) Schematic representation of the *SPL3* and *SPL9* loci. Regions tested in chromatin immunoprecipitation followed by qPCR (ChIP-qPCR) are depicted. Black boxes represent exons, and gray boxes indicate untranslated regions. Intergenic regions or introns are marked with lines.

(g) PolII enrichment at *SPL3* (left) and *SPL9* (right) in WT and *hag1-6* as determined by ChIP-qPCR. The means ± SE of three biological replicates as relative values to *Actin2/7* after normalization to input DNA are shown.

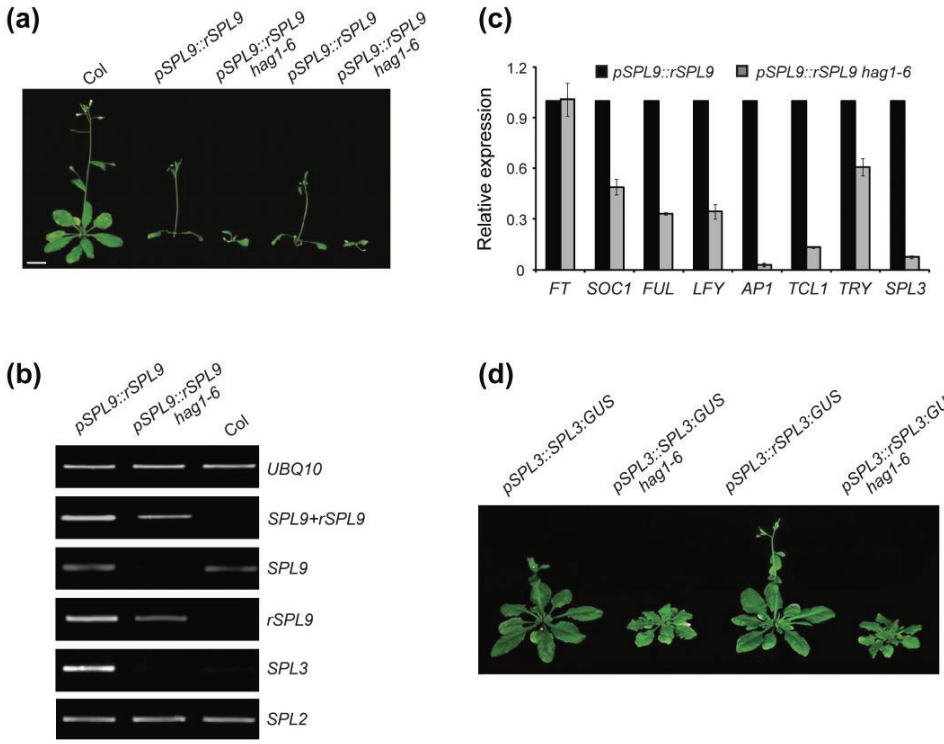
(a)
Col
pSPL9::rSPL9
pSPL9::rSPL9 hag1-6
pSPL9::rSPL9
pSPL9::rSPL9 hag1-6
(c)
pSPL9::rSPL9
pSPL9::rSPL9 hag1-6
Relative expression
1.2
0.9
0.6
0.3
0
FT
SOC1
FUL
LFY
AP1
TCL1
TRY
SPL3
(b)
pSPL9::rSPL9
pSPL9::rSPL9 hag1-6
Col
UBQ10
SPL9+rSPL9
SPL9
rSPL9
SPL3
SPL2
(d)
pSPL3::SPL3:GUS
pSPL3::SPL3:GUS hag1-6
pSPL3::rSPL3:GUS
pSPL3::rSPL3:GUS hag1-6

Figure 2.4 Regulation of miR156-resistant *SPL3* and *SPL9* by HAG1.

(a) Phenotype of 2 *pSPL9::rSPL9 hag1-6* lines from 2 independent crosses between *pSPL9::rSPL9* in WT and *hag1-6*. Scale bar: 1 cm.

(b) RT-PCR analysis of total *SPL9* (*SPL9*+*rSPL9*), *SPL9*, *rSPL9*, *SPL3*, and *SPL2* transcripts in *pSPL9::rSPL9* in WT, *pSPL9::rSPL9 hag1-6*, and WT plants. RNAs were isolated from plants that possessed 2 visible true leaves.

(c) RT-qPCR analysis of the transcript levels of *SPL3*- and *SPL9*-downstream target genes in *pSPL9::rSPL9* and *pSPL9::rSPL9 hag1-6*. Levels in *pSPL9::rSPL9* were set to 1 after normalization with *UBQ10*. Error bars represent se of 3 biological replicates.

(d) Phenotype of *pSPL3::SPL3:GUS* or *pSPL3::rSPL3:GUS*-containing WT and *hag1-6* plants.

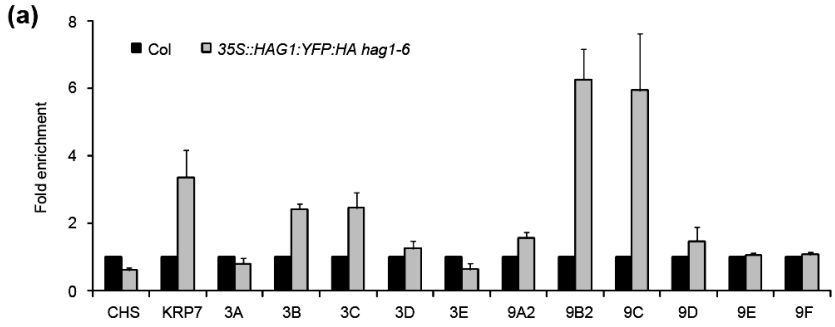

(b)

Genotype	First leaf bearing abaxial trichome (leaf number)
Col	6.77 ± 0.8
hag1-6	12.89 ± 1.3
prz1-1	12.2 ± 1.2
Col	6.11 ± 0.6
ada2a-3	5.28 ± 0.6

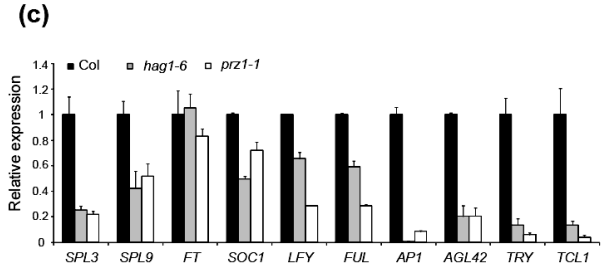

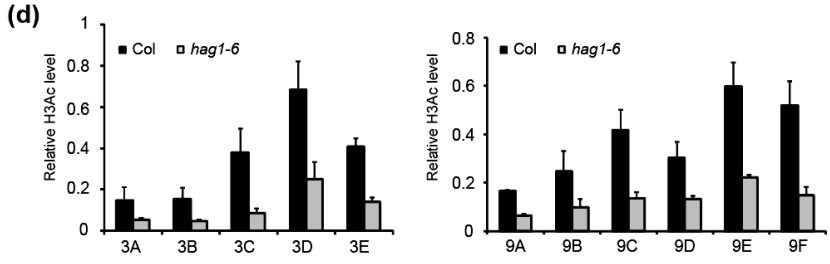

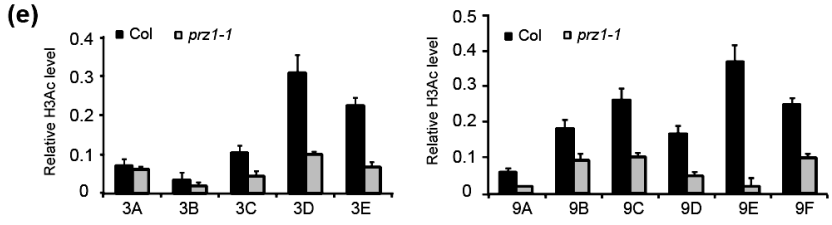

Figure 2.5 Control of *SPL* transcription by the HAG1/PRZ1-containing HAT complex.

(a) Direct association of HAG1:YFP:HA with *SPL3* and *SPL9* chromatin as determined by ChIP-qPCR using an anti-HA antibody. Regions tested are as depicted in Figure 2.3f. Values are the means ± standard error (SE) of three biological replicates obtained after normalization to input DNA.

(b) Abaxial trichome phenotypes of WT, *hag1-6*, *prz1-1*, and *ada2a-3*.

(c) Transcript levels of *SPL3*, *SPL9*, and their downstream target genes in WT, *hag1-6*, and *prz1-1* at the seven-leaf stage as determined by RT-qPCR. Error bars represent SE of three biological replicates.

(d, e) H3Ac levels within *SPL3* (left) and *SPL9* (right) chromatin from WT and *hag1-6* (d) or WT and *pzr1-1* (e). Values are the means ± SE of three biological replicates as relative values to *Actin2/7* after normalization to input DNA. Plant samples were harvested at the seven-leaf stage.

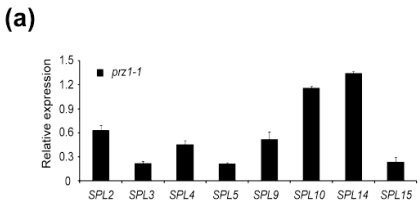

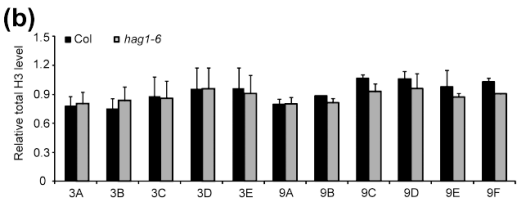

(c)

Genotype	First leaf bearing abaxial trichome (leaf number)
Col	6.8 ± 0.51
hag2-2	7.1 ± 0.21
ham1-1 ham2-1	7.4 ± 0.35
hac1-2 hac5-2	9.1 ± 0.29
haf1-2 haf2-5	8.9 ± 0.18
Ler	4.1 ± 1.89
elo3-1	5.6 ± 0.96

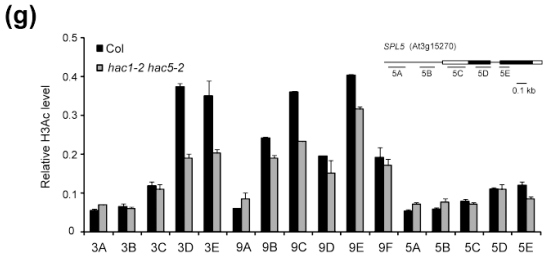

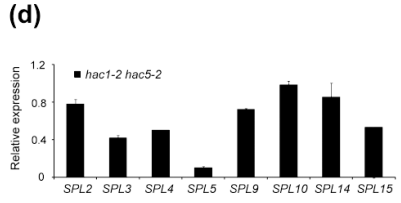

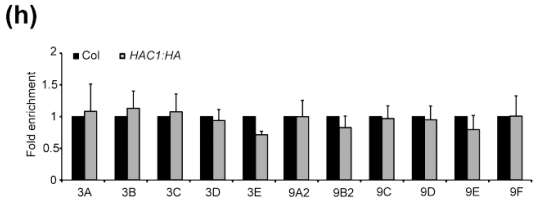

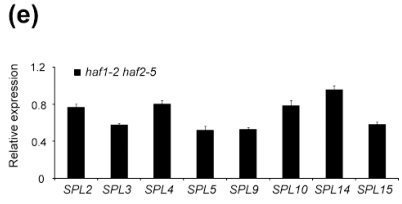

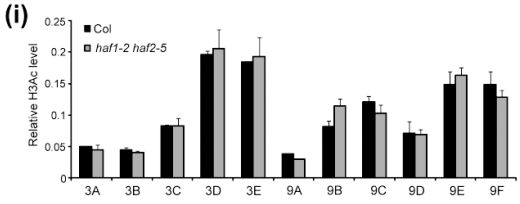

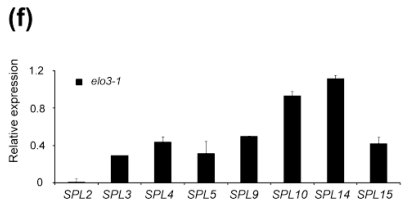

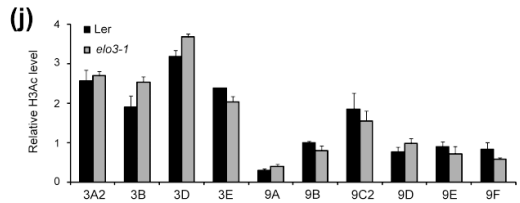

Figure 2.6 Role of other HATs in vegetative phase transition.

(a) RT-qPCR analysis of multiple *SPL* transcripts in *prz1-1*. Expression levels were first normalized to *UBQ10* and then to WT levels that were set to 1. Error bars represent se of 3 biological replicates.

(b) ChIP-qPCR analysis of total H3 levels at the *SPL3* and *SPL9* loci in WT and *hag1-6*. Regions tested are as depicted in Figure 2.3f (b,g,h). Shown are the means ± sd of 3 technical replicates as relative values to *Actin2/7* after normalization to input DNA.

(c) Abaxial trichome phenotypes of HAT mutants. Leaf numbers were scored as in Figure 2.1 c.

(d-f) RT-qPCR analysis of the transcript levels of multiple *SPL* genes in *hac1-2 hac5-2* (d), *haf1-2 haf2-5* (e), and *elo3-1* (f). Values were normalized first to *UBQ10* (d,e) or *PP2A3* (f) and then to WT levels that were set to 1. Error bars represent sd of 3 technical replicates.

(g, i, and j) ChIP-qPCR analysis of H3Ac levels at the *SPL3*, *SPL9*, and *SPL5* loci in *hac1-2 hac5-2* (g), *haf1-2 haf2-5* (i), and *elo3-1* (j). Shown are the means ± sd of 3 technical replicates as relative values to *Actin2/7* (g,i) or *PP2A3* (j) after normalization to input DNA. The experiment was repeated twice by using 2 independent biological replicates and a representative result is shown.

(h) ChIP-qPCR analysis for the enrichment of HAC1:HA within *SPL3* and *SPL9* chromatin. Regions tested are as depicted in Figure 2.3f. Values are the means ± se of 3 biological replicates obtained after normalization to input DNA.

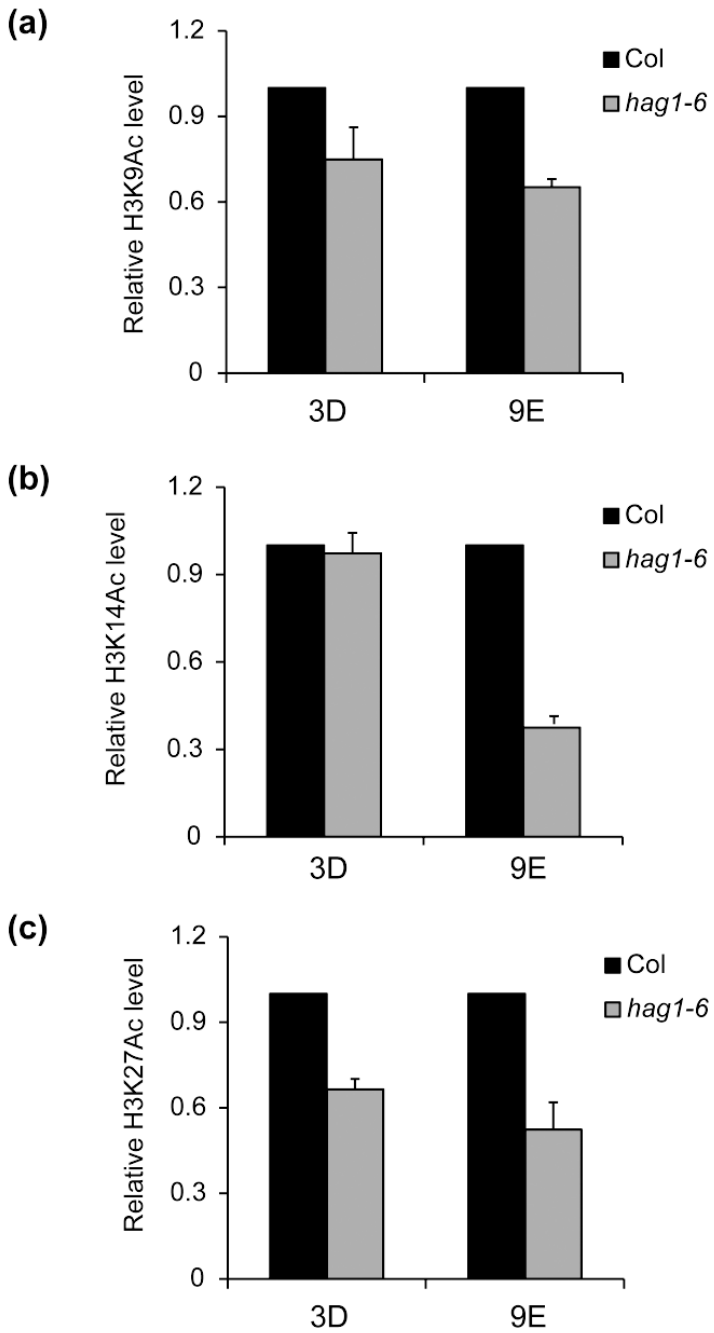
(a)
Relative H3K9Ac level
1.2
0.9
0.6
0.3
0
3D
9E
Col
hag1-6
(b)
Relative H3K14Ac level
1.2
0.9
0.6
0.3
0
3D
9E
Col
hag1-6
(c)
Relative H3K27Ac level
1.2
0.9
0.6
0.3
0
3D
9E
Col
hag1-6

Figure 2.7 H3K9Ac, H3K14Ac, H3K27Ac levels at the *SPL3* and *SPL9* loci in WT and *hag1-6*.

(a) ChIP-qPCR analysis using antibody against H3K9Ac. Regions tested are as depicted in Figure 2.3f. Shown are the means ± sd of 3 technical replicates as relative values to *Actin2/7* after normalization to input DNA (a-c). Plant samples were harvested at the seven-leaf stage (a-c).

(b) ChIP-qPCR analysis using antibody against H3K14Ac.

(c) ChIP-qPCR analysis using antibody against H3K27Ac.

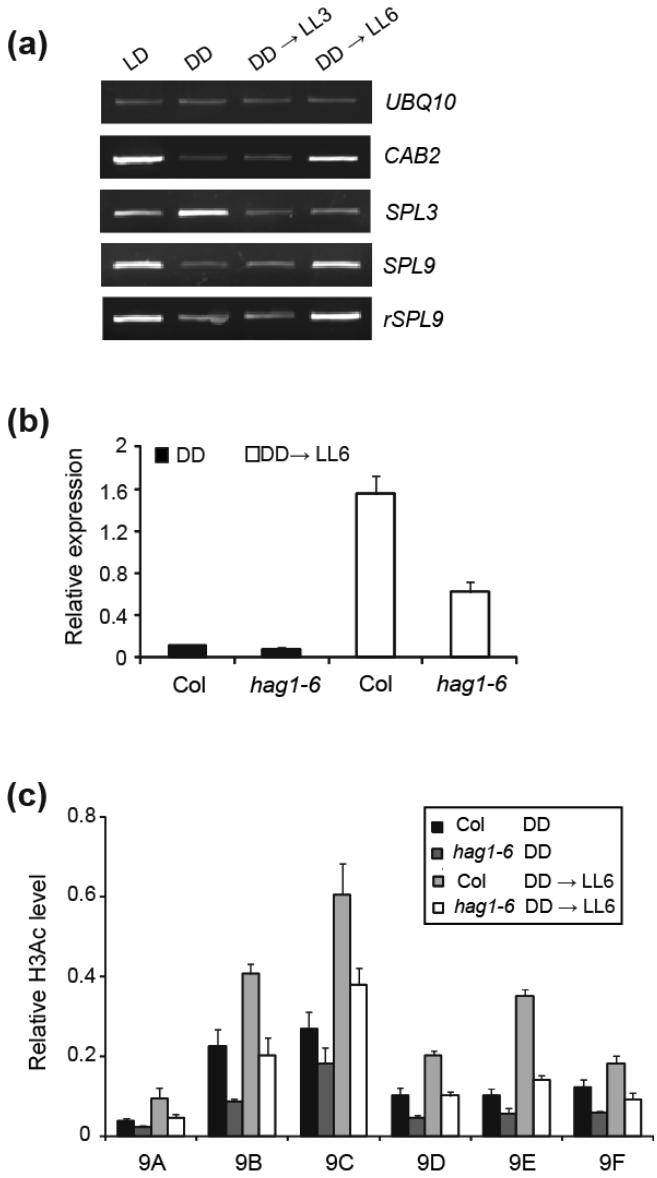
(a)
LD
DD
DD → LL3
DD → LL6
UBQ10
CAB2
SPL3
SPL9
rSPL9
(b)
DD
DD→ LL6
Relative expression
2
1.6
1.2
0.8
0.4
0
Col
hag1-6
Col
hag1-6
(c)
Relative H3Ac level
0.8
0.6
0.4
0.2
0
Col DD
hag1-6 DD
Col DD → LL6
hag1-6 DD → LL6
9A
9B
9C
9D
9E
9F

Figure 2.8 Light induction of *SPL9* is controlled by a miR156-independent epigenetic mechanism.

(a) RT-PCR analysis of *SPL3* and *SPL9* mRNA expression in *pSPL9::rSPL9* seedlings during the dark-to-light transition. Eight-day-old seedlings grown in long days were either kept in long days (LD) or transferred to darkness for 5 days without (DD) or with subsequent transfer to white light for 3 (DD → LL3) or 6 h (h; DD → LL6).

(b) RT-qPCR analysis of light-induced *SPL9* expression in WT and *hag1-6*. Two-week-old seedlings grown in LD were used for DD or DD → LL6 treatment as described in (a). Normalization was to *UBQ10*, and shown are the means ± standard error (SE) of three biological replicates.

(c) ChIP-qPCR analysis of H3Ac levels at *SPL9* in WT and *hag1-6* before and after light exposure. Plant samples were prepared as in (b). Regions tested are as depicted in Figure 2.3f. Values are the means ± SE of three biological replicates as relative values to *Actin2/7* after normalization to input DNA.

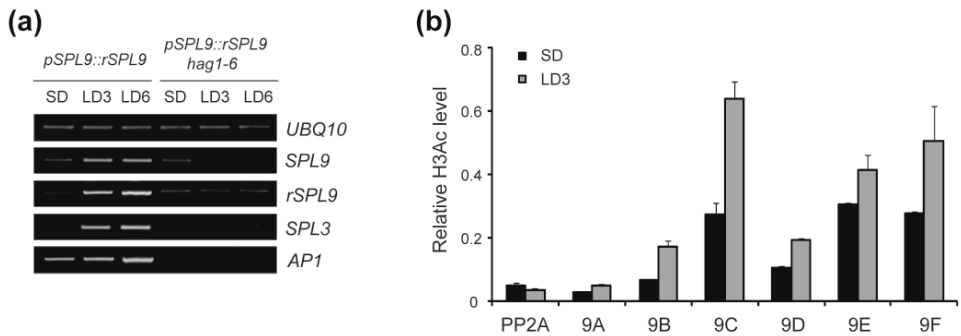

Figure 2.9 Transcriptional control of the photoperiodic induction of *SPL3* and *SPL9*.

(a) RT-PCR analysis of the transcript levels of *SPL3* and *SPL9* in *pSPL9::rSPL9* and *pSPL9::rSPL9 hag1-6* plants during photoperiodic transition. Plants grown for 4 weeks in SD were either kept in SD for 6 d (SD) or transferred to LD and further grown for 3 (LD3) or 6 d (LD6).

(b) ChIP-qPCR analysis of H3Ac levels at the *SPL9* loci in *pSPL9::rSPL9* plants during the photoperiodic transition. Plant samples were prepared as in (a). Regions tested are as depicted in Figure 2.3f. Shown are the means ± sd of 3 technical replicates as relative values to *Actin2/7* after normalization to input DNA. The data are from a representative experiment of 2 biological replicates.

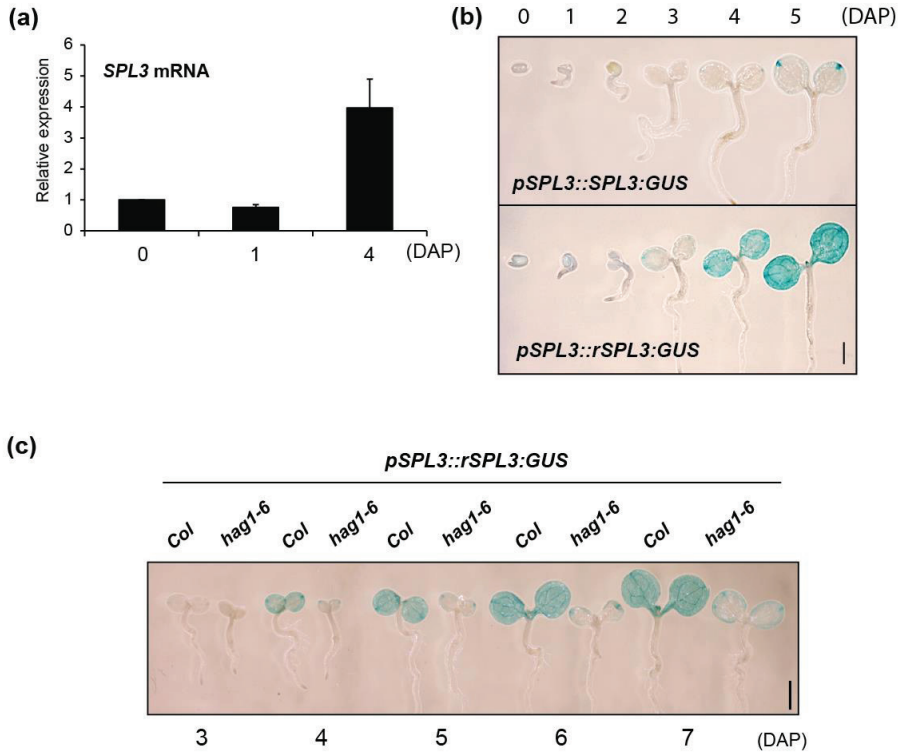
(a)
SPL3 mRNA
Relative expression
0
1
2
3
4
5
6
0
1
4
(DAP)
(b)
0 1 2 3 4 5 (DAP)
pSPL3::SPL3:GUS
pSPL3::rSPL3:GUS
(c)
pSPL3::rSPL3:GUS
Col
hag1-6
Col
hag1-6
Col
hag1-6
Col
hag1-6
Col
hag1-6
3
4
5
6
7
(DAP)
(d)
Relative H3Ac level
1 DAP
4 DAP
0
0.03
0.06
0.09
0.12
0.15
3A
3B
3C
3D
3E
(e)
Fold enrichment
1 DAP Col
4 DAP Col
1 DAP 35S::HAG1:YFP:HA hag1-6
4 DAP 35S::HAG1:YFP:HA hag1-6
0
1
2
3
4
CHS
3A
3B
3C
3D
3E

Figure 2.10 Transcriptional activation of *SPL3* by the germination-dependent targeting of HAG1.

(a) RT-qPCR analysis of *SPL3* mRNA expression during germination. Seeds were plated on Murashige and Skoog (MS) agar medium with 1% sucrose and grown for the indicated days in long day (LD) conditions.

(b) Histochemical GUS staining of transgenic plants harboring *pSPL3::SPL3:GUS* or *pSPL3::rSPL3:GUS*. Plants were grown for the indicated days in LD conditions. Scale bars: 1 mm (b, c).

(c) Histochemical GUS staining of transgenic plants harboring *pSPL3::rSPL3:GUS* in WT or *hag1-6* backgrounds. Plants were grown for the indicated days in LD conditions.

(d) ChIP-qPCR analysis of H3Ac levels at the *SPL3* locus in germinating seeds. Seed samples were prepared as in (a). Regions tested are as depicted in Figure 2.3f. The means ± standard error (SE) of three biological replicates as relative values to *UBQ11* after normalization to input DNA are shown.

(e) Targeting of HAG1:YFP:HA into *SPL3* chromatin in germinating seeds as determined by ChIP-qPCR using anti-HA antibody. Seed samples were prepared as in (a). Values are the means ± SE of three biological replicates obtained after normalization to input DNA.

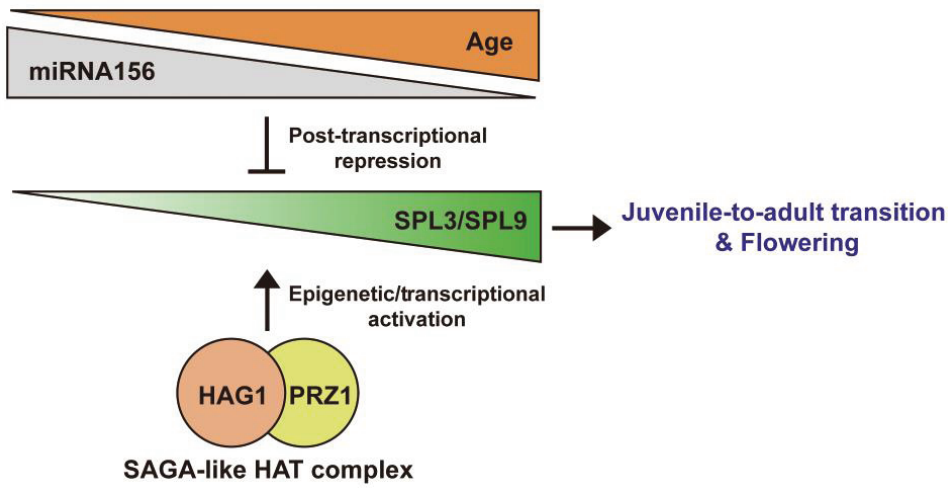

Figure 2.11 Schematic model for the regulation of *SPL3* and *SPL9* by the HAG1/PRZ1 containing SAGA-like complex.

HAG1/GCN5- and PRZ1/ADA2b-containing SAGA-like HAT complex directly controls the transcription of *SPLs*. This epigenetic control assures sufficient transcriptional output of *SPLs*. Then, the *SPL* transcript levels are subsequently fine-tuned by miR156-mediated post-transcriptional mechanism in accordance with age.

2.6 Discussion

The miR156-SPL module acts as a quantitative developmental clock that orchestrates phase transitions in Arabidopsis (Pulido & Laufs, 2010). However, accumulating evidence has shown that Arabidopsis is equipped with additional layers of regulation for SPLs. In this report, I provide evidence that HAG1 and PRZ1, Arabidopsis homologs of GCN5 and ADA2 of the SAGA complex, provide a miR156-independent transcriptional control mechanism for a group of *SPLs* through histone acetylation. Highly acetylated *SPL* chromatin seems to allow increased engagement and processivity of PolII. Although GCN5-mediated H3Ac in transcribed regions was reported to facilitate PolII progression by promoting nucleosome eviction in yeast (Sansó *et al*, 2011; Govind *et al*, 2007), HAG1/PRZ1-mediated H3Ac in the coding regions of *SPL3* and *SPL9* appears not to induce nucleosome eviction as evidenced by the comparable total H3 levels in WT and *hag1-6*.

HAG1/PRZ1-dependent histone acetylation may act as an important gear to attain the appropriate levels of *SPL* expression required for legitimate developmental phase transitions. The consistently high levels of *rSPL3* and *rSPL9* transcripts observed throughout development indicate that *SPL3* and *SPL9* transcription is facilitated by an active HAG1/PRZ1-containing complex regardless of plant age. Such robust transcription of *SPL*s may be a prerequisite for miR156-dependent post-transcriptional regulation; i.e., the HAG1/PRZ1-mediated transcriptional mechanism might be required for sufficient supply of *SPL* transcripts such that the miR156-mediated post-transcriptional mechanism can

gradually tune the final output of *SPL* transcripts in accordance with age (Figure 2.11).

Another important aspect to the HAG1/PRZ1-mediated transcription of *SPLs* might be in conveying environmental and developmental inductive cues to control phase transition. Although phase transitions are primarily related with developmental cues, plants are also able to modulate phase-transition programs depending on environmental conditions to gain higher reproductive success. This study shows that environmental changes such as shifts from dark-to-light or photoperiodic change from SD to long days (LD) can be transduced into the regulation of epigenetic status and *SPL* transcription. Moreover, I found that the initial induction of *SPL3* during post-embryonic growth is regulated by the specific targeting of HAG1-mediated histone acetylation activity. Low level of H3Ac at *SPL* loci in non-inductive conditions or developmental stages may determine the basal expression levels of *SPLs*. Upon exposure to inducing signals (such as light, photoperiod, and seed germination), HAT activity and H3Ac levels increase at *SPLs* and result in enhanced transcriptional competence. Although other, yet unrevealed, mechanisms and factors may also be required for conveying the environmental cues that lead to activation of *SPL* transcription, this study indicates that the HAG1/PRZ1-containing complex and histone acetylation are critical components of this process.

Chapter III

HAG1-mediated epigenetic reprogramming is essential for the acquisition of pluripotency in Arabidopsis

3.1 Abstract

Throughout their life cycle, plants must cope with environment where they germinated and withstand challenges that threaten their survival. To confront such challenges, plants have equipped themselves with high regenerative potential which allows them to regenerate lost parts or even whole organism upon damage. *De novo* regeneration of shoots can be achieved *in vitro* using a two-step process that involves the acquisition of pluripotency on callus induction media (CIM) and the formation of *de novo* shoots on shoot induction media (SIM). Recent reports have noted that root-meristem genes are highly induced in explants derived from even aerial tissues during incubation on CIM suggesting their potential role in establishing the pluripotency of callus. However, mechanisms underlying the induction of root genes upon callus formation and their role in *de novo* shoot regeneration remain unknown. In this study, I demonstrate that HAG1/AtGCN5 protein is induced in developing calli and plays a pivotal role in the activation of root-meristem genes. On CIM, HAG1 catalyzes histone acetylation at *WOX5/WOX14*, *SCR*, *PLT1*, and *PLT2* through direct targeting to their chromatin and activates their transcription. In turn, the transcription factors encoded by the root-meristem genes act as potency factors to establish competence for *de novo* regeneration of shoots on SIM.

3.2 Introduction

As to their sessile nature, plants are continuously exposed to environmental challenges that could threaten their survival. Therefore, plants have developed an ability to alter their developmental program in response to environmental cues. This plasticity allows most plant tissues to change their cellular fate, regenerate lost parts, and even reconstruct the entire organism.

Regeneration of tissues or whole plants can be achieved *in vitro* by modulating the ratio of two phytohormones: auxin and cytokinin (Skoog & Miller, 1957). Plant explants derived from roots, hypocotyls, cotyledons, or petals are placed on callus induction media (CIM) to acquire competence to form *de novo* organs. Next, *de novo* shoots or roots are regenerated from CIM-preincubated callus upon transfer to shoot induction media (SIM) supplemented with high cytokinin-to-auxin ratio or to high auxin-containing root induction media (RIM), respectively.

Due to its high regenerative potential, callus was long considered to be an unorganized mass of undifferentiated cells formed from virtually all plant cells. However, recent studies provided evidences that callus is formed by the proliferation of a subset of existing stem cell-like population in the pericycle adjacent to the xylem poles and shows gene expression profiles resembling those of the lateral root primordia (Atta *et al*., 2009; Sugimoto *et al*., 2010). Although a recent study has revealed the role of a few auxin-related root-meristem genes, *PLETHORAs* (*PLTs*), in *de novo* shoot regeneration (Kareem et at., 2015), the role of many other root-meristem genes induced on CIM and the molecular mechanisms underlying the acquisition of pluripotency for successful *de novo* shoot

regeneration remain unknown.

Epigenetic modifications are known to play pivotal roles in determining cellular fate. In mammals, differentiated cells are known to be generally enriched with condensed chromatin state, whereas pluripotent cells display open chromatin state and possess dynamic gene expression profiles (Gaspar-Maia *et al*., 2011). Several studies in Arabidopsis also suggest that the chromatin state of plants is also differentially regulated depending on cellular states (Zhao *et al*., 2001; Verdeil *et al*., 2007).

General Control Nonrepressed 5 (GCN5/HAG1) is a histone acetyltransferase that is well conserved in yeast, flies, plants, and mammals. HAG1 catalyzes histone acetylation on target chromatin and promotes transcriptional activation by facilitating transcription initiation and elongation (Sterner *et al*., 1999; Govind *et al*., 2007; Nagy & Tora, 2007; Sanso *et al*., 2011).

In this study, I show that HAG1 play an essential role in *de novo* shoot regeneration. Upon CIM incubation, histone acetylation at *WUSCHEL-RELATED HOMEOBOX 5* (*WOX5*)*/WOX14*, *SCARECROW* (*SCR*), *PLT1*, and *PLT2* is induced through increased HAG1 activity. This allows a high transcriptional output of the root-meristem genes on CIM which encode potency factors that establish competence for *de novo* shoot regeneration on SIM.

3.3 Materials and methods

3.3.1 Plant materials and growth conditions

hag1-6 (SALK_150784), *hag1-7* (SALK_106557), *wox7-1* (SALK_065801), *scr-3* (CS3997), and *scr-6* (SALK_032192) are all in the Columbia-0 (Col-0) background and were obtained from TAIR (http://www.arabidopsis.org). *wox14-1* (pst13645), which is in the Nossen (No) background, was obtained from RIKEN (http://www.brc.riken.jp/lab/epd/Eng). *wox5-1*, *wox5-3*, and *35::GVG-WOX5* were kind gifts from Thomas Laux (Universtät Freiburg, Germany). *pWOX::GFP-ER*, *pSCR::GFP-ER*, and *CYCB1;1:GUS* were provided by Elliot M. Meyerowitz (Caltech, USA), Ji-Young Lee (Seoul National University, South Korea), and Peter Doerner (University of Edinburgh, UK), respectively. These transgenic plants were crossed with *hag1-6*, and the plants homozygous both for the transgene and *hag1-6* were used for experiments. Seeds were germinated on Murashige and Skoog (MS) medium supplemented with 1% sucrose and buffered to pH 5.7 with 0.05% MES. Plants were grown under 100 μmol m^{-2} s^{-1} cool white fluorescent lights at 22°C in long days (LD) with a 16 hr light and 8 hr dark photoperiod.

3.3.2 Constructs and plant transformation

Construction details of the *35S::FLAG:HAG1* was previously described (Kim *et al*., 2015). *35S::FLAG:HAG1* was transformed into heterozygous *hag1-7* plants via *Agrobacterium*-mediated transformation using floral dip method (Clough & Bent, 1998). Homozygous transgenic *35S::FLAG:HAG1 hag1-7* plants were selected in the subsequent generations through genotyping.

To generate *pHAG1::HAG1:HA*, the genomic *HAG1* fragment including the 1.151 kb promoter region upstream of the start codon was amplified using HAG1 genomic entry-F (5′-CACCAGTTAAAACTGAAGCCGAACCA-3′) and HAG1 genomic entry-R (5′-TTGAGATTTAGCACCAGATTGGAG-3′) primers, cloned first into the pENTR™/SD/D-TOPO entry vector (Invitrogen), and subcloned subsequently into the pEarleyGate301 destination vector (Earley *et al*., 2006). *pHAG1::HAG1:HA* was transformed into heterozygous *hag1-6* via *Agrobacterium*-mediated transformation using floral dip method (Clough & Bent, 1998). Homozygous transgenic *pHAG1::HAG1:HA hag1-6* plants were selected in the subsequent generations. To generate the *UBI:::mCHERRY-GR-SCR*, the coding sequence of *SCR* was amplified using SCR_CDS_SalIF (5′-TTTGTCGACATGGCGGAATCCGGCGATTTCAAC-3′) and SCR_CDS_SacIR (5′-TTTGAGCTCCTAAGAACGAGGCGTCCAAGCAG-3′) primers and cloned first into the 35S-pPZP221-RbcS vector (Choi *et al*., 2012). Then, the *SCR* coding sequence and the Rubisco small subunit (RbcS) terminator was amplified using SCR_NOT1-F (5′-TTTGCGGCCGCTATGGCGGAATCCGGCGATTTCAAC-3′) and SCR_RbcS_MfeI-R (5′-TTTCAATTGCAAACATATAGTAGATGCGACG-3′) primers and subscloned into *UBI:::mCHERRY-GR-WUS* by removing the *WUS* coding sequence and the RbcS terminator with NotI and MfeI digestion and replacing them with the *SCR* coding sequence and the RbcS terminator. *UBI::mCHERRY-GR-SCR* was transformed into heterozygous *hag1-6*. Homozygous transgenic *UBI::mCHERRY-GR-SCR hag1-6* plants were selected in the subsequent generations through selection on BASTA media and genotyping.

3.3.3 Culture conditions

For callus induction, root-, cotyledon-, or hypocotyl-derived explants from 2 w- to 20 d-old seedlings were excised, transferred onto CIM, and cultured in the dark. Unless otherwise noted, the composition of CIM used in this study contains Gamborg's B5 medium with minimal organics (Sigma), 3% sucrose buffered to pH 5.7 with 0.05% MES, and 0.8% phytoagar supplemented with 0.5 mg/L 2,4-dichlorophenoxyacetic acid (2,4-D) and 0.1 mg kinetin. For shoot regeneration, root-derived explants incubated on CIM for 7 d were transferred onto SIM, and incubated under continuous fluorescent light at 22℃. SIM is consisted of Gamborg's B5 medium with minimal organics (Sigma), 3% sucrose buffered to pH 5.7 with 0.05% MES, and 0.8% phytoagar supplemented with 158 mg/L indole-3-acetic acid (IAA) and 894 mg/L N^6-(2-isopentenyl)adenine (2IP). For *de novo* root organogenesis, root-derived explants placed on CIM for 7 d were transferred onto RIM, and incubated under continuous dark at 22℃. The composition of RIM was identical to that of SIM except for 158 mg/L of IAA without 2IP. Regenerated shoots or roots were scored at indicated days after transfer onto the corresponding media.

3.3.4 Microscopy

50 μg/ml of propidium iodide was used for counterstaining of the cell outlines. Images were observed with confocal laser microscope (Carl Zeiss LSM700). At least 20 explants were observed and imaged to infer the representative pattern of each sample.

3.3.5 Immunoblot analysis

Total protein was extracted using protein extraction buffer (50 mM Tris-HCl pH 7.5, 150 mM NaCl, 10 mM $MgCl_2$, 5 mM EDTA, 0.6 mM PMSF, 80 μM MG132, proteinase inhibitor cocktail, and 10% glycerol). Protein samples were quantified using a protein assay kit (Bio-Rad), and 30 μg was subjected to western blot analysis. Anti-HA antibody (Abcam ab9110) was used at 1:3000 dilution for the detection of HAG1:HA protein.

3.3.6 Histochemical GUS assay

GUS staining was performed as described (Han *et al*, 2007). At least 30 root-derived explants were stained for each genotype to infer the representative pattern of each sample, and images were observed with stereomicroscope (Carl Zeiss STEM2000).

3.3.7 RNA sequencing analysis

Total RNA was isolated using Tri Reagent (MRC) and purified with RNeasy Mini Kit (Qiagen) to have an $OD_{260/280}$ ratio of 1.8 to 2.2. Library preparation and sequencing via Illumina HiSeq™ 2000 was performed by Beijing Genomics Institute (Hong Kong). Clean reads were mapped to the Col-0 genomic sequence (http://1001genomes.org/accessions.html) using SOAP aligner/soap2, and mismatches with no more than 2 bases were allowed in the alignment. Unless stated otherwise, differentially expressed genes (DEGs) were selected with FDR ≤ 0.001 and $|\log_2 Ratio| \geq 1$ as thresholds.

3.3.8 RT-qPCR analysis

3 μg of total RNA was reverse transcribed using M-MuLV reverse transcriptase (Fermentas) and oligo (dT) primer. Following reverse transcription (RT), quantitative PCR (qPCR) was performed on first-strand DNA with real-time PCR cycler (Qiagen Rotor Gene Q) by using SYBR Green I master mix (Kappa). Quantification using standard curves was performed to determine the amount of target genes in each sample. The transcript levels of each gene were normalized to the level of the internal control, *Ubiquitin 10* (*UBQ10*). The experiments were repeated at least three times for each gene. Gene-specific primers used for RT-qPCR analyses are as listed below.

Table 3-1 Oligonucleotides used for RT-qPCR analyses

Gene	Name	Sequence (5' to 3')
UBQ10	qUBQ10-F	GATTGTCAAGAGGAAGAGAAGGTGA
	qUBQ10-R	AAAGAGATAACAGGAACGGAAACATAGT
WOX5	WOX5-F	CCGACGTCTCTCAGATCACA
	WOX5-R	AGCTTAATCGAAGATCTAATGGCG
SCR	SCR-F	CTCTGCACTCTTTGACTCACTGG
	SCR-R	CTCCAACCGCTAATACATTCCGT
PLT1	PLT1-F	TGAGTCTTCAAGGAAACGCGAG
	PLT1-R	GAGGAGGAATCGTGAGCATTGT
PLT2	PLT2-F	GTAACCCTGGTCTGCTTCATGG
	PLT1-R	AATCGACTTTCACGGCTGGAAA
WOX14	WOX14-F	ACTAGGCATCGGTGGACTCC
	WOX14-R	AGGCTGCTTTCGTTTGGACC

3.3.9 ChIP-qPCR analysis

ChIP assays against H3Ac and HA were performed as previously described (Han *et al*., 2007; Johnson *et al*., 2002) using anti-H3Ac (Millipore 06-599) and anti-HA (Abcam ab9110) antibodies. For ChIP binding assays, β-glycerophosphate, sodium fluoride, and MG132 were added to all extraction and lysis buffers. The amount of immunoprecipitated DNA was quantified by qPCR as described in the above section. Relative amounts of each amplified product were determined by using the comparative $\Delta\Delta C_T$ method (Livak & Schmittgen, 2001). The amount of immunoprecipitated DNA was normalized to the respective input DNA (DNA isolated from chromatin that is cross-linked and fragmented under the same conditions as the immunoprecipitated DNA), and the fold enrichment was calculated by comparing the normalized value of each fragment to that of *UBQ11*. For ChIP binding assays, levels of nontransgenic control roots (R) were set to 1 after normalization to the levels of the input DNA. Primers used for ChIP-qPCR assays are listed in Table 3-2.

Table 3-2 Oligonucleotides used for ChIP-qPCR analyses

Gene	Name	Sequence (5' to 3')
UBQ11	UBQ11-F	TCAGTATATGTCTCGCAGCAAACTATC
	UBQ11-R	GACGACTCGGTCGGTCACG
WUS	WUS D-F	TCGATAGAAATGCCAAACGAC
	WUS D-R	GGATTCAACACAACGTGCAA'
WOX5	WOX A-F	CACCAAGGCTTTCTGATTATTCTTA
	WOX A-R	GATTGAAACATTGAATTTGTTCTCC
	WOX B-F	TATACACAGGCCCTAAAACGTAAAA
	WOX B-R	GAATCTGATCAGTTGTTGGAGTTCT
	WOX C-F	CCGACGTCTCTCAGATCACA
	WOX C-R	AGCTTAATCGAAGATCTAATGGCG
SCR	SCR A-F	TCCAATTCCTCTCAAGTAAAATGCC
	SCR A-R	TCAAAGTGTGGTACGATGTGCT
	SCR B-F	CTCGTCCTCCTCAATTACCCCT
	SCR B-R	GCTAGACTCTTTTATCAATGGTGGG
	SCR C-F	CTCTGCACTCTTTGACTCACTGG
	SCR C-R	CTCCAACCGCTAATACATTCCGT
PLT1	PLT1 A-F	ATGAGCTAGAACCCGTTGCATAT
	PLT1 A-R	AAACCTCAGTGAATATACGGCGA
	PLT1 B-F	TCTTCCTTTCTTCTCTGATTGGCT
	PLT1 B-R	AGGAGGCAAAGAAGAGTTGTTCG
	PLT1 C-F	TGAGTCTTCAAGGAAACGCGAG
	PLT1 C-R	GAGGAGGAATCGTGAGCATTGT

PLT2	PLT2 A-F	AAGCGAGCCATAGGTTTAACTTT
	PLT2 A-R	CCTTGCCTTACGTTCTCTCTCTAG
	PLT2 B (Ac)-F	TGATGCTTTCGATTTTACATGTCT
	PLT2 B (Ac)-R	GTGAGTTGGTGATAGAGGGAACG
	PLT2 B (binding) -F	GCCTCACATTCACTCTTCACAAAA
	PLT2 B (binding)-R	TGATGCTTTCGATTTTACATGTCT
	PLT2 C-F	GTAACCCTGGTCTGCTTCATGG
	PLT2 C-R	AATCGACTTTCACGGCTGGAAA’
WOX14	WOX14 A-F	CGGATGTAACAACAATACCTGG
	WOX14 A-R	AATCGAGTTTTACGGGTCAAGAT
	WOX14 B-F	TTCACTTTCTCATTGTCTTGTTCAT
	WOX14 B-R	CCTCAGTCATCACTCTCCCACT
	WOX14 In1-F	ACACTTGACCCATTGAGACTTTAG
	WOX14 In1-R	CGGTAGGTAAACTGTCTTCGAATG
	WOX14 C-F	ACTAGGCATCGGTGGACTCC
	WOX14 C-R	AGGCTGCTTTCGTTTGGACC

3.3.10 ChIP sequencing analysis

ChIP using anti-H3Ac antibody (Millipore 06-599) was performed as previously described (Han *et al*., 2007, Kim *et al*., 2015) except that protein agarose A beads (Santa Cruz 2001) was used instead of salmon sperm DNA/Protein A agarose beads (Upstate 16-157). Input and ChIPed DNA was eluted with 12 µl distilled water using MinElute PCR Purification Kit (Qiagen), and 2 µl of it was used for quantification using Qubit 2.0 Fluorometer (Life Technologies). Part of sample was also used for qPCR analysis to validate the enrichments patterns of known loci. 12 ng of ChIPed DNA and input DNA was pooled from 7 independent experiments, and their quality was assessed with 2100 (Agilent) and Lab ChIP GX (Caliper). Further procedures including DNA-end repair, adaptor ligation, amplification, construction of sequencing library, and sequencing using Illumina HiSeq™ 2000 were performed by Beijing Genomics Institute (Hong Kong). Sequenced reads were mapped to the reference genome of Col-0, and only uniquely mapped reads were selectively and used for analysis. Genome depth distributions of the uniquely mapped reads were obtained by BEDTools (http://bedtools.readthedocs.io/en/latest/). Aligned reads were analyzed using Model-based Analysis for ChIP-seq (MACS) to further analyze regions enriched with H3Ac peaks after normalization to the respective input DNA. ChIP seq data were visualized and analyzed using Integrated Genome Browser (IGB, http://bioviz.org/igb/index.html).

3.4 Result

3.4.1 Mutations in *HAG1* cause severely defective *de novo* shoot regeneration

To examine the role of HAG1 during *de novo* organ regeneration, I used two T-DNA insertion mutants of *HAG1* and tested for their ability to regenerate root and shoot. Both *hag1-6* and *hag1-7* mutants were capable of regenerating *de novo* roots when explants pre-incubated on CIM were transferred onto RIM (Figure 3.1a). However, *de novo* shoot regeneration was severely impaired in both mutants when CIM pre-incubated explants were transferred onto SIM (Figures 3.1a-3.1d). An overexpression of FLAG-tagged HAG1 (*35S::FLAG:HAG1 hag1-7*) and an introduction of HA-tagged HAG1 (*pHAG1::HAG1:HA hag1-6*) fully rescued the shoot regeneration defects of *hag1-7* and *hag1-6*, respectively (Figures 3.1a and 3.1b). The shoot regeneration defect of *hag1-6* was also observed when explants derived from aerial organs such as cotyledons and hypocotyls were used (Figure 3.1e). Next, I questioned if the defect of *hag1-6* could be rescued with elevated levels of exogenous cytokinin as cytokinin is well known to be essential for proper shoot regeneration. However, unlike wild type (WT; Col), *hag1-6* calli were not able to regenerate shoots even on media with high cytokinin concentrations (Figure 3.1f).

3.4.2 Global gene expression profiling reveals distinct expression dynamics in *hag1*

As an attempt to understand the role of HAG1 in *de no*vo shoot regeneration, I analyzed global gene-expression profiles of WT Col and *hag1-6* during the course

of *de novo* shoot regeneration by RNA sequencing (RNA-seq) analysis (Figure 3.2a). First, I analyzed the number of differentially expressed genes (DEGs) during the transition from roots to calli (R vs C), from calli to developing shoot progenitor cells (C vs S), and from shoot progenitor cells to visible shoots (S vs S2W). The largest number of DEGs was found in the R vs C comparison, representing a global gene-expression change during root to callus transition (Figure 3.2b). Smaller number of genes was differentially expressed in C vs S comparison, indicating that the process of early shoot regeneration accompanies differential expression of a subset of phase-specific genes. In *hag1-6*, the overall numbers of DEGs were significantly lower than in WT (Figure 3.2b). Importantly, the proportion of downregulated DEGs compared to upregulated DEGs, especially during the R to C transition, was higher in *hag1-6* than WT. While 3,783 genes were increased and 3,284 genes were decreased in WT during the R to C transition, only 1,903 genes were increased and 3,097 genes were decreased in *hag1-6* (Figure 3.2b). The increased proportion of downregulated DEGs in *hag1-6* is well correlated with the general role of HAG1 as a positive regulator of transcription.

Next, I analyzed a group of genes that showed a constant gene-expression profile at all time points (no change in gene expression; NC) in WT and *hag1-6*. The number of genes of which expression remained constant at all time points was higher in *hag1-6* (1,489 genes) compared to WT (1,002 genes) (Figure 3.2c). In this group, a large number of genes (607 genes) was specific to *hag1-6* (Figure 3.2d). Then I classified these *hag1-6*-specific NC genes based on their expression pattern in WT R vs WT C. Interestingly, the largest portion (58%) of these genes were upregulated during the R to C transition in WT (Figure 3.2e). It indicates that

many genes upregulated during callus formation in WT are not induced in developbping *hag1-6* calli and result in increased NC number in *hag1-6*. Together, the results from RNA-seq indicate that R to C transition is a crucial step in the course of *de novo* organogenesis which accompanies massive gene-expression changes and raise a possibility that HAG1 is required for the activation of many genes at this stage.

3.4.3 HAG1 plays a pivotal role on CIM

As a way to understand the role of HAG1 on CIM, I measured the expression levels of HAG1 protein during the R to C transition by immunoblot assay using the *pHAG1::HAG1:HA hag1-6* plants. HAG1 protein expression was increased during the R to C transition (Figure 3.3a). The *hag1-6* mutation resulted in the development of abnormal calli that have different texture, color, and faster growth compared to WT calli (Figure 3.3b). Consistent with the faster growth, the expression of the M/G2-phase marker *CYCB1;1* (Colón-Carmona *et al*., 1999) was higher in *hag1-6* calli than WT, indicating accelerated mitotic division (Figure 3.3c). Based on these results, I hypothesized that the main role of HAG1 on CIM might be in the activation of genes encoding potency factors that confer pluripotency in callus cells and, thus, competence for *de novo* shoot regeneration on the following SIM.

3.4.4 *WOX5* expression in calli is severely reduced in *hag1*

Root meristem genes are known to be induced upon incubation on CIM (Sugimoto *et al*., 2010). I was surprised to find from my RNA-seq data that the expression of

several genes involved in root-meristem maintenance was induced on CIM in WT but not in *hag1-6* (Figure 3.3d). Among these, the expression of *WOX5*, a quiescent center (QC)-specific gene crucial for root stem-cell maintenance, remained low at all stages in *hag1-6* (Figure 3.4a). Closer observation of *WOX5*-expression pattern using *pWOX5::GFP-ER* revealed that *WOX5* promoter activity spreads to the entire callus-forming regions on CIM in WT (Figure 3.4b). Upon transfer to SIM, *WOX5* promoter activity seemed to decrease gradually and was completely absent after 7 d on SIM. However, in *hag1-6* background, *WOX5* promoter activity was largely reduced at all time points observed. Next, I questioned whether the shoot regeneration defects of *hag1-6* observed with the aerial tissues (hypocotyl and cotyledon) are also correlated with the expression of *WOX5*, a root-specific gene. Although *WOX5* transcript levels were drastically increased upon callus induction in WT, this increase was not observed in *hag1-6* calli derived from hypocotyls and cotyledons (Figures 3.4c and 3.4d). Thus, I concluded that the shoot regeneration defect observed in root, hypocotyl, and cotyledon explants of *hag1-6* is strongly correlated with the absence of *WOX5* induction during CIM incubation.

3.4.5 *SCR* expression in calli is largely affected by *hag1* mutation

Root stem-cell niche is known to be maintained by two parallel pathways: the SCR and PLT pathways. I noted that the transcript levels of *SCR* were largely reduced on both CIM and SIM by the *hag1-6* mutation (Figure 3.5a). A closer examination of *SCR* expression in WT and *hag1-6* at various time points on CIM and SIM using *pSCR::GFP-ER* revealed that the *SCR* promoter, which is active in the endodermis and QC in roots, became activated in developing calli in the subepidermal layer but

repressed in the endodermis and QC on CIM (Figures 3.5b and 3.5c). Upon transfer onto SIM, the promoter activity of *SCR* gradually decreased and was completely absent after 7 d on SIM (Figure 3.5b). In *hag1-6*, *SCR* promoter activity was detected in the endodermis and QC at 1 d on CIM. However, its activity was largely reduced throughout later stages (Figures 3.5b and 3.5c). Next, I compared the expression of *SCR* in aerial tissue-derived calli of WT and *hag1-6*. *SCR* transcript level, which was sharply increased in CIM-incubated WT cotyledon explants, was not increased in *hag1-6* (Figure 3.5d). Transcript level of *SCR* in hypocotyl-derived calli was also reduced by *hag1-6* mutation (Figure 3.5e).

3.4.6 *PLT1* and *PLT2* transcript levels are severely reduced in *hag1*

PLT1 and *PLT2* were reported to be required for acquiring the competence to regenerate shoot progenitor cells (Kareem *et al*., 2015). The transcript levels of *PLT1* and *PLT2* were drastically increased upon CIM incubation in the root-, hypocotyl-, and cotyledon-derived calli in WT Col (Figures 3.6a-3.6f). However, their transcript levels were reduced in *hag1-6*, especially on CIM (Figures 3.6a-3.6f). These results indicate that the reduced *PLT1* and *PLT2* transcript levels in *hag1-6* are also correlated with the shoot- regeneration defect of *hag1-6*.

3.4.7 Genome-wide H3Ac profile of WT and *hag1* calli

To understand the role of HAG1 in the reprogramming of the epigenome during callus formation, I generated genome-wide maps of histone H3 acetylation (H3Ac) by chromatin immunoprecipitation (ChIP) followed by high-throughput DNA sequencing (ChIP-seq) using WT and *hag1-6* calli (Figures 3.7a-3.7c). H3Ac was

highly enriched at the transcription start site (TSS) in both WT and *hag1-6* (Figures 3.7a and 3.7b). In accordance with previous reports which have defined HAG1 as a gene-specific coactivator required for the expression of subset of genes rather than a global transcriptional regulator (Lee *et al*., 2000; Krebs *et al*., 2011; Bonnet *et al*., 2014), overall H3Ac-enrichment pattern in *hag1-6* was comparable to WT across all the five chromosomes of Arabidopsis, although some specific loci with lower H3Ac levels in *hag1-6* were also observed (Figures 3.7b and 3.7c).

3.4.8 H3Ac within *WOX5*, *SCR*, *PLT1*, and *PLT2* chromatin is directly controlled by HAG1

My ChIP-seq results showed that H3Ac levels within *WOX5, SCR, PLT1,* and *PLT2* chromatin are reduced in *hag1-6* calli compared to WT (Figures 3.8a-3.8d). For more detailed analysis of these loci, then I performed ChIP-qPCR analysis using WT and *hag1-6* roots, CIM-, and SIM-incubated explants. In WT, H3Ac levels at these loci were increased upon CIM incubation with highest levels in the TSS of these genes (Figures 3.8e-3.8h). However, in *hag1-6*, the H3Ac levels were lower compared to WT, specifically in CIM-incubated explants.

Next, I investigated whether *WOX5*, *SCR*, *PLT1*, and *PLT2* are direct targets of HAG1. ChIP assays using anti-HA antibody revealed that HAG1:HA protein indeed associates directly with the promoters and transcribed regions of *WOX5*, *SCR*, *PLT1*, and *PLT2*, but not with a negative control locus *WUS* (Figures 3.9a-3.9f). Importantly, the targeting of HAG1:HA to *WOX5*, *SCR*, *PLT1*, and *PLT2* loci was detected in CIM-incubated explants. This result is in concordance with the induction of HAG1 protein in CIM-incubated explants (Figure 3.3a) and also with

the preferential reduction of H3Ac levels in *hag1-6* explants on CIM (Figures 3.8e-3.8h).

3.4.9 *WOX5* and *WOX14* act redundantly in the control of *de novo* shoot regeneration

To reveal the link between the reduced expression of *WOX5* in *hag1-6* and the shoot-regeneration defect of *hag1* mutants, I obtained two T-DNA insertion mutants of *WOX5* and analyzed their shoot-regeneration phenotypes. Both *wox5-1* and *wox5-3* showed minor defects in shoot regeneration when the assays were performed using root explants, although the defects were more pronounced when hypocotyl explants were used (Figures 3.10a and 3.10b). Then, I assumed that other members of the *WOX* family might act redundantly with *WOX5* in conferring pluripotency to callus required for *de novo* shoot regeneration. Among the 15 *WOX*-family genes, *WOX7* and *WOX14* were chosen for test because these genes showed similar expression patterns with *WOX5* in WT and *hag1-6* calli (Figures 3.10c and 3.10d). When each single and *wox5-3 wox7-1 wox14-1* triple mutants were subjected to shoot-regeneration assay, *wox14-1* and the triple mutants showed severely impaired shoot-regeneration phenotypes (Figure 3.10e). Thus, *WOX5* and *WOX14* seem to have redundant roles, with *WOX14* major, in conferring competence for *de novo* shoot regeneration.

Next, I questioned if HAG1 also catalyzes histone acetylation at the *WOX14* locus. In WT, H3Ac levels were increased during CIM incubation, especially in the TSS of *WOX14* (Figures 3.10f and 3.10g). However, in *hag1-6*, H3Ac levels were not increased during CIM incubation and remained lower than WT. Moreover,

HAG1:HA protein enrichment at *WOX14* was detected only during CIM incubation (Figure 3.10h). Taken together, these results demonstrate that H3Ac catalyzed by HAG1 induces the transcriptional activation of *WOX5* and *WOX14*, two members of the *WOX*-family genes acting redundantly in conferring pluripotency to callus.

3.4.10 *WOX5* and *SCR* have additive roles in *de novo* shoot regeneration

As *SCR* displayed similar expression dynamics with *WOX5* during the course of *de novo* organogenesis, I studied if *SCR* also plays a role in *de novo* shoot regeneration by observing the phenotypes of two *scr* mutants; the *scr-3* with a nonsense mutation and the *scr-6* with a T-DNA insertion (Figure 3.11a). Compared to the previously reported *scr-3*, *scr-6* mutants displayed more severe phenotypes including smaller plant size and arrested root growth (Figure 3.11b). In correlation with the severity of plant phenotypes, *de novo* shoot regeneration was partially impaired in *scr-3*, whereas in *scr-6*, it was completely abolished (Figures 3.11c-3.11e). As the weak allele of *scr* mutants, *scr-3*, allowed for a chance to test genetic relationship between *WOX5* and *SCR*, then I made the *wox5-3 scr-3* double mutant through crossing and subject it to shoot-regeneration assay. *De novo* shoot regeneration as well as primary root growth were more severely impaired in *wox5-3 scr-3* compared to each single mutant (Figures 3.12a-3.12e). In concordance with the phenotypes, transcript levels of *PLT1* and *PLT2* in calli were additively reduced in *wox5-3 scr-3* compared to each single mutant (Figures 3.12f and 3.12g). Therefore, these results indicate that *WOX5* and *SCR* have additive roles in *de novo* shoot regeneration.

3.4.11 Activation of WOX5 on CIM partially rescues the shoot regeneration defect of *hag1*

As another way to test if *WOX5* and *SCR* might act as potency determining factors, I introgressed the dexamethasone (DEX)-inducible *UBI::mCHERRY-GR-SCR* and *35S::GVG-WOX5* into *hag1-6* from WT Col background and analyzed shoot regeneration phenotypes (Figures 3.13a-3.13c). Activation by DEX-induced nuclear translocalization of SCR did not rescue the shoot-generation defect of *hag1-6* (Figure 3.13a). However, the activation of WOX5 on CIM but not on SIM partially rescued the shoot-regeneration defect of *hag1-6* both in hypocotyl- and root-derived explants (Figure 3.13b). The DEX treatment induced the formation of pale shoot-like structures on *hag1-6* calli (Figure 3.13c). Although other yet-to-be-known factors are also likely to be required for complete rescue of the shoot-regeneration defect of *hag1-6*, the results above strongly support the notion that deactivation of *WOX5* expression in *hag1-6* callus should be a partial reason for its defect in shoot regeneration and WOX5 is one of the potency factors conferring regenerative competence in callus.

3.5 Figures

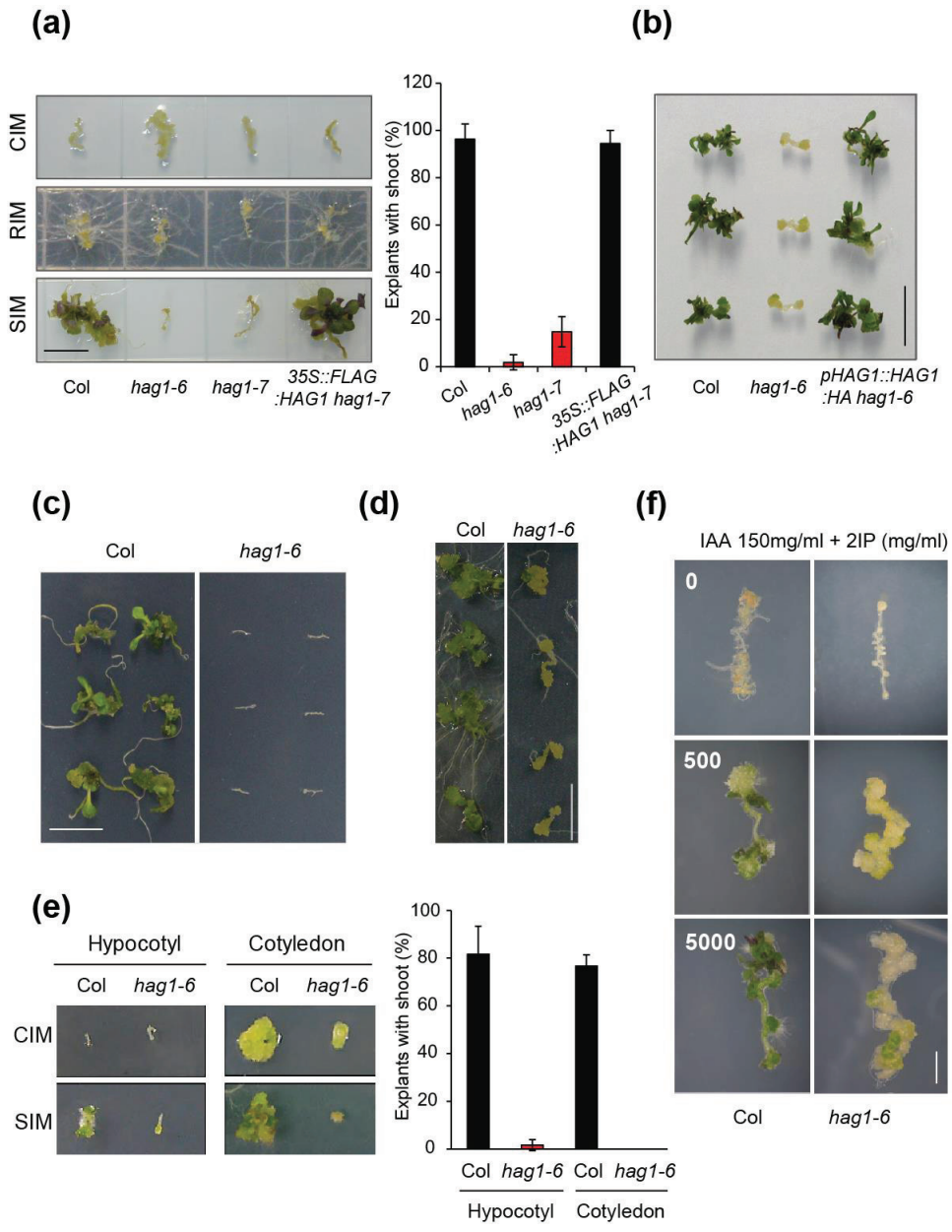
(a)
CIM
RIM
SIM
Col
hag1-6
hag1-7
35S::FLAG :HAG1 hag1-7
Explants with shoot (%)
120
100
80
60
40
20
0
Col
hag1-6
hag1-7
35S::FLAG :HAG1 hag1-7
(b)
Col
hag1-6
pHAG1::HAG1 :HA hag1-6
(c)
Col
hag1-6
(d)
Col
hag1-6
(e)
Hypocotyl
Cotyledon
Col
hag1-6
Col
hag1-6
CIM
SIM
Explants with shoot (%)
100
80
60
40
20
0
Col
hag1-6
Col
hag1-6
Hypocotyl
Cotyledon
(f)
IAA 150mg/ml + 2IP (mg/ml)
0
500
5000
Col
hag1-6

Figure 3.1 Mutations in *hag1* cause severe defects in *de novo* shoot regeneration.

(a) Callus, *de novo* shoot, and root formation in wild-type (WT; Col), *hag1-6*, *hag1-7*, and *35S::FLAG:HAG1 hag1-7* root explants. Root explants were transferred onto callus induction media (CIM) for 1 week (w) and then transferred onto fresh CIM, shoot induction media (SIM), or root induction media (RIM) for callus, *de novo* shoot, or root induction, respectively. Graph on right shows the percentage of explants with shoots scored at 18 days (d) on SIM. Scale bar: 1 cm.

(b) *De novo* shoot regeneration using Col, *hag1-6,* and *pHAG1::HAG1:HA hag1-6* root explants. Shoot regeneration assay was performed as in (a). Scale bar: 1 cm.

(c) *De novo* shoot regeneration assay using Col and *hag1-6* root explants on CIM and SIM with different composition. Root segments were cut and transferred onto CIM containing 2.2 mM 2,4-dichlorophenoxyacetic acid (2,4-D) and 0.2 mM kinetin for 4 d and then transferred onto SIM containing 5.0 mM isopentenyladenine (2IP) and 0.9 mM indole-3-acetic acid (IAA). Scale bar: 1 cm.

(d) *De novo* shoot regeneration assay using Col and *hag1-6* on Murashige and Skoog (MS)-based CIM and SIM. Root explants were transferred onto MS-based CIM (instead of Gamborg's B5) for 4 d and then transferred onto MS-based SIM. Scale bar: 1 cm.

(e) *De novo* shoot regeneration in Col and *hag1-6* cotyledon or hypocotyl explants. Graph on right shows the percentage of explants with shoots scored at 18 d on SIM. Scale bar: 1 cm.

(f) Shoot regeneration assay using Col and *hag1-6* root explants on media with different cytokinin (2IP) to auxin (IAA) ratios. Col and *hag1-6* root explants were

transferred onto 150 mg/ml IAA-containing media supplemented with 0, 500, or 5,000 mg/ml 2IP. Scale bar: 2 mm.

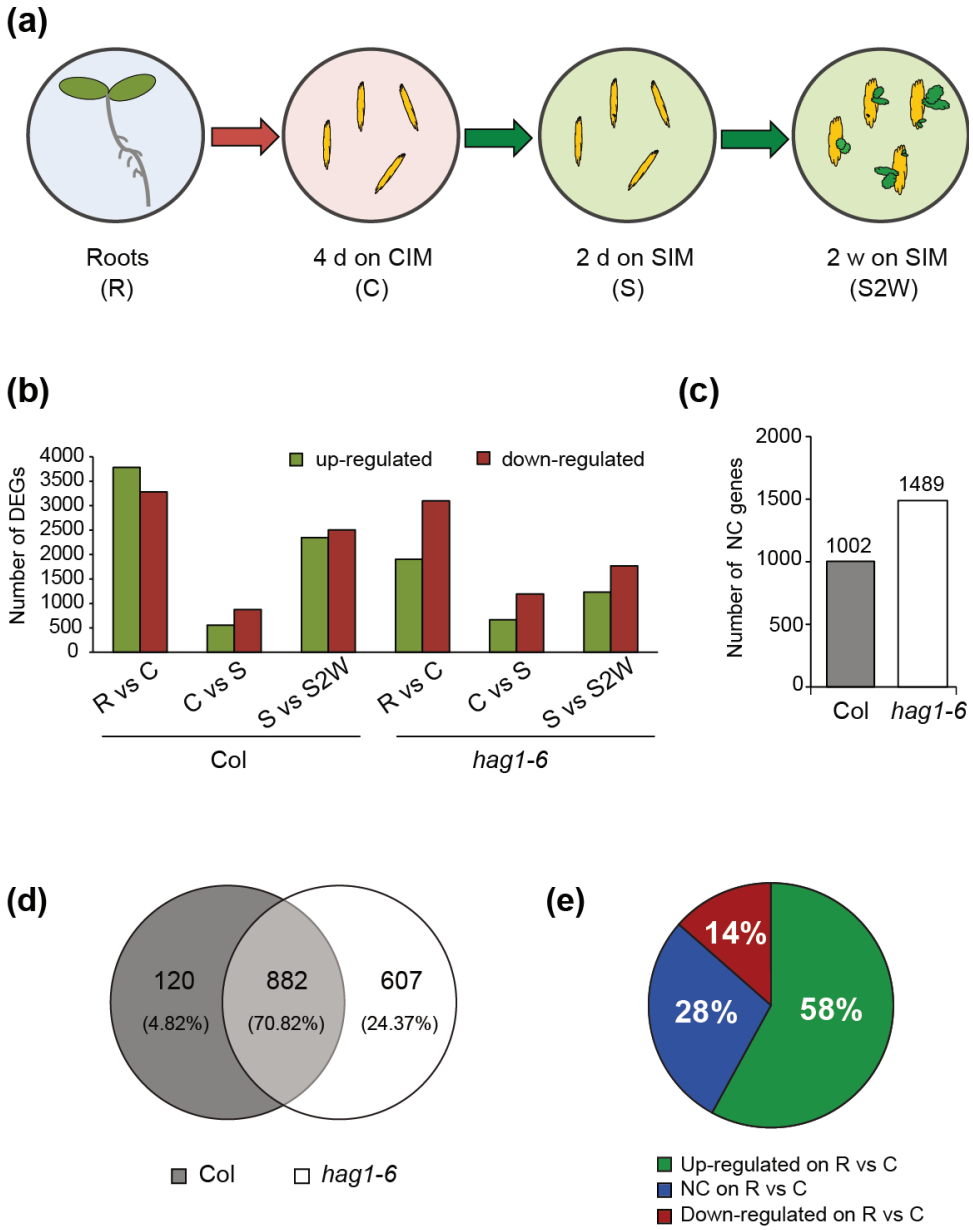
(a)
Roots
(R)
4 d on CIM
(C)
2 d on SIM
(S)
2 w on SIM
(S2W)
(b)
Number of DEGs
4000
3500
3000
2500
2000
1500
1000
500
0
up-regulated
down-regulated
R vs C
C vs S
S vs S2W
R vs C
C vs S
S vs S2W
Col
hag1-6
(c)
Number of NC genes
2000
1500
1000
500
0
1002
1489
Col
hag1-6
(d)
120
(4.82%)
882
(70.82%)
607
(24.37%)
Col
hag1-6
(e)
14%
28%
58%
Up-regulated on R vs C
NC on R vs C
Down-regulated on R vs C

Figure 3.2 Global gene expression profiling reveals distinct expression dynamics in *hag1*.

(a) Schematics illustrating sample preparation for the RNA-seq analyses.

(b) Statistic chart of differentially expressed genes (DEGs) in Col and *hag1-6* (green: up- regulated genes, $\log_2$ ratio ≤ 1; red: down-regulated genes, $\log_2$ ratio ≥ 1; FDR < 0.05).

(c) Number of genes representing no-change in expression (NC) in Col and *hag1-6*.

(d) Venn-diagram of the comparison of NC genes either overlapping or non-overlapping between Col and *hag1-6*.

(e) Classification of the NC genes of *hag1-6* based on their expression patterns in Col R vs Col C.

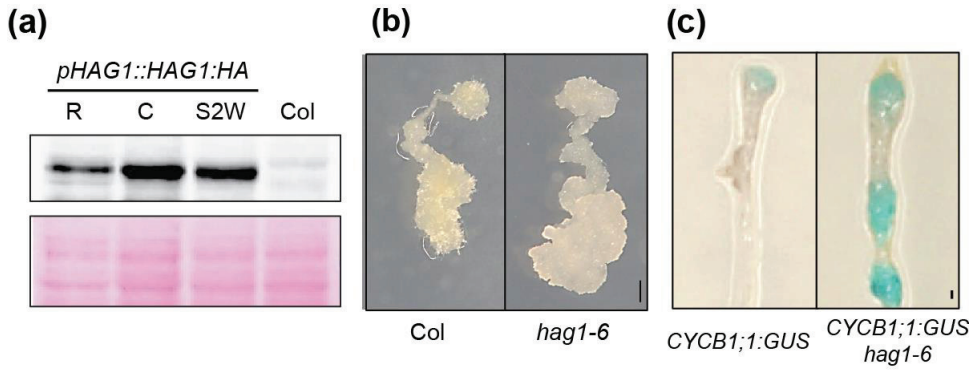

(d)

Gene	Col				*hag1-6*			
	R	C	S	S2W	R	C	S	S2W
WOX5	27	**377**	670	6	15	**86**	10	1
PLT1	129	**1275**	1042	24	110	**426**	352	4
PLT2	93	**535**	218	22	87	**256**	60	3
SHR	403	**1282**	1196	325	334	**482**	747	514
SCR	641	**577**	980	249	399	**288**	169	124

Figure 3.3 HAG1 plays a pivotal role on CIM.

(a) Immunoblot analysis of HAG1:HA protein. Roots (R), 1 w CIM-incubated root explants (C), and 1 w CIM-incubated + 2 w SIM-incubated root explants (S2W) of *pHAG1::HAG1:HA* were subjected to immunoblot analysis using α-HA antibody. 1 w CIM-incubated Col root explants (Col) were used as negative control. Ponceau staining was performed as loading control.

(b) Callus phenotype of *hag1-6*. Col and *hag1-6* root explants had been transferred onto CIM for 4 w before taken picture. Scale bar: 1 mm.

(c) Histochemical GUS staining of *CYCB1;1:GUS* and *CYCB1;1:GUS hag1-6* root explants at 4 d on CIM. Scale bar: 1 mm

(d) Reduced expression of root meristem genes in *hag1-6* as revealed by RNA-seq. Numbers represent normalized read counts.

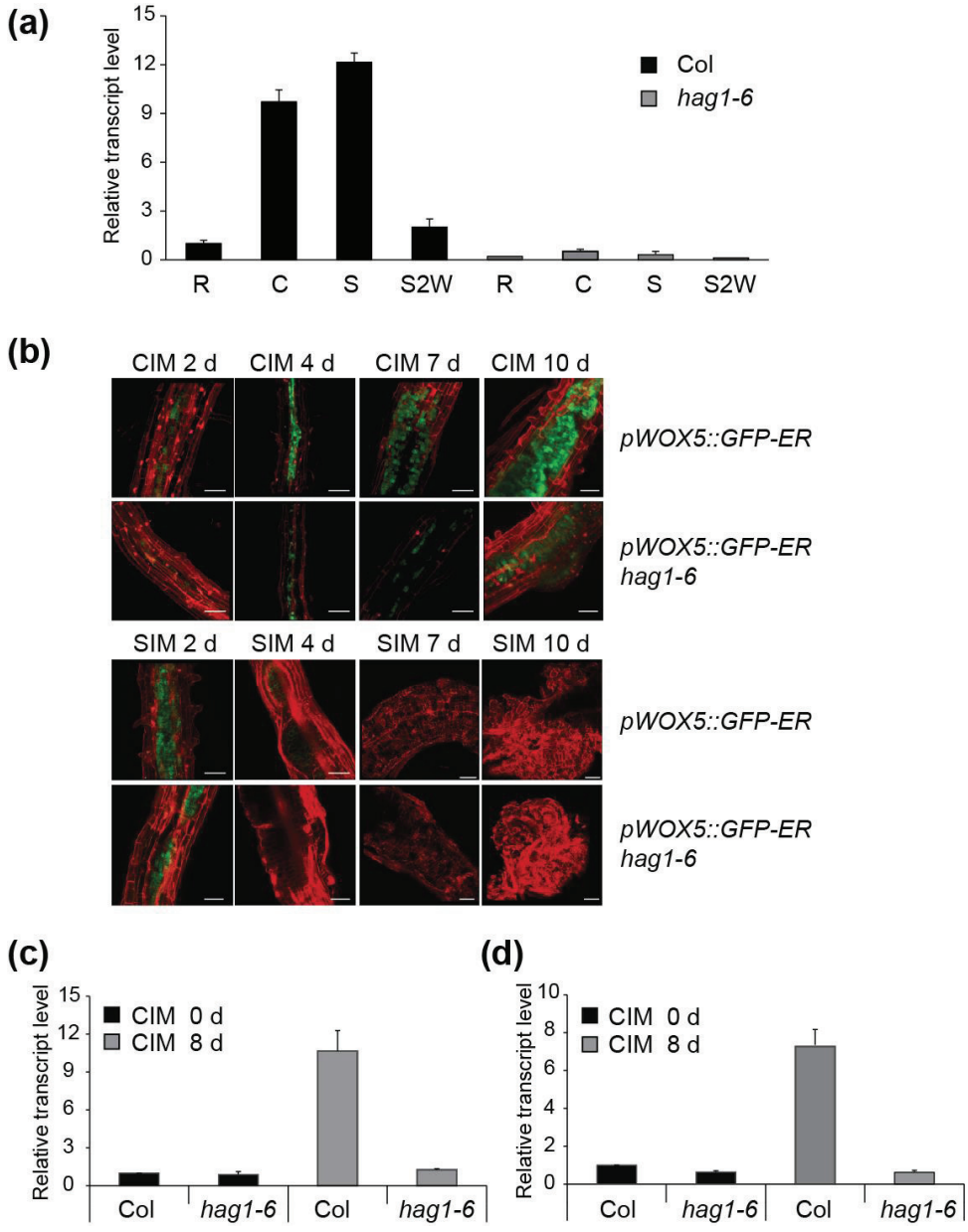
(a)
Relative transcript level
15
12
9
6
3
0
Col
hag1-6
R
C
S
S2W
R
C
S
S2W
(b)
CIM 2 d
CIM 4 d
CIM 7 d
CIM 10 d
pWOX5::GFP-ER
pWOX5::GFP-ER
hag1-6
SIM 2 d
SIM 4 d
SIM 7 d
SIM 10 d
pWOX5::GFP-ER
pWOX5::GFP-ER
hag1-6
(c)
Relative transcript level
15
12
9
6
3
0
CIM 0 d
CIM 8 d
Col
hag1-6
Col
hag1-6
(d)
Relative transcript level
10
8
6
4
2
0
CIM 0 d
CIM 8 d
Col
hag1-6
Col
hag1-6

Figure 3.4 *WOX5* expression is severely reduced in *hag1*.

(a) Transcript level of *WOX5* in Col and *hag1-6* roots (R), 4-d CIM explants (C), 4-d CIM + 2-d SIM explants (S), and 4-d CIM + 2-w SIM explants (S2W) as determined by reverse transcription followed by quantitative polymerase chain reaction (RT-qPCR) analysis. Level of Col R was set to 1 after normalization with *Ubiquitin 10* (*UBQ10*). Values are the means ± SE of three biological replicates.

(b) *pWOX5::GFP-ER* expression in Col and *hag1-6* at various time points on CIM and SIM. Cellular outlines were visualized with propidium iodide (PI) staining (red). Scale bars: 50 μm.

(c and d) Transcript levels of *WOX5* in Col and *hag1-6* hypocotyl (c) and cotyledon (d) explants at indicated days on CIM. Col levels at CIM 0 d were set to 1 after normalization with *UBQ10*. Values are the means ± SE of three biological replicates.

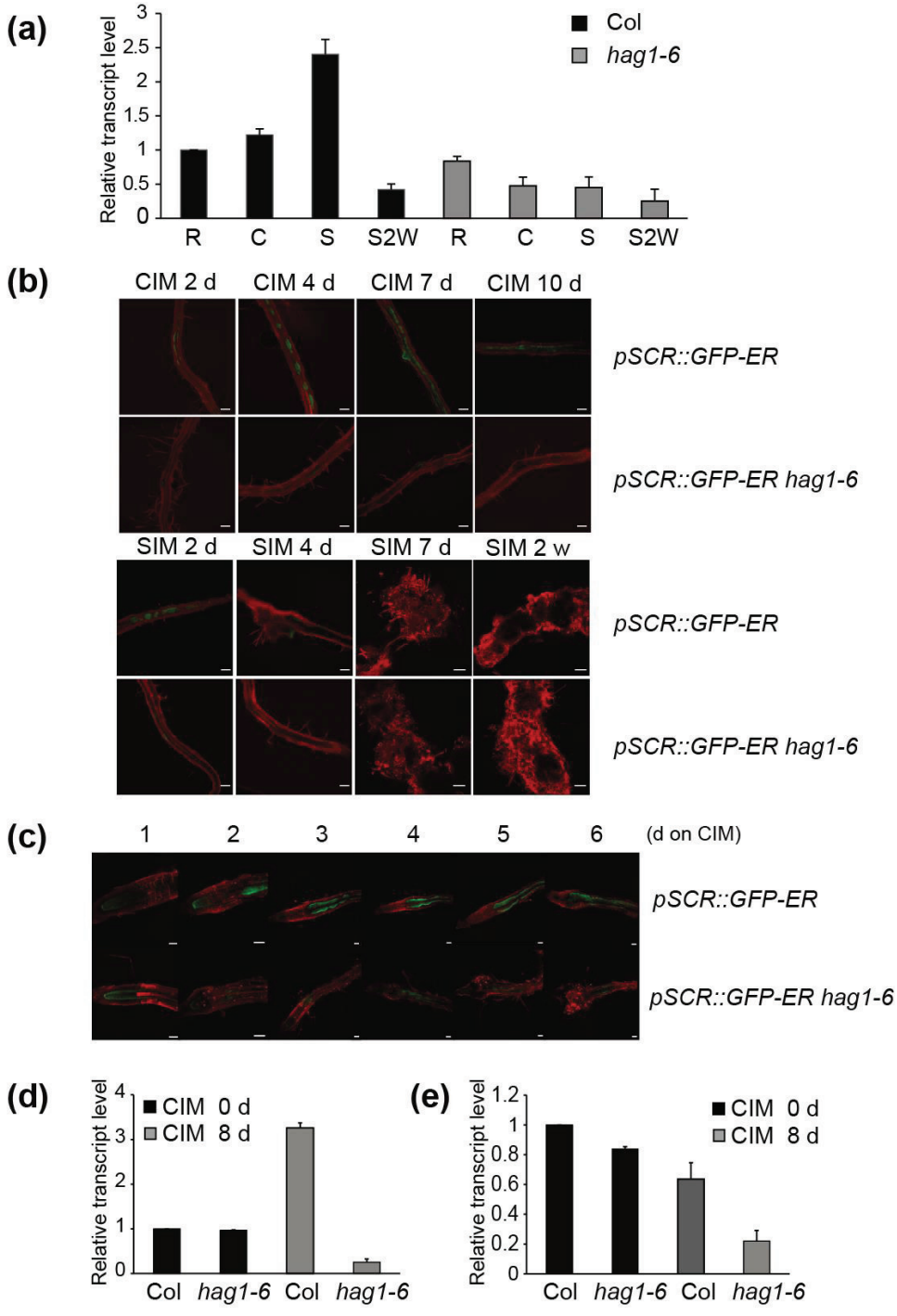
(a)
Relative transcript level
3
2.5
2
1.5
1
0.5
0
R
C
S
S2W
R
C
S
S2W
Col
hag1-6
(b)
CIM 2 d
CIM 4 d
CIM 7 d
CIM 10 d
pSCR::GFP-ER
pSCR::GFP-ER hag1-6
SIM 2 d
SIM 4 d
SIM 7 d
SIM 2 w
pSCR::GFP-ER
pSCR::GFP-ER hag1-6
(c)
1
2
3
4
5
6
(d on CIM)
pSCR::GFP-ER
pSCR::GFP-ER hag1-6
(d)
Relative transcript level
4
3
2
1
0
CIM 0 d
CIM 8 d
Col
hag1-6
Col
hag1-6
(e)
Relative transcript level
1.2
1
0.8
0.6
0.4
0.2
0
CIM 0 d
CIM 8 d
Col
hag1-6
Col
hag1-6

Figure 3.5 *SCR* expression in callus is largely affected by *hag1* mutation.

(a) Transcript level of *SCR* in Col and *hag1-6* roots (R), 4-d CIM explants (C), 4-d CIM + 2-d SIM explants (S), and 4-d CIM + 2-w SIM explants (S2W). Level of Col R was set to 1 after normalization with *UBQ10*. Values are the means ± SE of three biological replicates.

(b) *pSCR::GFP-ER* expression in Col and *hag1-6* at various time points on CIM and SIM. Cellular outlines were visualized with PI staining. Scale bars: 50 μm.

(c) *pSCR::GFP-ER* expression in Col and *hag1-6* root tips at indicated days on CIM.

(d and e) Transcript levels of *SCR* in Col and *hag1-6* hypocotyl (d) and cotyledon (e) explants at indicated days on CIM. See Figures 3.4c and 3.4d for data presentation.

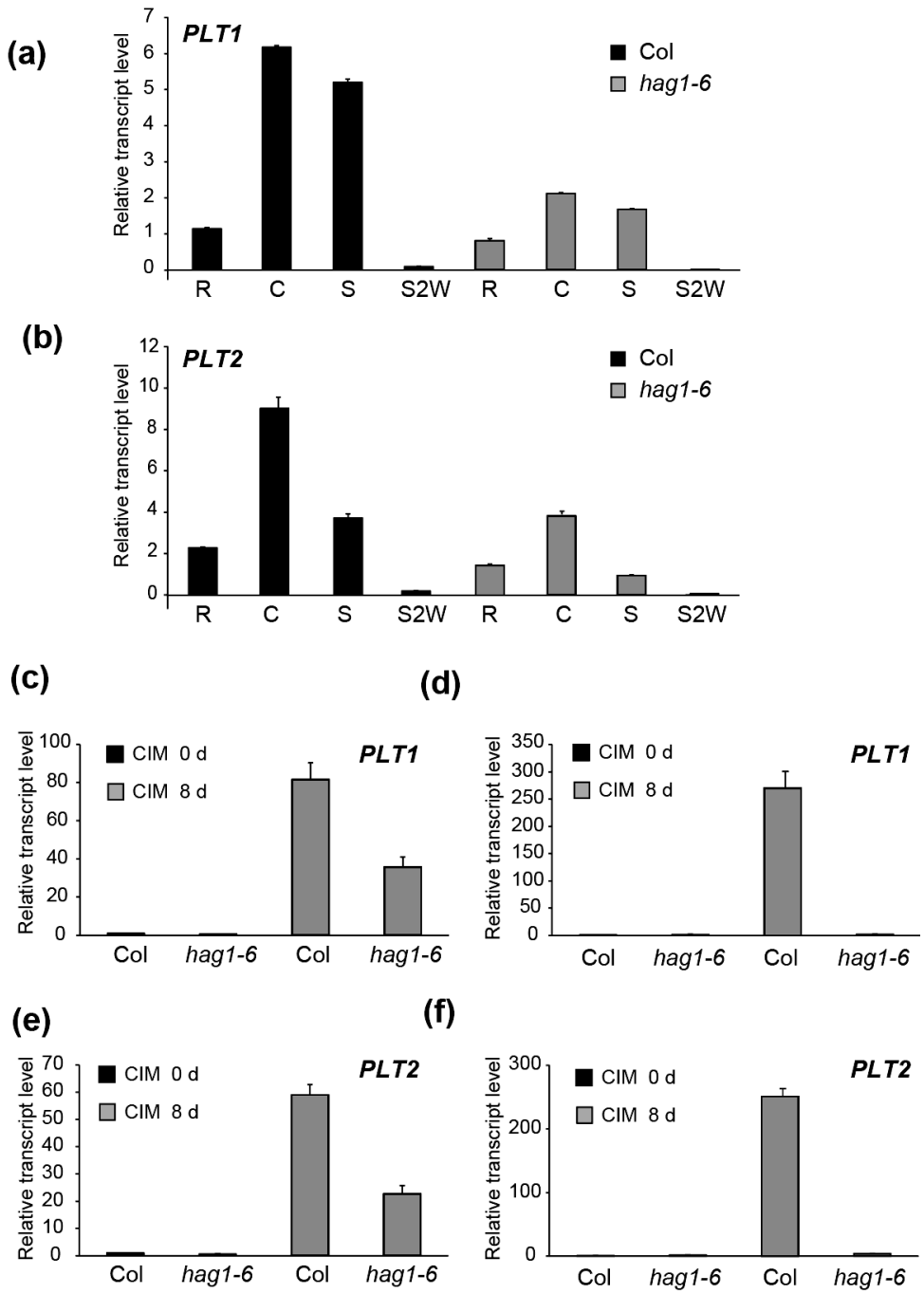
(a)
PLT1
Relative transcript level
Col
hag1-6
R
C
S
S2W
(b)
PLT2
(c)
(d)
CIM 0 d
CIM 8 d
(e)
(f)

Figure 3.6 *PLT1* and *PLT2* expressions in callus are largely affected by *hag1* mutation.

(a and b) Transcript levels of *PLT1* (a) and *PLT2* (b) in Col and *hag1-6* roots (R), 4-d CIM explants (C), 4-d CIM + 2-d SIM explants (S), and 4-d CIM + 2-w SIM explants. Levels of Col R were set to 1 after normalization with *UBQ10*. Values are the means ± SE of three biological replicates.

(c-f) Transcript levels of *PLT1* (c and d) and *PLT2* (e and f) in Col and *hag1-6* hypocotyl (c and e) and cotyledon (d and f) explants at indicated days on CIM. Col levels at CIM 0 d were set to 1 after normalization with *UBQ10*. Values are the means ± SE of three biological replicates.

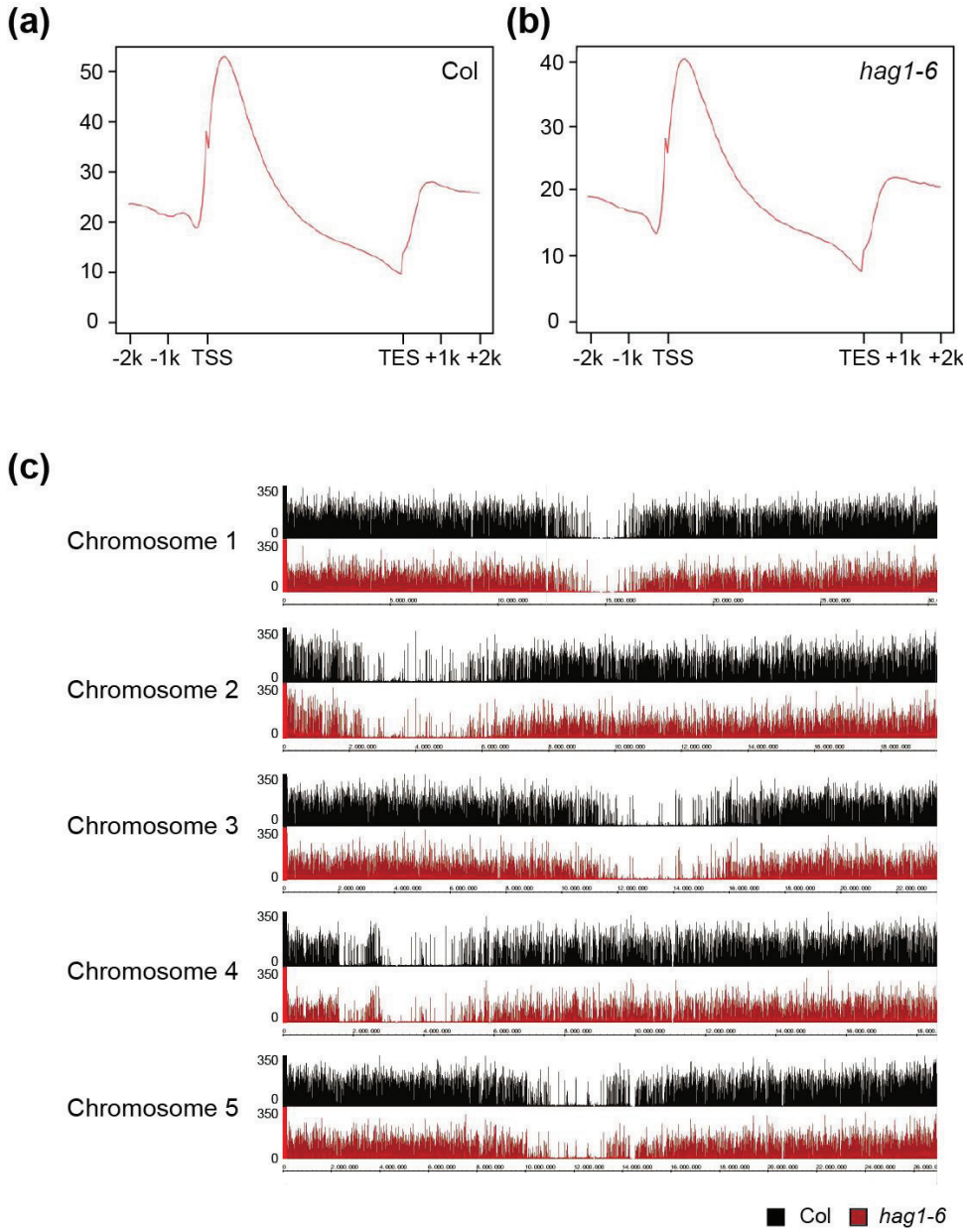
(a)
Col
50
40
30
20
10
0
-2k -1k TSS
TES +1k +2k
(b)
hag1-6
40
30
20
10
0
-2k -1k TSS
TES +1k +2k
(c)
Chromosome 1
Chromosome 2
Chromosome 3
Chromosome 4
Chromosome 5
350
0
Col
hag1-6

Figure 3.7 Genome-wide H3Ac enrichment in WT and *hag1-6* calli.

(a and b) Gene depth distribution of H3Ac in Col (a) and *hag1-6* (b). TSS and TES indicate transcription start site and transcription end site, respectively.

(c) Genome-wide enrichment of H3Ac in Col and *hag1-6* over the five Arabidopsis chromosomes.

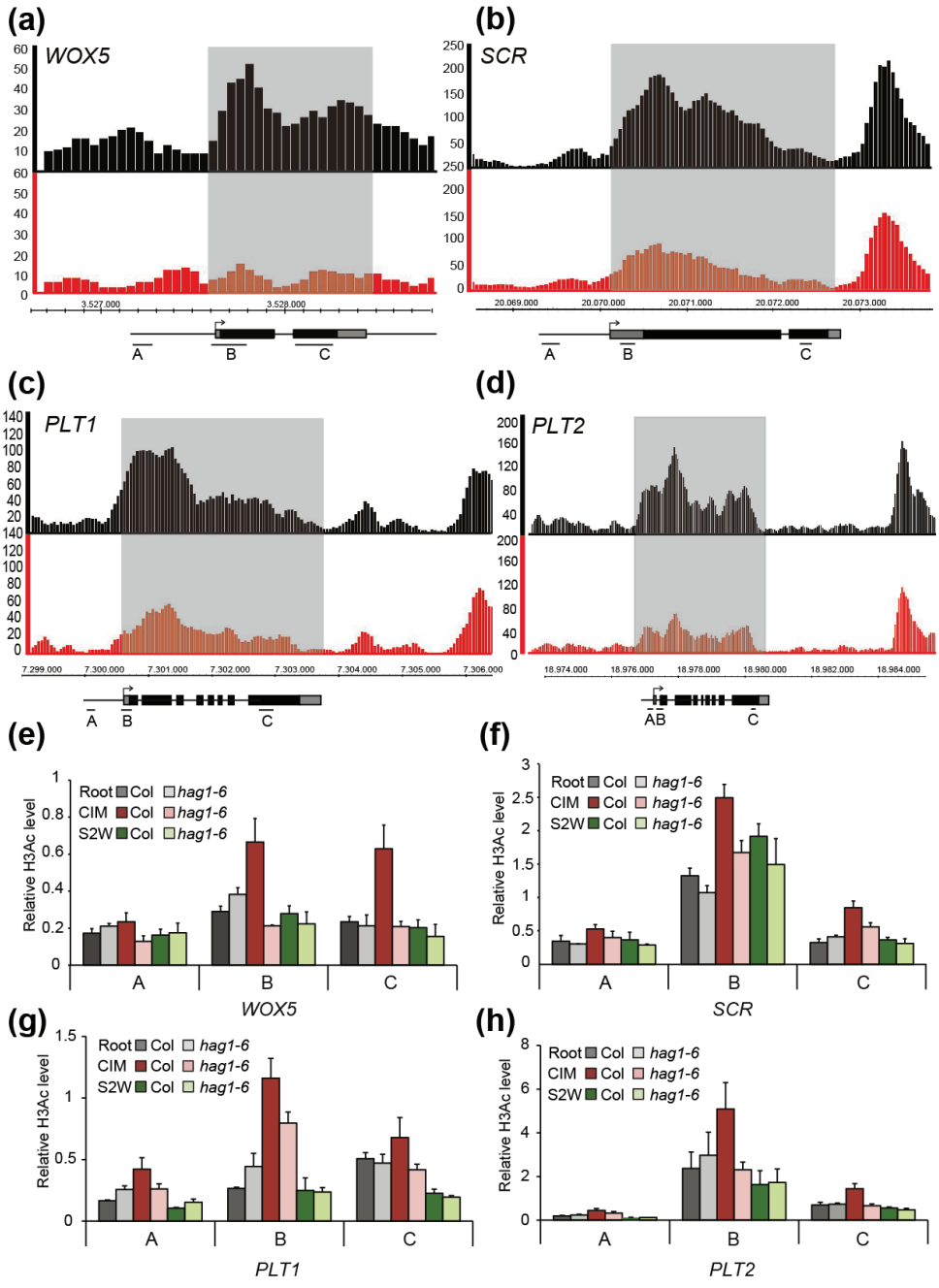
(a)
WOX5
(b)
SCR
(c)
PLT1
(d)
PLT2
(e)
Relative H3Ac level
Root Col hag1-6
CIM Col hag1-6
S2W Col hag1-6
A
B
C
WOX5
(f)
SCR
(g)
PLT1
(h)
PLT2

Figure 3.8 H3Ac is reduced at *WOX5*, *SCR*, *PLT1*, and *PLT2* loci in *hag1* compared to WT.

(a-d) H3Ac enrichment as determined by ChIP-seq at *WOX5* (a), *SCR* (b), *PLT1* (c), and *PLT2* (d) loci in Col (upper black diagram) and *hag1-6* (lower red diagram) calli. Schematic representation of each locus is depicted at the bottom. Exons are indicated as boxes whereas intergenic sequences and introns are marked with lines. 5' and 3' UTRs are represented as gray boxes. Transcription start sites are indicated with arrows.

(e-h) ChIP followed by qPCR (ChIP-qPCR) analysis of H3Ac levels at *WOX5* (e), *SCR* (f), *PLT1* (g), and *PLT2* (h) loci in Col and *hag1-6.* Root, 1-w CIM (CIM), and 1-w CIM + 2-w SIM (S2W) samples were used for the assays. Regions tested are indicated in the schematics (a-d). Values are the means ± SE of three biological replicates as relative values to *UBQ11* after normalization to input DNA.

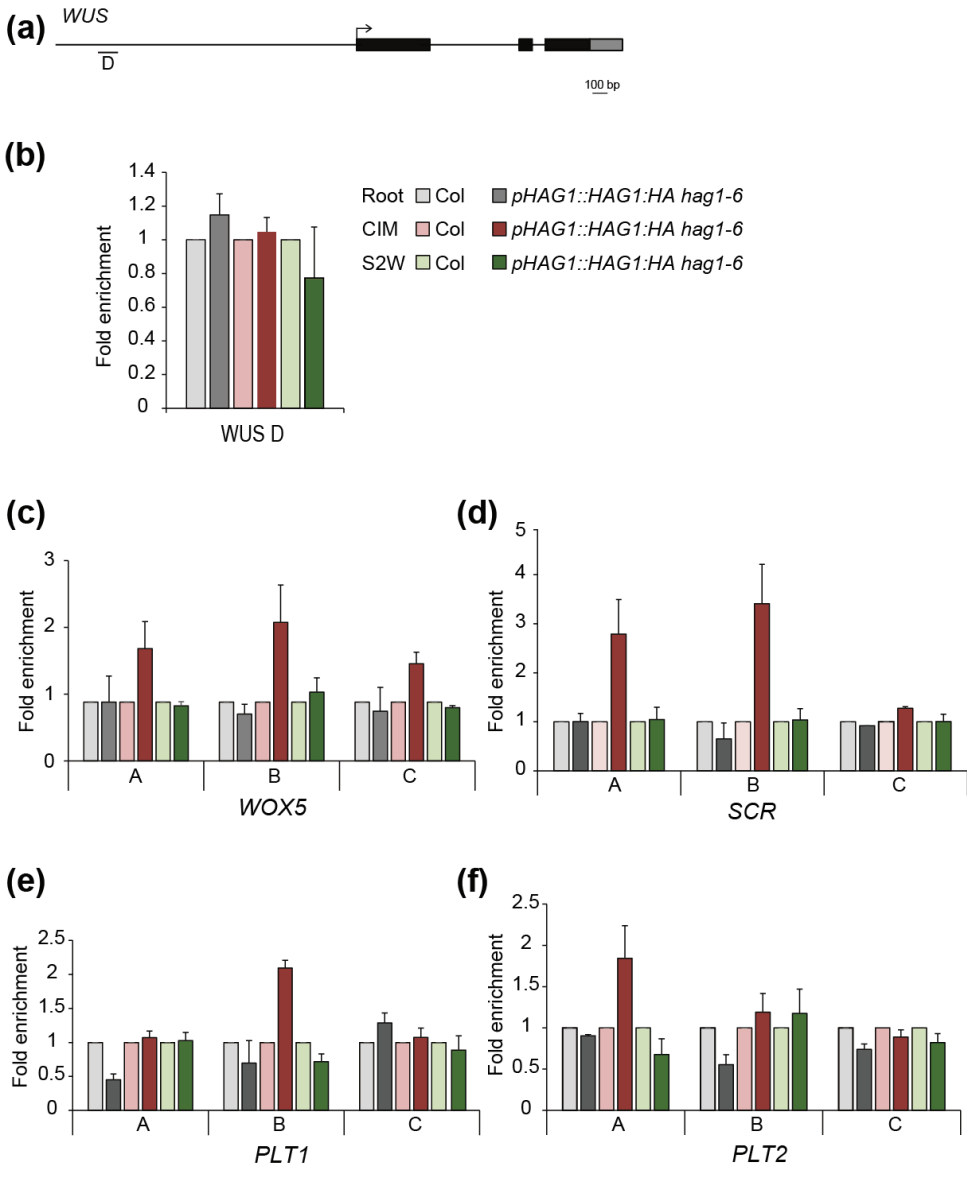
(a)
WUS
D
100 bp
(b)
Fold enrichment
1.4
1.2
1
0.8
0.6
0.4
0.2
0
WUS D
Root Col pHAG1::HAG1:HA hag1-6
CIM Col pHAG1::HAG1:HA hag1-6
S2W Col pHAG1::HAG1:HA hag1-6
(c)
Fold enrichment
3
2
1
0
A
B
C
WOX5
(d)
Fold enrichment
5
4
3
2
1
0
A
B
C
SCR
(e)
Fold enrichment
2.5
2
1.5
1
0.5
0
A
B
C
PLT1
(f)
Fold enrichment
2.5
2
1.5
1
0.5
0
A
B
C
PLT2

Figure 3.9 Direct targeting of HAG1:HA to *WOX5*, *SCR*, *PLT1*, and *PLT2* loci.

(a) Schematic representation of the *WUS* locus. See Figures 3.8a-3.8d for interpretation of the schematic. The region tested in ChIP-qPCR (Kwon *et al*., 2005) is indicated.

(b-f) Direct targeting of HAG1:HA protein to *WOX5* (c), *SCR* (d), *PLT1* (e), and *PLT2* (f) chromatin as determined by ChIP-qPCR analysis. Root, 1-w CIM (CIM), and 1-w CIM + 2-w SIM (S2W) samples were used for the assays. WUS D was used as a negative-control region (b). Values are the means ± SE of three biological replicates obtained after normalization to input DNA.

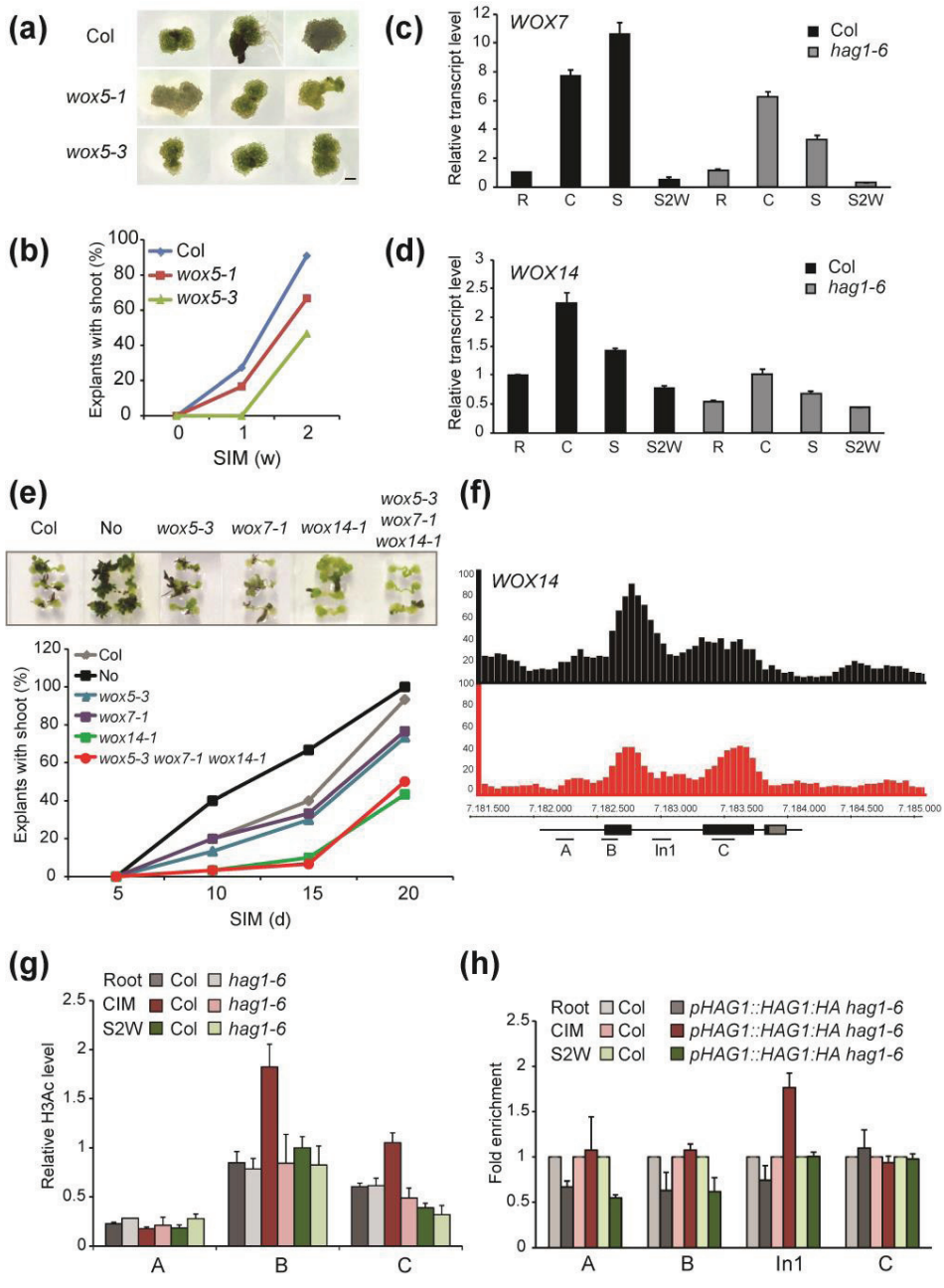
(a)
Col
wox5-1
wox5-3
(b)
Explants with shoot (%)
Col
wox5-1
wox5-3
SIM (w)
(c)
WOX7
Relative transcript level
Col
hag1-6
R C S S2W R C S S2W
(d)
WOX14
Relative transcript level
Col
hag1-6
R C S S2W R C S S2W
(e)
Col No wox5-3 wox7-1 wox14-1 wox5-3 wox7-1 wox14-1
Explants with shoot (%)
Col
No
wox5-3
wox7-1
wox14-1
wox5-3 wox7-1 wox14-1
SIM (d)
(f)
WOX14
A B In1 C
(g)
Root Col hag1-6
CIM Col hag1-6
S2W Col hag1-6
Relative H3Ac level
A B C
(h)
Root Col pHAG1::HAG1:HA hag1-6
CIM Col pHAG1::HAG1:HA hag1-6
S2W Col pHAG1::HAG1:HA hag1-6
Fold enrichment
A B In1 C

Figure 3.10 Mutations in *WOX*-clade genes cause defects in *de novo* shoot formation.

(a) *De novo* shoot regeneration using Col, *wox5-1*, and *wox5-3* hypocotyl explants. Scale bar: 1 mm.

(b) Percentage of explants with *de novo* shoots in Col, *wox5-1*, and *wox5-3* hypocotyl explants scored at indicated weeks on SIM.

(c and d) Transcript levels of *WOX7* (c) and *WOX14* (d) in Col and *hag1-6* roots (R), 4-d CIM explants (C), 4-d CIM + 2-d SIM explants (S), and 4-d CIM + 2-w SIM explants. Levels of Col R were set to 1 after normalization with *UBQ10*. Values are the means ± SE of three biological replicates.

(e) *De novo* shoot regeneration using Col, Nossen (No), *wox5-3*, *wox7-1*, *wox14-1*, and *wox5-3 wox7-1 wox14-1* root explants. No was used as WT control for *wox14-1*.

(f) H3Ac enrichment as determined by ChIP-seq at the *WOX14* locus of Col (upper black diagram) or *hag1-6* (lower red diagram) calli. Schematic representation of the *WOX14* locus is depicted at the bottom.

(g) ChIP-qPCR analysis of H3Ac levels at the *WOX14* loci of Col and *hag1-6*. Regions tested are indicated in the schematic in (d). See Figures 3.8e-3.8h for sample preparation and data presentation (e and f).

(h) Direct targeting of HAG1:HA protein to *WOX14* chromatin as determined by ChIP-qPCR analysis. Regions tested are as indicated in (f).


(a)
SALK_032192
TGG(W) → TGA (STOP)
scr-6
scr-3
100 bp

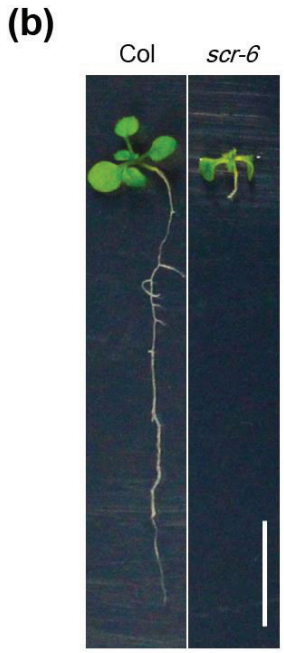
(b)
Col
scr-6


(c)
Col
scr-3
Col
scr-6

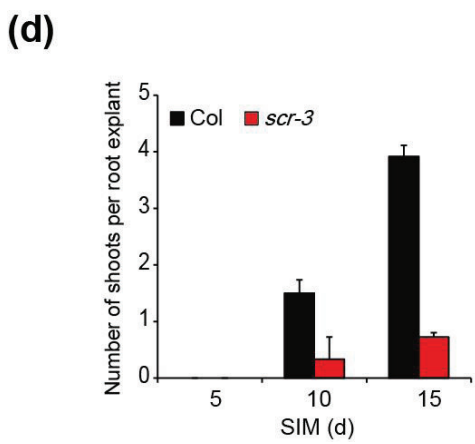
(d)
Number of shoots per root explant
Col
scr-3
0
1
2
3
4
5
5
10
15
SIM (d)

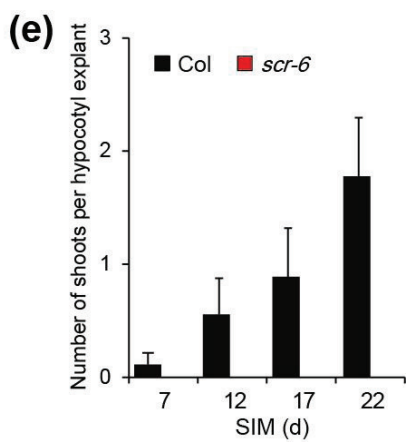
(e)
Number of shoots per hypocotyl explant
Col
scr-6
0
1
2
3
7
12
17
22
SIM (d)

Figure 3.11 Mutations in *SCR* cause severe defects in *de novo* shoot regeneration.

(a) Schematic representation of the *SCR* locus. The T-DNA insertion position of *scr-6* and the point mutation in *scr-3* are depicted. See Figures 3.8a-3.8d for interpretation of the schematic.

(b) Root phenotype of *scr-6.*Col and *scr-6* were grown vertically for 2 w before taken picture. Scale bar: 1 cm.

(c-e) *De novo* shoot regeneration using Col and *scr* mutants; *scr-3* and *scr-6* (c). The number of shoots per root explant was scored for Col and *scr-3* (d), and the number of shoots per hypocotyl explant was scored for Col and *scr-6* (e) at the indicated days on SIM. Scale bar: 1 mm.

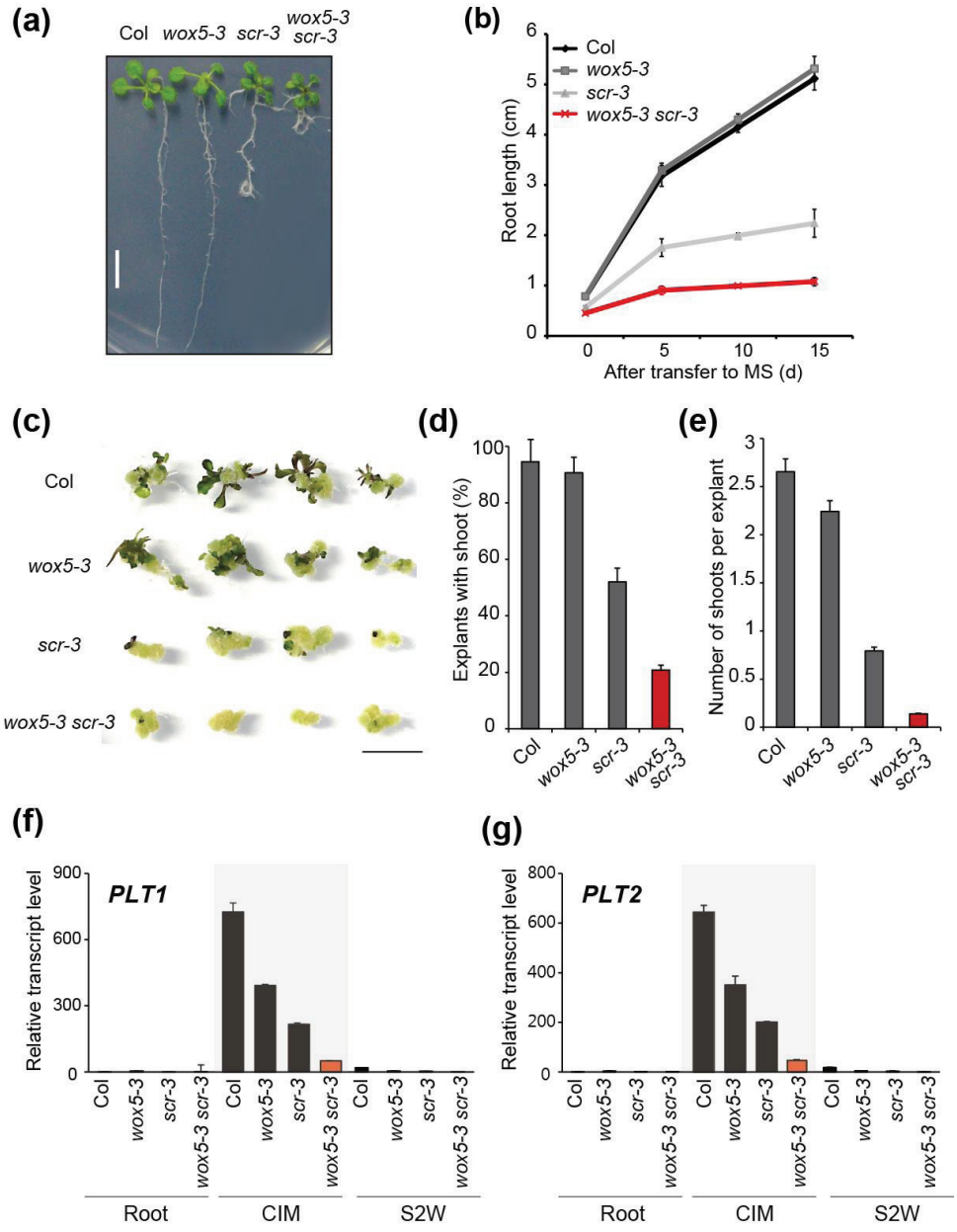
(a)
Col
wox5-3
scr-3
wox5-3 scr-3
(b)
Col
wox5-3
scr-3
wox5-3 scr-3
Root length (cm)
After transfer to MS (d)
(c)
Col
wox5-3
scr-3
wox5-3 scr-3
(d)
Explants with shoot (%)
(e)
Number of shoots per explant
(f)
PLT1
Relative transcript level
Root
CIM
S2W
(g)
PLT2
Relative transcript level
Root
CIM
S2W

Figure 3.12 Mutations in *WOX5* and *SCR* have additive effects on *de novo* shoot regeneration.

(a and b) Root phenotypes of Col, *wox5-3*, *scr-3*, and *wox5-3 scr-3* seedlings. Col, *wox5-3*, *scr-3*, and *wox5-3 scr-3* seeds were germinated on MS media. At 5 days after germination (DAG), seedlings at similar developmental stages were transferred onto fresh MS and grown vertically. The picture was taken after 15 d on fresh MS (a). Root lengths measured at indicated days after transfer to fresh MS (b). Scale bar: 1 cm.

(c-e) *De novo* shoot regeneration of Col, *wox5-3*, *scr-3*, and *wox5-3 scr-3* root explants. The picture was taken at 15 d on SIM (c). The percentage of explants with shoots (d), and the number of shoots per explants (e) were scored at 15 d on SIM. Scale bar: 1 cm.

(f and g) Transcript levels of *PLT1* (f) and *PLT2* (g) in Col, *wox5-3*, *scr-3*, and *wox5-3 scr-3* roots, 1-w CIM explants (CIM), and 1-w CIM + 2-w SIM explants (S2W) as determined by RT-qPCR analysis. Levels of Col root were set to 1 after normalization with *UBQ10*. Values are the means ± SE of three biological replicates.

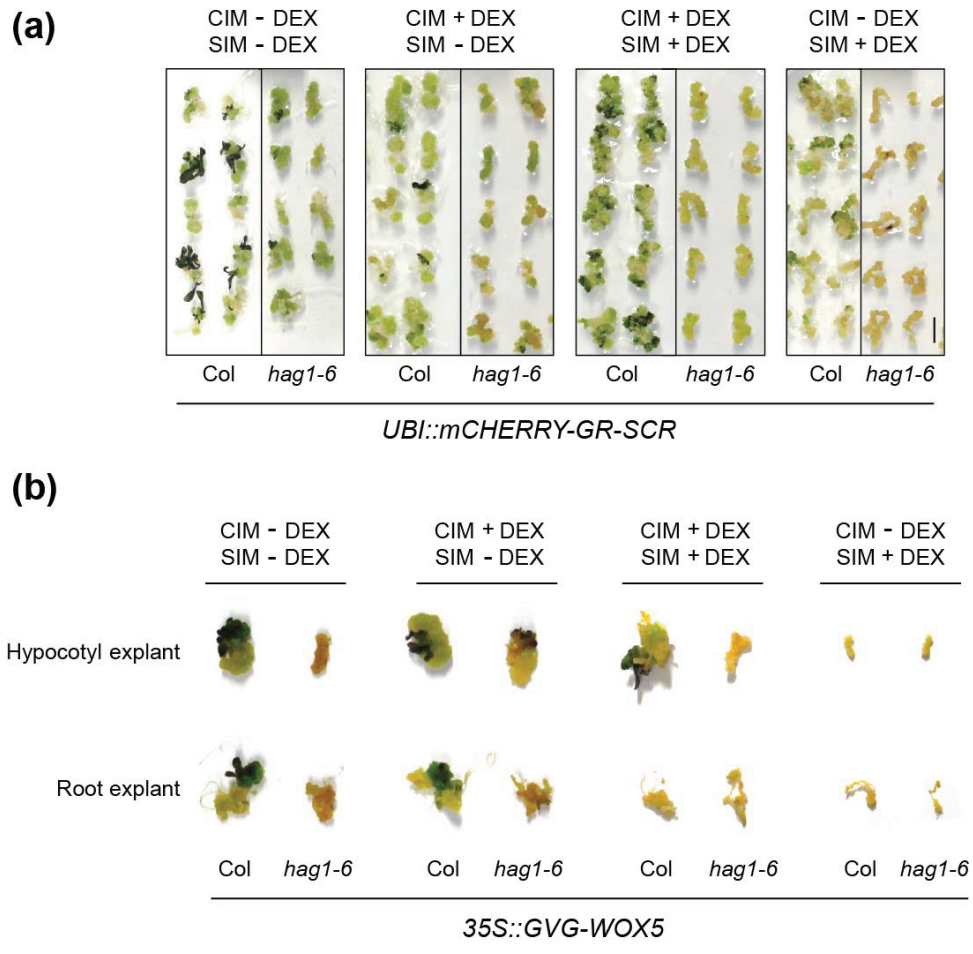
(a)
CIM - DEX
SIM - DEX
CIM + DEX
SIM - DEX
CIM + DEX
SIM + DEX
CIM - DEX
SIM + DEX
Col
hag1-6
Col
hag1-6
Col
hag1-6
Col
hag1-6
UBI::mCHERRY-GR-SCR
(b)
CIM - DEX
SIM - DEX
CIM + DEX
SIM - DEX
CIM + DEX
SIM + DEX
CIM - DEX
SIM + DEX
Hypocotyl explant
Root explant
Col
hag1-6
Col
hag1-6
Col
hag1-6
Col
hag1-6
35S::GVG-WOX5
(c)
35S::GVG-WOX5
35S::GVG-WOX5 hag1-6

Figure 3.13 Activation of WOX5 on CIM partially rescues the shoot regeneration defect of *hag1*.

(a) Activation of SCR by dexamethasone (DEX) treatment of *UBI::mCHERRY-GR-SCR* in Col and *hag1-6*. Root explants of homozygous *UBI::mCHERRY-GR-SCR* and *UBI::mCHERRY-GR-SCR hag1-6* transgenic plants were transferred onto the indicated combinations of CIM and SIM supplemented with or without 0.5 μM DEX.

(b) Activation of WOX5 by DEX treatment of *35S::GVG-WOX5* in Col and *hag1-6*. Hypocotyl and root explants of homozygous *35S::GVG-WOX5* and *35S::GVG-WOX5 hag1-6* transgenic plants were transferred onto the indicated combinations of CIM and SIM supplemented with or without 20 μM DEX.

(c) Morphology of shoots regenerated from *35S::GVG-WOX5* and *35S::GVG-WOX5 hag1-6* root explants. The explants were treated with 20 μM DEX on- CIM and further incubated on DEX-free SIM. Scale bar: 1 mm.

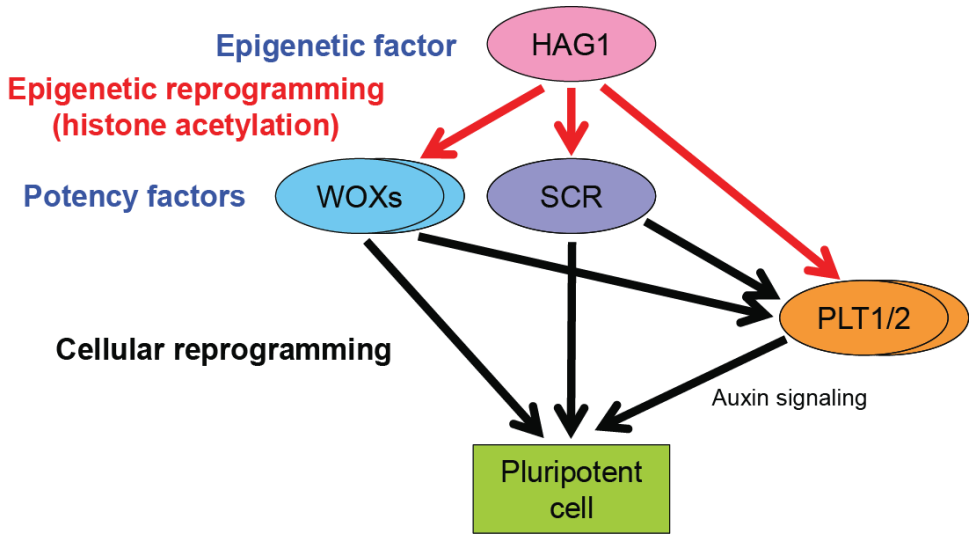

Figure 3.14 Acquisition of pluripotency during *de novo* organogenesis in plant cells by the HAG1-WOX5/WOX14/SCR/PLT1/PLT2 pathway.

Upon callus induction, HAG1 mediates epigenetic reprogramming of *WOX5*/*WOX14*, *SCR*, and *PLT1*/*PLT2* by catalyzing histone H3 acetylation of their chromatin. This epigenetic control on CIM assures the proper induction of these root transcription factors that act as potency factors to establish the pluripotency and competence to regenerate shoots on SIM.

3.6 Discussion

In this study, I provide evidence that HAG1, Arabidopsis homolog of GCN5, is highly expressed on CIM and activate a group of root meristem genes through epigenetic reprogramming to establish callus pluripotency (Figure 3.14). Loss of *HAG1* or root meristem genes such as *WOX5*, *SCR* and as well as the previously reported *PLT*s, leads to defective *de novo* shoot regeneration indicating that proper control these genes are indispensable for the acquisition of pluripotency. In mammals, GCN5/HAG1 is known to be highly expressed in mammalian embryonic stem cells (ESCs) and act as critical regulator during initiation of cellular reprogramming by associating with MYC, one of the OSKM (OCT4, SOX2, KLF4, and MYC) factors required for somatic cell reprogramming (Lin *et al*., 2007; Martínez-Cerdeño *et al*., 2012; Hirsch *et al*., 2015). Therefore, the role of HAG1 in the epigenetic reprogramming of differentiated cells for the establishment of pluripotency is likely to be well conserved in mammals and plants.

Induction of WOX5 result in partial rescue of *hag1* shoot regeneration defect. A recent report proposed that organogenesis is achieved by two distinct steps in which PLT3/7 target *PLT1/2* for acquisition of competence and *CUC2* for the completion of shoot regeneration (Kareem *et al*., 2015). However, in *hag1-6*, the expressions of *CUC2* as well as the major shoot meristem maintenance factor, *WUS* were both expressed at higher levels than WT. This might seem controversial considering the role of CUC2 and WUS as critical factors for *de novo* shoot formation (Laux *et al*., 1996; Mayer *et al*., 1998; Gallois *et al*., 2002, 2004). It is likely that the process *de novo* shoot formation is equipped with multiple pathways

and defect in *hag1* is due to the reduced expression of root genes in CIM rather than the misexpression of shoot genes in SIM. Furthermore, the increased expression of shoot genes could not compensate the loss of pluripotency resulted from the reduced expression of root genes in CIM indicating that these potency factors might affect the patterning rather than the expression of shoot genes in SIM. However, it is worth noting that several chlorophyll A/B-binding protein (*CAB*)-encoding genes are downregulated in *hag1*. Because *WOX5*-induced shoots in *hag1* produced shoots which lacked chlorophyll accumulation, and *CAB2* is known as a direct target of HAG1 **(**Benhamed *et al*., 2006**)**, it is tempting to suggest that *CAB2* might be the second target of HAG1 for the formation of complete *de novo* shoots.

Another phenotype of *hag1* (as well as *scr*) is the formation of callus with high proliferation rate. Studies in mammals provided evidence that the cell-cycle machinery can be coupled to the maintenance of pluripotency (Coronado *et al*., 2013; Gonzales *et al*., 2015). However, the possible crosstalk between callus pluripotency and the cell-cycle control is not yet revealed. Whether the over-proliferation is another cause for the loss of pluripotency in *hag1*, and whether root meristem genes are involved in this process remains to be elucidated in further studies.

References

Colón-Carmona, A., You, R., Haimovitch-Gal, T., Doerner, P. (1999). Spatio-temporal analysis of mitotic activity with a labile cyclin-GUS fusion protein. *Plant J*. **20:** 503-508.

Anzola, J.M., Sieberer, T., Ortbauer, M., Butt, H., Korbei, B., Weinhofer, I., Mullner, A.E., and Luschnig, C. (2010). Putative Arabidopsis transcriptional adaptor protein (PROPORZ1) is required to modulate histone acetylation in response to auxin. *Proc. Natl. Acad. Sci. USA* **107:** 10308-10313.

Atta, R., Laurens, L., Boucheron-Dubuisson, E., Guivarc'h, A., Carnero, E., Giraudat-Pautot, V., Rech, P., and Chriqui, D. (2009). Pluripotency of Arabidopsis xylem pericycle underlies shoot regeneration from root and hypocotyl explants grown in vitro. *Plant J*. **57:** 626-644.

Axtell, M.J., and Bowman, J.L. (2008). Evolution of plant microRNAs and their targets. *Trends Plant Sci.* **13:** 343-349.

Banno, H., Ikeda, Y., Niu, Q.W., and Chua, N.H. (2001). Overexpression of Arabidopsis ESR1 induces initiation of shoot regeneration. *Plant Cell* **13:** 2609-2618.

Benhamed, M., Bertrand, C., Servet, C., and Zhou, D.X. (2006). Arabidopsis

GCN5, HD1, and TAF1/HAF2 interact to regulate histone acetylation required for light-responsive gene expression. *Plant Cell* **18:** 2893-2903.

Benhamed, M., Martin-Magniette, M.L., Taconnat, L., Bitton, F., Servet, C., De Clercq, R., De Meyer, B., Buysschaert, C., Rombauts, S., Villarroel, R., Aubourg, S., Beynon, J., Bhalerao, R.P., Coupland, G., Gruissem, W., Menke, F.L., Weisshaar, B., Renou, J.P., Zhou, D.X., and Hilson, P. (2008). Genome-scale Arabidopsis promoter array identifies targets of the histone acetyltransferase GCN5. *Plant J.* **56:** 493-504

Berdasco, M., Alcazar, R., Garcia-Ortiz, M.V., Ballestar, E., Fernandez, A.F., Roldan-Arjona, T., Tiburcio, A.F., Altabella, T., Buisine, N., Quesneville, H., Baudry, A., Lepiniec, L., Alaminos, M., Rodriguez, R., Lloyd, A., Colot, V., Bender, J., Canal, M.J., Esteller, M., and Fraga, M.F. (2008). Promoter DNA hypermethylation and gene repression in undifferentiated Arabidopsis cells. *PLoS ONE* **3:** e3306.

Bertrand, C., Bergounioux, C., Domenichini, S., Delarue, M., and Zhou, D.X. (2003). Arabidopsis histone acetyltransferase AtGCN5 regulates the floral meristem activity through the WUSCHEL/AGAMOUS pathway. *J. Biol. Chem.* **278:** 28246-28251.

Bertrand, C., Benhamed, M., Li, Y.F., Ayadi, M., Lemonnier, G., Renou, J.P., Delarue, M., and Zhou, D.X. (2005). Arabidopsis HAF2 gene encoding TATA-

binding protein (TBP)-associated factor TAF1, is required to integrate light signals to regulate gene expression and growth. *J. Biol. Chem.* **280:** 1465-1473.

Bird, A. (2002). DNA methylation patterns and epigenetic memory. *Genes Dev.* **16:** 6-21.

Birnbaum, K.D., and Alvarado, A.S. (2008). Slicing across kingdoms: regeneration in plants and animals. *Cell* **132:** 697-710.

Birney, E. *et al.* (The ENCODE Project Consortium) (2007). Identification and analysis of functional elements in 1% of the human genome by the ENCODE pilot project. *Nature* **447:** 799-816.

Bonnet, J., Wang, C.Y., Baptista, T., Vincent, S.D., Hsiao, W.C., Stierle, M., Kao, C.F., Tora, L., Devys, D. (2014). The SAGA coactivator complex acts on the whole transcribed genome and is required for RNA polymerase II transcription. *Genes Dev.* **28:** 1999–2012.

Bouyer, D., Roudier, F., Heese, M., Andersen, E.D., Gey, D., Nowack, M.K., Goodrich, J., Renou, J.P., Grini, P.E., Colot, V., and Schnittger, A. (2011). Polycomb repressive complex 2 controls the embryo-to-seedling phase transition. *PLoS Genet.* **7:** e1002014.

Bratzel, F., Lopez-Torrejon, G., Koch, M., Del Pozo, J.C., and Calonje, M.

(2010). Keeping cell identity in Arabidopsis requires PRC1 RING-finger homologs that catalyze H2A monoubiquitination. *Curr. Biol*. **20:** 1853-1859.

Cantone, I., and Fisher, A.G. (2013). Epigenetic programming and reprogramming during development. *Nat. Struct. Mol. Biol.* **20:** 282-289.

Cary, A.J., Che, P., and Howell, S.H. (2002). Developmental events and shoot apical meristem gene expression patterns during shoot development in Arabidopsis thaliana. *Plant J.* **32:** 867-877.

Chanvivattana, Y., Bishopp, A., Schubert, D., Stock, C., Moon, Y.H., Sung, Z.R., and Goodrich, J. (2004). Interaction of Polycomb-group proteins controlling flowering in Arabidopsis. *Development* **131:** 5263-5276.

Che, P., Gingerich, D.J., Lall, S., and Howell, S.H. (2002). Global and hormone-induced gene expression changes during shoot development in Arabidopsis. *Plant Cell* **14:** 2771-2785.

Che, P., Lall, S., and Howell, S.H. (2007). Developmental steps in acquiring competence for shoot development in Arabidopsis tissue culture. *Planta* **226:** 1183-1194.

Che, P., Lall S., Nettleton, D., and Howell, S.H. (2006). Gene expression programs during shoot, root, and callus development in Arabidopsis tissue culture.

Plant Physiol. **141:** 620-637.

Choi, Y., Gehring, M., Johnson, L., Hannon, M., Harada, J.J., Goldberg, R.B., Jacobsen, S.E., and Fischer, R.L. (2002). DEMETER, a DNA glycosylase domain protein, is required for endosperm gene imprinting and seed viability in arabidopsis. *Cell* **110:** 33-42.

Clough, S.J., and Bent, A.F. (1998). Floral dip: a simplified method for Agrobacterium-mediated transformation of Arabidopsis thaliana. *Plant J.* **16:** 735-743.

Cohen, R., Schocken, J., Kaldis, A., Vlachonasios, K.E., Hark, A.T., and McCain, E.R. (2009). The histone acetyltransferase GCN5 affects the inflorescence meristem and stamen development in Arabidopsis. *Planta* **230:** 1207-1221.

Coleman-Derr, D., and Zilberman, D. (2012). DNA methylation, H2A.Z, and the regulation of constitutive expression. *Cold Spring Harb. Symp. Quant. Biol.* **77:** 147-154.

Colville, A., Alhattab, R., Hu, M., Labbe, H., Xing, T., and Miki, B. (2011). Role of HD2 genes in seed germination and early seedling growth in Arabidopsis. *Plant Cell Rep*. **30:** 1969-1979.

Coronado, D., Godet, M., Bourillot, P.Y., Tapponnier, Y., Bernat, A., Petit, M., Afanassieff, M., Markossian, S., Malashicheva, A., Iacone, R., Anastassiadis, K., and Savatier, P. (2013). A short G1 phase is an intrinsic determinant of naive embryonic stem cell pluripotency. *Stem Cell Res.* **10:** 118-131.

D'Agostino, I.B., and Kieber, J.J. (1999). Phosphorelay signal transduction: the emerging family of plant response regulators. *Trends Biochem. Sci.* **24:** 452-456.

D'Agostino, I.B., Deruere, J., and Kieber, J.J. (2000). Characterization of the response of the Arabidopsis response regulator gene family to cytokinin. *Plant Physiol.* **124:** 1706-1717.

Duclercq, J., Sangwan-Norreel, B., Catterou, M., and Sangwan, R.S. (2011). De novo shoot organogenesis: from art to science. *Trends Plant Sci.* **16:** 597-606.

Earley, K.W., Haag, J.R., Pontes, O., Opper, K., Juehne, T., Song, K., and Pikaard, C.S. (2006). Gateway-compatible vectors for plant functional genomics and proteomics. *Plant J.* **45:** 616-629.

Farrona, S., Coupland, G., and Turck, F. (2008). The impact of chromatin regulation on the floral transition. *Semin. Cell Dev. Biol.* **19:** 560-573.

Finnegan, E.J., and Kovac, K.A. (2000). Plant DNA methyltransferases. *Plant Mol. Biol.* **43:** 189-201.

Fraga, M.F., Ballestar, E., Montoya, G., Taysavang, P., Wade, P.A., and Esteller, M. (2003). The affinity of different MBD proteins for a specific methylated locus depends on their intrinsic binding properties. *Nucleic Acids Res.* **31:** 1765-1774.

Furuta, K., Kubo, M., Sano, K., Demura, T., Fukuda, H., Liu, Y.G., Shibata, D., and Kakimoto, T. (2011). The CKH2/PKL chromatin remodeling factor negatively regulates cytokinin responses in Arabidopsis calli. *Plant Cell Physiol.* **52:** 618-628.

Gallois, J.L., Woodward, C., Reddy, G.V., and Sablowski, R. (2002). Combined SHOOT MERISTEMLESS and WUSCHEL trigger ectopic organogenesis in Arabidopsis. *Development* **129:** 3207-3217.

Gallois, J.L., Nora, F.R., Mizukami, Y., and Sablowski, R. (2004). WUSCHEL induces shoot stem cell activity and developmental plasticity in the root meristem. *Genes Dev.* **18:** 375-380.

Gaspar-Maia, A., Alajem, A., Meshorer, E., and Ramalho-Santos, M. (2011). Open chromatin in pluripotency and reprogramming. *Nat. Rev. Mol. Cell Biol.* **12:** 36-47.

Georgieva, E.I., Lopez-Rodas, G., Sendra, R., Grobner, P., and Loidl, P. (1991). Histone acetylation in Zea mays. II. Biological significance of post-translational histone acetylation during embryo germination. *J. Biol. Chem*. **266:** 18751-18760.

Gordon, S.P., Heisler, M.G., Reddy, G.V., Ohno, C., Das, P., and Meyerowitz, E.M. (2007). Pattern formation during de novo assembly of the Arabidopsis shoot meristem. *Development* **134:** 3539-3548.

Govind, C.K., Zhang, F., Qiu, H., Hofmeyer, K., and Hinnebusch, A.G. (2007). Gcn5 promotes acetylation, eviction, and methylation of nucleosomes in transcribed coding regions. *Mol. Cell* **25:** 31-42.

Guo, A.Y., Zhu, Q.H., Gu, X., Ge, S., Yang, J., and Luo, J. (2008). Genome-wide identification and evolutionary analysis of the plant specific SBP-box transcription factor family. *Gene* **418:** 1-8.

Han, S.K., Song, J.D., Noh, Y.S., and Noh, B. (2007). Role of plant CBP/p300-like genes in the regulation of flowering time. *Plant J.* **49:** 103-114.

Hark, A.T., Vlachonasios, K.E., Pavangadkar, K.A., Rao, S., Gordon, H., Adamakis, I.D., Kaldis, A., Thomashow, M.F., and Triezenberg, S.J. (2009). Two Arabidopsis orthologs of the transcriptional coactivator ADA2 have distinct biological functions. *Biochim. Biophys. Acta* **1789:** 117-124.

Hassan, A.H., Prochasson, P., Neely, K.E., Galasinski, S.C., Chandy, M., Carrozza, M.J., and Workman, J.L. (2002). Function and selectivity of bromodomains in anchoring chromatin-modifying complexes to promoter

nucleosomes. *Cell* **111:** 369-379.

Heo, J.B., and Sung, S. (2011). Vernalization-mediated epigenetic silencing by a long intronic noncoding RNA. *Science* **331:** 76-79.

Hirsch, C. L. *et al.* (2015). Myc and SAGA rewire an alternative splicing network during early somatic cell reprogramming. *Genes Dev.* **29:** 803–816.

Ikeda, Y., Banno, H., Niu, Q.W., Howell, S.H., and Chua, N.H. (2006). The ENHANCER OF SHOOT REGENERATION 2 gene in Arabidopsis regulates CUP-SHAPED COTYLEDON 1 at the transcriptional level and controls cotyledon development. *Plant Cell Physiol.* **47:** 1443-1456.

Johnson, L., Cao, X., and Jacobsen, S. (2002). Interplay between two epigenetic marks: DNA methylation and histone H3 lysine 9 methylation. *Curr. Biol*. **12:** 1360-1367.

Jung, J.H., Ju, Y., Seo, P.J., Lee, J.H., and Park, C.M. (2012). The SOC1-SPL module integrates photoperiod and gibberellic acid signals to control flowering time in Arabidopsis. *Plant J.* **69:** 577-588.

Kang, M.J., Jin, H.S., Noh, Y.S., and Noh, B. (2015). Repression of flowering under a noninductive photoperiod by the HDA9-AGL19-FT module in Arabidopsis. *New Phytol.* **206:** 281-294.

Kareem, A., Durgaprasad, K., Sugimoto, K., Du, Y., Pulianmackal, A.J., Trivedi, Z.B., Abhayadev, P.V., Pinon, V., Meyerowitz, E.M., Scheres, B., and Prasad, K. (2015). PLETHORA Genes Control Regeneration by a Two-Step Mechanism. *Curr. Biol.* **25:** 1017-1030.

Kaufmann, K., Muiño, J.M., Østerås, M., Farinelli, L., Krajewski, P., and Angenent, G.C. (2010). Chromatin immunoprecipitation (ChIP) of plant transcription factors followed by sequencing (ChIP-SEQ) or hybridization to whole genome arrays (ChIP-CHIP). *Nat. Protoc*. **5:** 457-472.

Kidner, C.A., and Martienssen, R.A. (2004). Spatially restricted microRNA directs leaf polarity through ARGONAUTE1. *Nature* **428:** 81-84.

Kim, J.Y., Oh, J.E., Noh, Y.S., and Noh, B. (2015). Epigenetic control of juvenile-to-adult phase transition by the Arabidopsis SAGA-like complex. *Plant J.* **83:** 537-545.

Konig, A.C., Hartl, M., Pham, P.A., Laxa, M., Boersema, P.J., Orwat, A., Kalitventseva, I., Plochinger, M., Braun, H.P., Leister, D., Mann, M., Wachter, A., Fernie, A.R., and Finkemeier, I. (2014). The Arabidopsis class II sirtuin is a lysine deacetylase and interacts with mitochondrial energy metabolism. *Plant Physiol.* **164:** 1401-1414.

Kornet, N., and Scheres, B. (2009). Members of the GCN5 histone acetyltransferase complex regulate PLETHORA-mediated root stem cell niche maintenance and transit amplifying cell proliferation in Arabidopsis. *Plant Cell* **21:** 1070-1079.

Krebs, A.R., Karmodiya, K., Lindahl-Allen, M., Struhl, K., Tora, L. (2011). SAGA and ATAC histone acetyl transferase complexes regulate distinct sets of genes and ATAC defines a class of p300-independent enhancers. *Mol. Cell* **44:** 410.

Kwon, C.S., Chen, C., Wagner, D. (2005). WUSCHEL is a primary target for transcriptional regulation by SPLAYED in dynamic control of stem cell fate in Arabidopsis. *Genes Dev.* **19:** 992-1003.

Laplaze, L., Benkova, E., Casimiro, I., Maes, L., Vanneste, S., Swarup, R., Weijers, D., Calvo, V., Parizot, B., Herrera-Rodriguez, M.B., Offringa, R., Graham, N., Doumas, P., Friml, J., Bogusz, D., Beeckman, T., and Bennett, M. (2007). Cytokinins act directly on lateral root founder cells to inhibit root initiation. *Plant Cell* **19:** 3889-3900.

Latrasse, D., Benhamed, M., Henry, Y., Domenichini, S., Kim, W., Zhou, D.X., and Delarue, M. (2008). The MYST histone acetyltransferases are essential for gametophyte development in Arabidopsis. *BMC Plant Biol*. **8:** 121.

Laux, T., Mayer, K.F., Berger, J., and Jurgens, G. (1996). The WUSCHEL gene

is required for shoot and floral meristem integrity in Arabidopsis. *Development* **122:** 87-96.

Lee, T.I., Causton, H.C., Holstege, F.C., Shen, W.C., Hannett, N., Jennings, E.G., Winston, F., Green, M.R., Young, R.A. (2000) Redundant roles for the TFIID and SAGA complexes in global transcription. *Nature* **6787:** 701-4.

Li, C., Xu, J., Li, J., Li, Q., and Yang, H. (2014). Involvement of Arabidopsis histone acetyltransferase HAC family genes in the ethylene signaling pathway. *Plant Cell Physiol.* **55:** 426-435.

Li, W., Liu, H., Cheng, Z.J., Su, Y.H., Han, H.N., Zhang, Y., and Zhang, X.S. (2011). DNA methylation and histone modifications regulate de novo shoot regeneration in Arabidopsis by modulating WUSCHEL expression and auxin signaling. *PLoS Genet.* **7:** e1002243.

Lin, W., Srajer, G., Evrard, Y.A., Phan, H.M., Furuta, Y., Dent, S.Y. (2007). Developmental potential of Gcn5−/− embryonic stem cells in vivo and in vitro. *Dev. Dyn.* **236:** 1547–1557.

Lindroth, A.M., Park, Y.J., McLean, C.M., Dokshin, G.A., Persson, J.M., Herman, H., Pasini, D., Miro, X., Donohoe, M.E., Lee, J.T., Helin, K., and Soloway, P.D. (2008). Antagonism between DNA and H3K27 methylation at the imprinted Rasgrf1 locus. *PLoS Genet.* **4:** e1000145.

Liu, C., Li, L.C., Chen, W.Q., Chen, X., Xu, Z.H., and Bai, S.N. (2013a). HDA18 affects cell fate in Arabidopsis root epidermis via histone acetylation at four kinase genes. *Plant Cell* **25:** 257-269.

Liu, X., Chen, C.Y., Wang, K.C., Luo, M., Tai, R., Yuan, L., Zhao, M., Yang, S., Tian, G., Cui, Y., Hsieh, H.L., and Wu, K. (2013b). PHYTOCHROME INTERACTING FACTOR3 associates with the histone deacetylase HDA15 in repression of chlorophyll biosynthesis and photosynthesis in etiolated Arabidopsis seedlings. *Plant Cell* **25:** 1258-1273.

Livak, K.J., and Schmittgen, T.D. (2001). Analysis of Relative Gene Expression Data Using Real-Time Quantitative PCR and the 2−ΔΔCT Method. *Methods* **25:** 402-408.

Long, J.A., Ohno, C., Smith, Z.R., and Meyerowitz, E.M. (2006). TOPLESS regulates apical embryonic fate in Arabidopsis. *Science* **312:** 1520-1523.

Luger, K., Mader, A.W., Richmond, R.K., Sargent, D.F., and Richmond, T.J. (1997). Crystal structure of the nucleosome core particle at 2.8 A resolution. *Nature* **389:** 251-260.

Luo, M., Yu, C.W., Chen, F.F., Zhao, L., Tian, G., Liu, X., Cui, Y., Yang, J.Y., and Wu, K. (2012). Histone deacetylase HDA6 is functionally associated with

AS1 in repression of KNOX genes in arabidopsis. *PLoS Genet.* **8:** e1003114.

Mao, Y., Pavangadkar, K.A., Thomashow, M.F., and Triezenberg, S.J. (2006). Physical and functional interactions of Arabidopsis ADA2 transcriptional coactivator proteins with the acetyltransferase GCN5 and with the cold-induced transcription factor CBF1. *Biochim. Biophys. Acta* **1759:** 69-79.

Martínez-Cerdeño, V., Lemen, J.M., Chan, V., Wey, A., Lin, W., Dent, S.R., Knoepfler, P.S. (2012) N-Myc and GCN5 Regulate Significantly Overlapping Transcriptional Programs in Neural Stem Cells. *PLoS ONE* **7:** e39456.

Mayer, K.F., Schoof, H., Haecker, A., Lenhard, M., Jurgens, G., and Laux, T. (1998). Role of WUSCHEL in regulating stem cell fate in the Arabidopsis shoot meristem. *Cell* **95:** 805-815.

Mizzen, C.A., Yang, X.J., Kokubo, T., Brownell, J.E., Bannister, A.J., Owen-Hughes, T., Workman, J., Wang, L., Berger, S.L., Kouzarides, T., Nakatani, Y., and Allis, C.D. (1996). The TAF(II)250 subunit of TFIID has histone acetyltransferase activity. *Cell* **87:** 1261-1270.

Nagy, Z., and Tora, L. (2007). Distinct GCN5/PCAF-containing complexes function as co-activators and are involved in transcription factor and global histone acetylation. *Oncogene* **26:** 5341-5357.

Nelissen, H., Fleury, D., Bruno, L., Robles, P., De Veylder, L., Traas, J., Micol, J.L., Van Montagu, M., Inzé, D., and Van Lijsebettens, M. (2005). The elongata mutants identify a functional Elongator complex in plants with a role in cell proliferation during organ growth. *Proc. Natl. Acad. Sci. USA* **102:** 7754-7759.

Ogas, J., Cheng, J.C., Sung, Z.R., and Somerville, C. (1997). Cellular differentiation regulated by gibberellin in the Arabidopsis thaliana pickle mutant. *Science* **277:** 91-94.

Ogas, J., Kaufmann, S., Henderson, J., and Somerville, C. (1999). PICKLE is a CHD3 chromatin-remodeling factor that regulates the transition from embryonic to vegetative development in Arabidopsis. *Proc. Natl Acad. Sci. USA* **96:** 13839-13844.

Pandey, R., Muller, A., Napoli, C.A., Selinger, D.A., Pikaard, C.S., Richards, E.J., Bender, J., Mount, D.W., and Jorgensen, R.A. (2002). Analysis of histone acetyltransferase and histone deacetylase families of Arabidopsis thaliana suggests functional diversification of chromatin modification among multicellular eukaryotes. *Nucleic Acids Res*. **30:** 5036-5055.

Peaucelle, A., Morin, H., Traas, J., and Laufs, P. (2007). Plants expressing a miR164-resistant CUC2 gene reveal the importance of post-meristematic maintenance of phyllotaxy in Arabidopsis. *Development* **134:** 1045-1050.

Perrella, G., Lopez-Vernaza, M.A., Carr, C., Sani, E., Gossele, V., Verduyn, C., Kellermeier, F., Hannah, M.A., and Amtmann, A. (2013). Histone deacetylase complex1 expression level titrates plant growth and abscisic acid sensitivity in Arabidopsis. *Plant Cell* **25:** 3491-3505.

Pulido, A., and Laufs, P. (2010). Co-ordination of developmental processes by small RNAs during leaf development. *J. Exp. Bot*. **61:** 1277-1291.

Qiao, M., Zhao, Z., Song, Y., Liu, Z., Cao, L., Yu, Y., Li, S., and Xiang, F. (2012). Proper regeneration from in vitro cultured Arabidopsis thaliana requires the microRNA-directed action of an auxin response factor. *Plant J.* **71:** 14-22.

Raisner, R.M., Hartley, P.D., Meneghini, M.D., Bao, M.Z., Liu, C.L., Schreiber, S.L., Rando, O.J., and Madhani, H.D. (2005). Histone variant H2A.Z marks the 5' ends of both active and inactive genes in euchromatin. *Cell* **123:** 233-248.

Rauch, C., Trieb, M., Wibowo, F.R., Wellenzohn, B., Mayer, E., and Liedl, K.R. (2005). Towards an understanding of DNA recognition by the methyl-CpG binding domain 1. *J. Biomol. Struct. Dyn.* **22,** 695-706.

Rhoades, M.W., Reinhart, B.J., Lim, L.P., Burge, C.B., Bartel, B., and Bartel, D.P. (2002). Prediction of plant microRNA targets. *Cell* **110:** 513-520.

Riou-Khamlichi, C., Huntley, R., Jacqmard, A., and Murray, J.A. (1999).

Cytokinin activation of Arabidopsis cell division through a D-type cyclin. *Science* **283:** 1541-1544.

Sakai, H., Honma, T., Aoyama, T., Sato, S., Kato, T., Tabata, S., and Oka, A. (2001). ARR1, a transcription factor for genes immediately responsive to cytokinins. *Science* **294:** 1519-1521.

Sansó, M., Vargas-Pérez, I., Quintales, L., Antequera, F., Ayté, J., and Hidalgo, E. (2011). Gcn5 facilitates Pol II progression, rather than recruitment to nucleosome-depleted stress promoters, in Schizosaccharomyces pombe. *Nucleic Acids Res.* **39:** 6369-6379.

Schubert, D., Clarenz, O., and Goodrich, J. (2005). Epigenetic control of plant development by Polycomb-group proteins. *Curr. Opin. Plant Biol.* **8:** 553-561.

Servet, C., Conde e Silva, N., and Zhou, D.X. (2010). Histone acetyltransferase AtGCN5/HAG1 is a versatile regulator of developmental and inducible gene expression in Arabidopsis. *Mol. Plant* **3:** 670-677.

Shemer, O., Landau, U., Candela, H., Zemach, A., and Eshed Williams, L. (2015). Competency for shoot regeneration from Arabidopsis root explants is regulated by DNA methylation. *Plant Sci.* **238:** 251-261.

Sieberer, T., Hauser, M.T., Seifert, G.J., and Luschnig, C. (2003). PROPORZ1,

a putative Arabidopsis transcriptional adaptor protein, mediates auxin and cytokinin signals in the control of cell proliferation. *Curr. Biol.* **13:** 837-842.

Skirycz, A., Radziejwoski, A., Busch, W., Hannah, M.A., Czeszejko, J., Kwasniewski, M., Zanor, M.I., Lohmann, J.U., De Veylder, L., Witt, I., and Mueller-Roeber, B. (2008). The DOF transcription factor OBP1 is involved in cell cycle regulation in Arabidopsis thaliana. *Plant J.* **56:** 779-792.

Skoog, F., and Miller, C.O. (1957). Chemical regulation of growth and organ formation in plant tissues cultured in vitro. *Symp. Soc. Exp. Biol.* **11:** 118-130.

Strahl, B.D., and Allis, C.D. (2000). The language of covalent histone modifications. *Nature* **403:** 41-45.

Sterner, D.E., Grant, P.A., Roberts, S.M., Duggan, L.J., Belotserkovskaya, R., Pacella, L.A., Winston, F., Workman, J.L., and Berger, S.L. (1999). Functional organization of the yeast SAGA complex: distinct components involved in structural integrity, nucleosome acetylation, and TATA-binding protein interaction. *Mol. Cell Biol.* **19:** 86-98.

Sterner, D.E., and Berger, S.L. (2000). Acetylation of histones and transcription-related factors. *Microbiol. Mol. Biol. Rev.* **64:** 435-459.

Stockinger, E.J., Mao, Y., Regier, M.K., Triezenberg, S.J., and Thomashow,

M.F. (2001). Transcriptional adaptor and histone acetyltransferase proteins in Arabidopsis and their interactions with CBF1, a transcriptional activator involved in cold-regulated gene expression. *Nucleic Acids Res*. **29:** 1524-1533.

Sugimoto, K., Jiao, Y., and Meyerowitz, E.M. (2010). Arabidopsis regeneration from multiple tissues occurs via a root development pathway. *Dev. Cell* **18:** 463-471.

Suzuki, Y., Kawazu, T., and Koyama, H. (2004). RNA isolation from siliques, dry seeds, and other tissues of Arabidopsis thaliana. *Biotechniques* **37:** 542-544.

Swiezewski, S., Liu, F., Magusin, A., and Dean, C. (2009). Cold-induced silencing by long antisense transcripts of an Arabidopsis Polycomb target. *Nature* **462:** 799-802.

Tajima, Y., Imamura, A., Kiba, T., Amano, Y., Yamashino, T., and Mizuno, T. (2004). Comparative studies on the type-B response regulators revealing their distinctive properties in the His-to-Asp phosphorelay signal transduction of Arabidopsis thaliana. *Plant Cell Physiol.* **45:** 28-39.

Tanaka, M., Kikuchi, A., and Kamada, H. (2008). The Arabidopsis histone deacetylases HDA6 and HDA19 contribute to the repression of embryonic properties after germination. *Plant Physiol.* **146:** 149-161.

Telfer, A., Bollman, K.M., and Poethig, R.S. (1997). Phase change and the regulation of trichome distribution in Arabidopsis thaliana. *Development* **124:** 645-654.

Tessadori, F., van Zanten, M., Pavlova, P., Clifton, R., Pontvianne, F., Snoek, L.B., Millenaar, F.F., Schulkes, R.K., van Driel, R., Voesenek, L.A., Spillane, C., Pikaard, C.S., Fransz, P., and Peeters, A.J. (2009). Phytochrome B and histone deacetylase 6 control light-induced chromatin compaction in Arabidopsis thaliana. *PLoS Genet.* **5:** e1000638.

To, T.K., and Kim, J.M. (2014). Epigenetic regulation of gene responsiveness in Arabidopsis. *Front. Plant Sci.* **4:** 548.

To, T.K., Kim, J.M., Matsui, A., Kurihara, Y., Morosawa, T., Ishida, J., Tanaka, M., Endo, T., Kakutani, T., Toyoda, T., Kimura, H., Yokoyama, S., Shinozaki, K., and Seki, M. (2011). Arabidopsis HDA6 regulates locus-directed heterochromatin silencing in cooperation with MET1. *PLoS Genet.* **7:** e1002055.

Tsai, M.C., Manor, O., Wan, Y., Mosammaparast, N., Wang, J.K., Lan, F., Shi, Y., Segal, E., and Chang, H.Y. (2010). Long noncoding RNA as modular scaffold of histone modification complexes. *Science* **329:** 689-693.

Ueno, Y., Ishikawa, T., Watanabe, K., Terakura, S., Iwakawa, H., Okada, K., Machida, C., and Machida, Y. (2007). Histone deacetylases and ASYMMETRIC

LEAVES2 are involved in the establishment of polarity in leaves of Arabidopsis. *Plant Cell* **19:** 445-457.

van Bakel, H., Nislow, C., Blencowe, B.J., and Hughes, T.R. (2010). Most "dark matter" transcripts are associated with known genes. *PLoS Biol.* **8:** e1000371.

Vlachonasios, K.E., Thomashow, M.F., and Triezenberg, S.J. (2003). Disruption mutations of ADA2b and GCN5 transcriptional adaptor genes dramatically affect Arabidopsis growth, development, and gene expression. *Plant Cell* **15:** 626-638.

Verdeil, J.L., Alemanno, L., Niemenak, N., and Tranbarger, T.J. (2007). Pluripotent versus totipotent plant stem cells: dependence versus autonomy? *Trends Plant Sci.* **12:** 245-252.

Wang, C., Gao, F., Wu, J., Dai, J., Wei, C., and Li, Y. (2010). Arabidopsis putative deacetylase AtSRT2 regulates basal defense by suppressing PAD4, EDS5 and SID2 expression. *Plant Cell Physiol*. **51:** 1291-1299.

Wang, J.W., Schwab, R., Czech, B., Mica, E., and Weigel, D. (2008). Dual effects of miR156-targeted SPL genes and CYP78A5/KLUH on plastochron length and organ size in Arabidopsis thaliana. *Plant Cell* **20:** 1231-1243.

Wang, J.W., Czech, B., and Weigel, D. (2009). miR156-regulated SPL transcription factors define an endogenous flowering pathway in Arabidopsis

thaliana. *Cell* **138**: 738-749.

Wang, L., Kim, J., and Somers, D.E. (2013). Transcriptional corepressor TOPLESS complexes with pseudoresponse regulator proteins and histone deacetylases to regulate circadian transcription. *Proc. Natl Acad. Sci. USA* **110:** 761-766.

Wang, Z., Zang, C., Cui, K., Schones, D.E., Barski, A., Peng, W., and Zhao, K. (2009). Genome-wide mapping of HATs and HDACs reveals distinct functions in active and inactive genes. *Cell* **138:** 1019-1031.

Woo, H.R., Dittmer, T.A., and Richards, E.J. (2008). Three SRA-domain methylcytosine-binding proteins cooperate to maintain global CpG methylation and epigenetic silencing in Arabidopsis. *PLoS Genet.* **4:** e1000156.

Wu, G., and Poethig, R.S. (2006). Temporal regulation of shoot development in Arabidopsis thaliana by miR156 and its target SPL3. *Development* **133:** 3539-3547.

Wu, G., Park, M.Y., Conway, S.R., Wang, J.W., Weigel, D., and Poethig, R.S. (2009). The sequential action of miR156 and miR172 regulates developmental timing in Arabidopsis. *Cell* **138:** 750-759.

Xu, K., Liu, J., Fan, M., Xin, W., Hu, Y., and Xu, C. (2012). A genome-wide transcriptome profiling reveals the early molecular events during callus initiation in

Arabidopsis multiple organs. *Genomics* **100:** 116-124.

Yamaguchi, A., Wu, M.F., Yang, L., Wu, G., Poethig, R.S., and Wagner, D. (2009). The microRNA-regulated SBP-box transcription factor SPL3 is a direct upstream activator of LEAFY, FRUITFULL, and APETALA 1. *Dev. Cell* **17:** 268-278.

Yang, L., Conway, S.R., and Poethig, R.S. (2011). Vegetative phase change is mediated by a leaf-derived signal that represses the transcription of miR156. *Development* **138:** 245-249.

Yano, R., Takebayashi, Y., Nambara, E., Kamiya, Y., and Seo, M. (2013). Combining association mapping and transcriptomics identify HD2B histone deacetylase as a genetic factor associated with seed dormancy in Arabidopsis thaliana. *Plant J.* **74:** 815-828.

Yoder, J.A., Walsh, C.P., and Bestor, T.H. (1997a). Cytosine methylation and the ecology of intragenomic parasites. *Trends Genet.* **13:** 335-340.

Yoder, J.A., Soman, N.S., Verdine, G.L., and Bestor, T.H. (1997b). DNA (cytosine-5)-methyltransferases in mouse cells and tissues. Studies with a mechanism-based probe. *J. Mol. Biol. Mol.* **270:** 385-395.

Yu, N., Cai, W.J., Wang, S., Shan, C.M., Wang, L.J., and Chen, X.Y. (2010).

Temporal control of trichome distribution by microRNA156-targeted SPL genes in Arabidopsis thaliana. *Plant Cell* **22:** 2322-2335.

Yu, S., Galvão, V.C., Zhang, Y.C., Horrer, D., Zhang, T.Q., Hao, Y.H., Feng, Y.Q., Wang, S., Schmid, M., and Wang, J.W. (2012). Gibberellin regulates the Arabidopsis floral transition through miR156-targeted SQUAMOSA promoter binding-like transcription factors. *Plant Cell* **24:** 3320-3332.

Yu, S., Cao, L., Zhou, C.M., Zhang, T.Q., Lian, H., Sun, Y., Wu, J., Huang, J., Wang, G., and Wang, J.W. (2013). Sugar is an endogenous cue for juvenile-to-adult phase transition in plants. *eLife* **2:** e00269.

Zhang, H., Bishop, B., Ringenberg, W., Muir, W.M., and Ogas, J. (2012). The CHD3 remodeler PICKLE associates with genes enriched for trimethylation of histone H3 lysine 27. *Plant Physiol.* **159:** 418-432.

Zhang, H., Rider, S.D., Jr., Henderson, J.T., Fountain, M., Chuang, K., Kandachar, V., Simons, A., Edenberg, H.J., Romero-Severson, J., Muir, W.M., and Ogas, J. (2008). The CHD3 remodeler PICKLE promotes trimethylation of histone H3 lysine 27. *J. Biol. Chem*. **283:** 22637-22648.

Zhang, T.Q., Lian, H., Tang, H., Dolezal, K., Zhou, C.M., Yu, S., Chen, J.H., Chen, Q., Liu, H., Ljung, K., and Wang, J.W. (2015). An intrinsic microRNA timer regulates progressive decline in shoot regenerative capacity in plants. *Plant*

Cell **27:** 349-360.

Zhao, J., Morozova, N., Williams, L., Libs, L., Avivi, Y., and Grafi, G. (2001). Two phases of chromatin decondensation during dedifferentiation of plant cells: distinction between competence for cell fate switch and a commitment for S phase. *J. Biol. Chem*. **276:** 22772-22778.

Zilberman, D. (2008). The evolving functions of DNA methylation. *Curr. Opin. Plant Biol.* **11:** 554-559.

Zilberman, D., Gehring, M., Tran, R.K., Ballinger, T., and Henikoff, S. (2007). Genome-wide analysis of Arabidopsis thaliana DNA methylation uncovers an interdependence between methylation and transcription. *Nat. Genet.* **39:** 61-69.

국문 초록

하나의 개체를 이루는 수많은 세포들은 모두 동일한 유전정보를 가지고 있다. 하지만 개별 세포는 서로 다른 모양을 가지고 다양한 기능을 수행하는 여러 종류의 세포타입(cell type)으로 분화하게 되며, 발달단계에 따라 특이적이며 안정적인 유전자 발현 패턴을 보이게 된다. 이렇게 동일한 유전정보가 발달 과정 및 주변 환경에 따라 선택적으로 발현되는 현상은 후성유전학적 메커니즘에 의해 조절된다.

후성유전학적 조절이란 DNA 염기서열 자체는 변화하지 않은 채로 특정 유전자의 발현이 조절되어 유전정보가 달라지는 현상을 뜻한다. 널리 알려진 후성유전학적 조절 메커니즘으로는 DNA 메틸화, ATP-의존적 리모델링이나 히스톤 변형을 통한 크로마틴 변형, 핵 내 위치 결정, 이형 히스톤 삽입 및 RNA 간섭이 있다.

이러한 후성유전학적 조절 메커니즘 중에서도 히스톤 변형을 통한 크로마틴 변형은 타깃 유전자 발현에 직접적인 영향을 미칠 수 있다는 점에서 많은 주목을 받아왔다. 특히 히스톤 아세틸화를 통한 히스톤 변형은 히스톤 아세틸화효소에 의해 매개되는데, 이는 전사가 활발히 일어나는 진정염색질에 널리 분포되어 있다. 히스톤 아세틸화효소들은 아세틸기(CH_3COO^-)를 N-말단 히스톤 꼬리의 리신 잔기에 붙이는 반응을 촉매 한다. 히스톤 아세틸기는 리신의 양전화를 중성화하여 음전하를 띤 DNA와 히스톤 간 결합을 느슨하게 만든다. 그 결과 전사인자들이 DNA에 효율적으로

결합할 수 있도록 하거나, 아세틸화된 히스톤을 선택적으로 인지하는 단백질들이 결합하여 작용할 수 있도록 하여 궁극적으로는 유전자 발현 활성을 유도한다.

이러한 배경을 바탕으로 본 연구에서는 애기장대 히스톤 아세틸화 효소 중 하나로 Gcn5-related N-acetyltransferase (GNAT) family에 속해있는 HAG1/AtGCN5가 식물의 발달 전이 및 식물세포 전형성능에 미치는 역할을 규명하였다.

먼저, HAG1과 PRZ1/ADA2b를 함유한 SAGA-유사 히스톤 아세틸화효소 복합체가 식물의 juvenile-to-adult 발달 전이를 조절하는 메커니즘에 대한 연구를 수행하였다. 애기장대의 경우 vegetative transition은 miR156에 의한 전사 후 조절을 받는 SQUAMOSA PROMOTER BINDING PROTEIN-LIKE (SPL) factor에 의해 결정된다고 알려져 왔다. 본 연구에서는 HAG1과 PRZ1이 *SPL* 유전자들의 염색질에 직접 H3Ac를 매개하여 juvenile-to-adult 발달 전이 시기에 중요한 영향을 미친다는 것을 밝혔다. 뿐만 아니라 이처럼 HAG1을 통해 이루어지는 후성유전학적 조절이 빛, 광주기, 혹은 후배자 발생에서도 miR156과는 독립적인 메커니즘으로 *SPL*의 전사를 촉진시킨다는 결론을 얻었다.

두 번째 부분에서는 HAG1이 캘러스에서의 전형성능 유도 및 줄기재생에 있어서 핵심적인 역할을 수행한다는 것을 밝혔다. 그 동안 캘러스는 모든 식물 세포로부터 유래 할 수 있는 탈분화 된 세포의 군집으로

여겨져 왔다. 하지만 최근 들어 캘러스가 내초 세포의 분열을 통해 형성되며, 그 과정에서 뿌리 분열조직 및 곁뿌리 발달의 경우와 유사한 유전체 발현 패턴을 보인다는 결론이 도출되어 식물 세포의 전형성능에 대한 관점이 재정립 되고 있다. 본 연구에서는 캘러스가 형성될 때 HAG1이 뿌리 분열조직에서 발현되는 여러 유전자들이 캘러스에서도 발현되도록 촉진시킨다는 사실을 발견하였다. 구체적으로, 캘러스가 형성될 때 HAG1은 *WOX5/WOX14*, *SCR*, *PLT1*과 *PLT2*의 염색질에 결합하여 히스톤의 아세틸 메커니즘을 통해 이들 유전자의 발현을 촉진시킨다. 나아가 HAG1에 의하여 캘러스에서 발현이 유도된 WOX5/WOX14와 SCR, PLT1 및 PLT2는 전형성능을 부여하는 형성능 유도인자들(potency factors)로 작용하여 이후 줄기재생을 가능하게 함을 알 수 있었다.

주요어: HAG1, 캘러스, 줄기재생, 히스톤 아세틸화, juvenile-to-adult 발달 전이

학 번: 2007-22838